

2000-08-01

Kinetic Studies on the Reaction of Hydroxyl Radicals with Aromatic Compounds

Paul Chadwick
Technological University Dublin

Follow this and additional works at: <https://arrow.tudublin.ie/scienmas>

 Part of the [Chemistry Commons](#)

Recommended Citation

Chadwick, P. (2000). *Kinetic studies on the reaction of hydroxyl radicals with aromatic compounds*. Masters dissertation. Technological University Dublin. doi:10.21427/D7N898

This Theses, Masters is brought to you for free and open access by the Science at ARROW@TU Dublin. It has been accepted for inclusion in Masters by an authorized administrator of ARROW@TU Dublin. For more information, please contact arrow.admin@tudublin.ie, aisling.coyne@tudublin.ie, vera.kilshaw@tudublin.ie.

KINETIC STUDIES ON THE REACTION OF
HYDROXYL RADICALS WITH AROMATIC
COMPOUNDS

A thesis submitted to
DUBLIN INSTITUTE OF TECHNOLOGY

For the degree of
MASTER OF PHILOSOPHY

by
PAUL CHADWICK B.A.(Moderator), G.R.S.C.

Based on research carried out in
School of Chemistry, Dublin Institute of Technology, Kevin St., Dublin 8

under the supervision of
DR. JACK TREACY

Declaration

I certify that this thesis, which I now submit for examination for the award of Master of Philosophy, is entirely my own work and has not been taken from the work of others, save and to the extent that such work has been cited and acknowledged within the text of my work.

This thesis was prepared according to the regulations for post-graduate studies by research of the Dublin Institute of Technology and has not been submitted in whole or in part for an award in any other Institute or University.

The Institute has permission to keep, to lend or to copy this thesis in whole or in part, on condition that any such use of the material of the thesis be duly acknowledged.

A handwritten signature in cursive script, reading "Paul Chadwick", written over a horizontal line.

PAUL CHADWICK

Acknowledgements

I wish to thank Dr. Mary Gurrie, Ms. Barbara O'Leary, Dr. Nick Holmes and Dr. John O'Reilly for their continual support in all matters chemical and other.

In addition, I wish to thank Professor Howard Sidebottom, Dr. John Wenger and all the postgraduate students at UCD Atmospheric Chemistry Dept.

I would like to thank my parents and family for providing me with the time, support and finance to gain a masters in chemistry.

Mostly, I wish to thank Tracy for her continual understanding and support throughout my less affluent years.

Finally, I want to thank the players, management and staff of Liverpool FC, who throughout my third level career have endeavored to make every effort to finish each season in March, thereby allowing me to concentrate on my studies.

TABLE OF CONTENTS

	Page
ABSTRACT	i
1.0 GENERAL INTRODUCTION	1
1.1 THE ATMOSPHERE	4
1.1.1 Thermosphere	4
1.1.2 Mesosphere	4
1.1.3 Stratosphere	5
1.1.4 Troposphere	9
1.2 THE POLLUTED TROPOSPHERE	15
1.3 PHOTOCHEMICAL OZONE CREATION POTENTIAL (POCP)	23
2.0 INTRODUCTION TO AROMATIC COMPOUNDS	30
2.1 AROMATIC COMPOUNDS	31
2.1.1 Aromatics in Fuel	31
2.1.2 Aromatics in Industry	35
2.1.3 Toxicology of Aromatics	36
2.2 ATMOSPHERIC CHEMISTRY OF AROMATICS	39
2.2.1 Reactions of Aromatic compounds with OH radicals	39

2.2.2	Product studies	42
2.3	EXPERIMENTAL TECHNIQUES	48
2.3.1	Absolute methods	48
2.3.2	Relative rate method	52
2.4	PREVIOUSLY REPORTED RATE DATA	55
2.4.1	Room temperature rate data	55
2.4.2	Temperature dependant rate data	66
2.4.3	Aims of this work	68
3.0	EXPERIMENTAL	74
3.1	MATERIALS	75
3.2	APPARATUS	75
3.3	PROCEDURE	77
3.4	ANALYSIS	78
4.0	RESULTS	81
4.1	ROOM TEMPERATURE OH RADICAL REACTIONS	82
4.2	TEMPERATURE DEPENDANT OH RADICAL REACTIONS	94

4.3	ROOM TEMPERATURE Cl ATOM REACTIONS	107
5.0	DISCUSSION	110
5.1	PHOTOLYSIS OF O ₃ /H ₂ MIXTURES AS A SOURCE OF OH RADICALS	111
5.2	ISOTOPE EFFECTS	114
5.3	MONOALKYL SUBSTITUTED BENZENES	119
5.4	DIALKYL SUBSTITUTED BENZENES	125
5.5	TRI- AND TETRAMETHYL SUBSTITUTED BENZENES	135
5.6	HALOTOLUENES	142
5.7	CORRELATIONS	147
5.8	ATMOSPHERIC IMPLICATIONS	153
6.0	LITERATURE REFERENCES	155

List of Figures

No.		Page
1.1	Regions of the atmosphere based on the temperature variation with altitude.	3
1.2	Plot of the partial pressure of ozone as a function of altitude for the tropical regions.	6
1.3	Reaction pathway for the oxidation of methane in the troposphere.	13
1.4	Generalised scheme for reaction of OH radicals with saturated VOCs (RCH ₃) in the troposphere.	21
2.1	The toxicological pathway for Benzene in the body.	38
2.2	Reaction pathway following H-atom abstraction from Toluene by OH radicals in the presence of NO _x .	43
2.3	Reaction pathway following OH addition to Toluene in the presence of NO _x .	45
3.1	Schematic diagram of experimental apparatus.	76
4.1	Plots in the form of equation XII for the reaction of Toluene with OH radicals using irradiated O ₃ /H ₂ O mixtures and irradiated O ₃ /H ₂ mixtures as the source of OH radicals at 298±2K and 1 atm total pressure.	85
4.2	Plots in the form of equation XII for the reaction of Toluene-h ₈ and Toluene-d ₈ with OH radicals at 298K and 1 atm total pressure.	86
4.3	Plots in the form of equation XII for the reaction of Toluene, Ethylbenzene, n-Propylbenzene and n-Butylbenzene with OH radicals at 298±2K and 1 atm total pressure.	87
4.4	Plots in the form of equation XII for the reaction of a series of Alkylbenzenes with OH radicals at 298±2K and 1 atm total pressure.	88
4.5	Plots in the form of equation XII for the reaction of 2-Fluorotoluene, 3-Fluorotoluene and 4-Fluorotoluene with OH radicals at 298±2K and 1 atm total pressure.	89
4.6	Plots in the form of equation XII for the reaction of 2-Chlorotoluene, 3-Chlorotoluene and 4-Chlorotoluene with OH radicals at 298±2K and 1 atm total pressure.	90

4.7	Plot in the form of equation XII for the reaction of 1,2,4,5-Tetramethylbenzene with OH radicals at $298\pm 2\text{K}$ and 1 atm total pressure.	91
4.8	Plots in the form of equation XII for the reaction of ortho-Diethylbenzene, Indane and Tetralin with OH radicals at $298\pm 2\text{K}$ and 1 atm total pressure.	92
4.9	Plots in the form of equation XII for the reaction of toluene with OH radicals over the temperature range 243 – 323K and at 1 atm total pressure.	95
4.10	Arrhenius plot for the reaction of Toluene with OH radicals over the temperature range 243 – 323K and at 1 atm total pressure.	96
4.11	Plots in the form of equation XII for the reaction of 3-Fluorotoluene with OH radicals over the temperature range 248 – 323K and at 1 atm total pressure.	97
4.12	Arrhenius plot for the reaction of 3-Fluorotoluene with OH radicals over the temperature range 248 – 323K and at 1 atm total pressure.	98
4.13	Plots in the form of equation XII for the reaction of 3-Chlorotoluene with OH radicals over the temperature range 243 – 323K and at 1 atm total pressure.	99
4.14	Arrhenius plot for the reaction of 3-Chlorotoluene with OH radicals over the temperature range 243 – 323K and at 1 atm total pressure.	100
4.15	Plots in the form of equation XII for the reaction of Indane with OH radicals over the temperature range 245 – 323K and at 1 atm total pressure.	101
4.16	Arrhenius plot for the reaction of Indane with OH radicals over the temperature range 245 – 323K and at 1 atm total pressure.	102
4.17	Plots in the form of equation XII for the reaction of Tetralin with OH radicals over the temperature range 243 – 323K and at 1 atm total pressure.	103
4.18	Arrhenius plot for the reaction of Tetralin with OH radicals over the temperature range 243 – 323K and at 1 atm total pressure.	104
4.19	Plots in the form of equation XII for the reaction of Indane and Tetralin With Cl atoms at $298\pm 2\text{K}$ and at 1 atm total pressure.	108
5.1	Plot of Δk versus number of CH_2 groups for this series of Monoalkylbenzenes.	123

5.2	Resonance structures following addition of OH radicals to the ortho, meta and para positions of Toluene.	139
-----	--	-----

List of Tables

No.		
1.1	Average percentage of main tropospheric constituents under clean air conditions.	11
1.2	VOC emissions by country in kTonnes for the member states of the EU in 1985, 1990 and 1994.	17
1.3	European Union and World Health Organisation population information and vegetation concentration thresholds for Ozone.	19
1.4	The POCPs for the 69 VOCs studied by Derwent and Jenkin showing the mean and one standard deviation for each VOC relative to ethene.	26
1.5	Emissions and POCP-weighted emissions for each hydrocarbon type.	28
1.6	Emissions and POCP-weighted emissions for the main source categories of hydrocarbons in the atmosphere.	29
2.1	Typical % hydrocarbon composition of petrol.	31
2.2	Structures and Research Octane Numbers (R.O.N.) for a series of hydrocarbons containing 7- carbon atoms.	33
2.3	Structures and Research Octane Numbers (R.O.N.) of the most frequently used oxygenates in motor fuel.	34
2.4	Rate constants for the reaction of OH radicals with Aromatic compounds at room temperature and at, or close to, the high pressure limit.	60
2.5	Temperature dependant parameters $k = A \exp(-B/T)$ for the reaction of OH radicals with Aromatic compounds.	69
3.1	Substrate aromatics, reference organics and gas chromatographic conditions used in this work.	79
4.1	Rate constant ratios, k_{36}/k_{37} , and calculated rate constants for the reaction of OH radicals with Aromatic compounds at $298 \pm 2K$ and 1 atm total pressure.	93
4.2	Rate constant ratios, k_{36}/k_{37} , and calculated rate constants for the reaction of OH radicals with a series of Aromatic compounds over the temperature range 243 – 323K and at 1 atm total pressure.	105

4.3	Arrhenius parameters for the reaction of OH radicals with selected Aromatic compounds over the temperature range 243 – 323K and at 1 atm total pressure.	106
4.4	Rate constant ratios, k_{39}/k_{40} , and calculated rate constants for the reaction of Cl atoms with Indane and Tetralin at 298±2K and 1 atm total pressure.	109
5.1	Rate constants for the reaction of OH radicals with Toluene- h_8 and Toluene- d_8 at room temperature and at, or close to, the high pressure limit.	118
5.2	Rate constants for the reaction of OH radicals with a series of alkyl substituted benzenes at room temperature and at, or close to, the high pressure limit.	120
5.3	Ionisation Potentials and room temperature OH radical rate constants for a series of monoalkyl substituted benzenes.	124
5.4	Rate constants for the reaction of OH radicals with a series of Aromatic compounds at room temperature and at, or close to, the high pressure limit.	126
5.5	Rate constants for the reaction of Cyclopentane, Cyclohexane, Indane and Tetralin with OH and NO ₃ radicals and Cl atoms at 298K.	132
5.6	Relative rate constants (per active Hatom) for H-atom abstraction from a series of Aromatic compounds by various radicals in solution phase.	134
5.7	Rate constants for the reaction of OH radicals with a series of methyl substituted benzenes at room temperature and at, or close to, the high pressure limit.	136
5.8	Rate constants for the reaction of OH radicals with a series of Halotoluenes at room temperature and at, or close to, the high pressure limit.	143
5.9	Calculated rate constants based on Electrophilic Substituent Constants versus experimental rate constants for reaction of OH with selected Aromatic compounds.	149
5.10	Calculated rate constants based on Ionisation Potentials versus experimental rate constants for reaction of OH with selected Aromatic compounds.	152
5.11	Room temperature rate constants and atmospheric lifetimes with Respect to reaction with the OH radical for the Aromatic compounds Studied in this work.	154

ABSTRACT

The results of a kinetic study on the reactions of hydroxyl radicals with selected aromatic compounds are presented in this thesis. Rate constants (in units $10^{-12} \text{ cm}^3 \text{ molecule}^{-1} \text{ s}^{-1}$) were obtained using a relative rate method for the following reactions at $298 \pm 2 \text{ K}$ and 1 atm. total pressure:

$k(\text{OH} + \text{toluene-}h_8) = 5.94 \pm 0.22$	$k(\text{OH} + 2\text{-fluorotoluene}) = 2.09 \pm 0.07$
$k(\text{OH} + \text{toluene-}d_8) = 5.77 \pm 0.07$	$k(\text{OH} + 3\text{-fluorotoluene}) = 4.40 \pm 0.07$
$k(\text{OH} + \text{ethylbenzene}) = 6.34 \pm 0.29$	$k(\text{OH} + 4\text{-fluorotoluene}) = 3.03 \pm 0.14$
$k(\text{OH} + \text{n-propylbenzene}) = 7.21 \pm 0.29$	$k(\text{OH} + 2\text{-chlorotoluene}) = 2.45 \pm 0.22$
$k(\text{OH} + \text{n-butylbenzene}) = 9.52 \pm 0.50$	$k(\text{OH} + 3\text{-chlorotoluene}) = 4.72 \pm 0.50$
$k(\text{OH} + \text{o-diethylbenzene}) = 12.47 \pm 0.43$	$k(\text{OH} + 4\text{-chlorotoluene}) = 3.46 \pm 0.43$
$k(\text{OH} + \text{indane}) = 23.86 \pm 1.88$	
$k(\text{OH} + \text{tetralin}) = 26.46 \pm 1.30$	
$k(\text{OH} + 1,2,4,5\text{-tetramethylbenzene}) = 51.57 \pm 3.4$	

Arrhenius parameters were determined using a relative rate method for the following reactions over the temperature range 243-323K and at 1 atm. total pressure:

OH + toluene	$k = 2.41 \times 10^{-12} \exp(269 \pm 24/T)$
OH + indane	$k = 21.6 \times 10^{-12} \exp(30 \pm 7/T)$
OH + tetralin	$k = 42.5 \times 10^{-12} \exp(-141 \pm 24/T)$
OH + 3-fluorotoluene	$k = 1.41 \times 10^{-12} \exp(314 \pm 13/T)$
OH + 3-chlorotoluene	$k = 2.22 \times 10^{-12} \exp(222 \pm 35/T)$

Rate constants for the reaction of chlorine atoms with indane and tetralin were obtained using a relative rate method at 298 ± 2 K and 1 atm. total pressure:

$$k(\text{Cl} + \text{indane}) = 2.28 \pm 0.18$$

$$k(\text{Cl} + \text{tetralin}) = 3.30 \pm 0.12$$

The results of this kinetic study show that there is a small but systematic increase in the reactivity of OH radicals towards monoalkyl substituted benzenes with increasing length of the alkyl side-chain, in contrast to previous investigations. Furthermore, the reactivity with OH radicals is greatly enhanced when the alkyl substituent is in the form of a saturated ring (indane and tetralin). It is proposed that this enhanced reactivity is due to a greater contribution from the abstraction pathway. This proposition is supported by the results of temperature dependant studies and reaction with chlorine atoms.

The presence of a fluorine or chlorine substituent on the aromatic ring (fluorotoluene and chlorotoluene isomers) results in a decrease in reactivity with OH radicals, relative to toluene, due to the negative inductive effect of the halogen. The fluorotoluenes are less reactive with OH radicals than the corresponding chlorotoluene isomers, consistent with electronegativity trends, while the position of the substituent on the ring has a measurable influence on the reactivity.

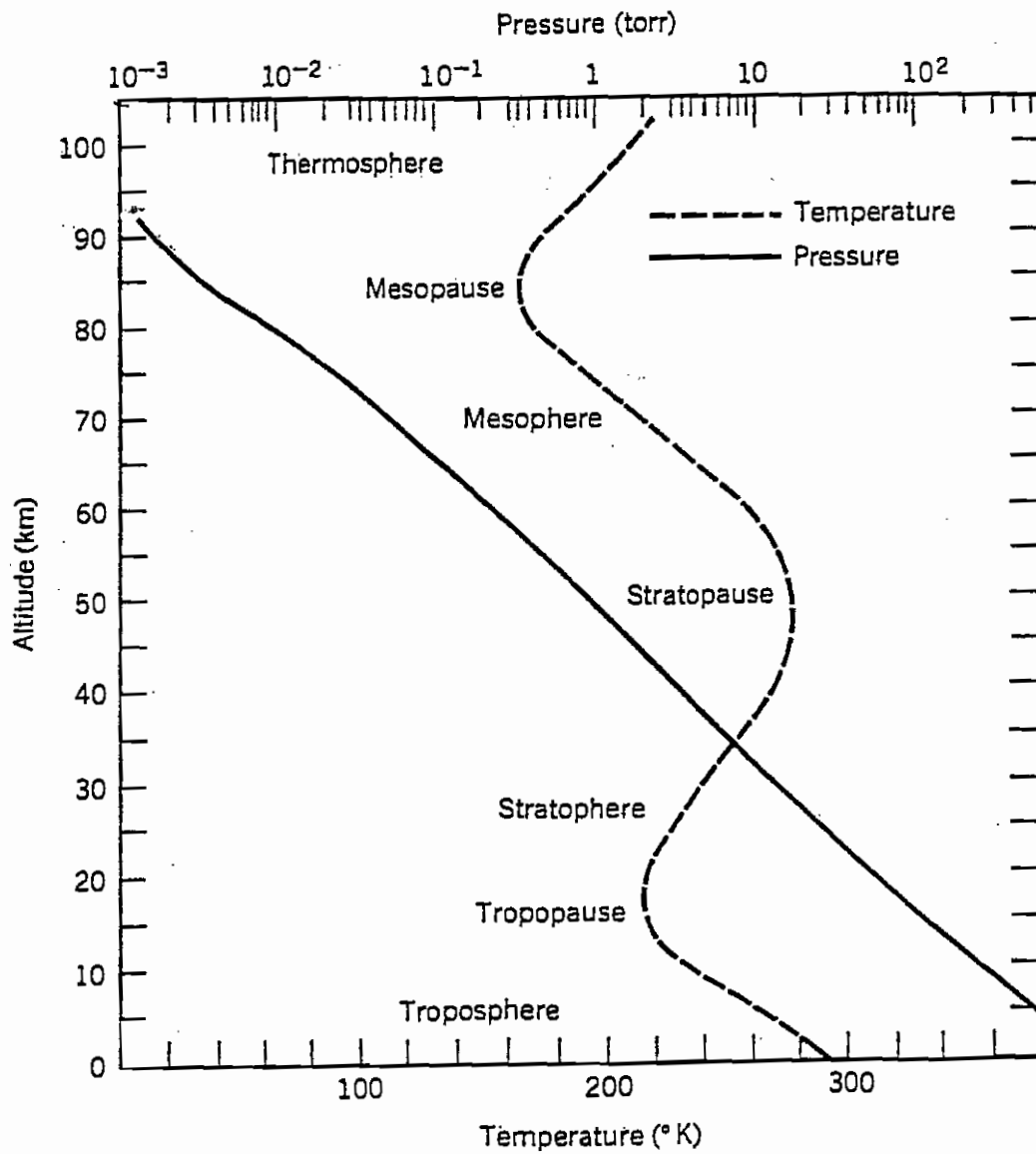
Finally, the contribution of these aromatic compounds to photochemical oxidant formation is assessed in terms of their atmospheric lifetimes.

1.0 GENERAL INTRODUCTION

Ever since the Earth was formed the chemical composition of the atmosphere has been evolving. It has now reached an equilibrium which can sustain life. The natural “unpolluted” atmosphere is made up almost entirely of nitrogen, oxygen, argon and water vapour. In the past few centuries the development of industry has led to an increase in man-made pollution which has disturbed the equilibrium and affected human health, ecosystems and climatic change. This chapter outlines the basic chemistry of the unpolluted and polluted atmosphere and emphasises the key species involved.

The atmosphere is divided into layers defined in terms of temperature. Figure 1.1 is a plot of average atmospheric temperature for mid-latitudes as a function of altitude together with the effect on pressure of increasing altitude. The pressure continually decreases with increasing altitude from 101 kPa at sea level to 10^{-3} kPa at about 100 km. The temperature steadily decreases with altitude up to ~15 km at a rate of about 6.5 K/km. Known as the troposphere, this region is an area of much interest to atmospheric chemists. From the tropopause (the top of the troposphere) the stratosphere extends for a further 50 km in altitude. Temperature increases with altitude in the stratosphere owing to the absorption of short-wavelength radiation by ozone. Above the stratopause, from 50 to 85 km, is the mesosphere over which the temperature decreases again with altitude down to 175 K where the atmosphere is at its coolest. The uppermost layer is the thermosphere which, together with the mesosphere, is sometimes known as the ionosphere. The chemistry of each of the layers is described in greater detail in the following section.

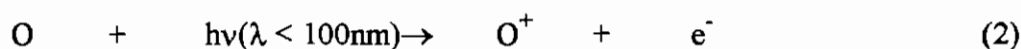
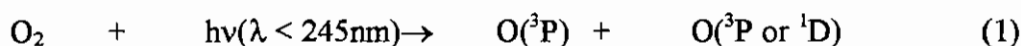
Figure 1.1 Regions of the atmosphere based on the temperature variation with altitude [47].



1.1 THE ATMOSPHERE

1.1.1 Thermosphere

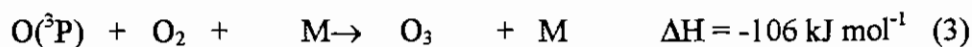
Photodissociation of molecular oxygen (reaction 1) and subsequent photoionisation (reaction 2) by ultra-violet photons takes place at very high altitudes:



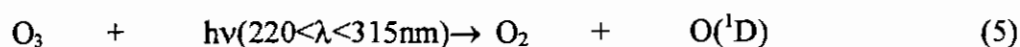
O^+ can react exothermally with both molecular oxygen and molecular nitrogen leading to a very high concentration of charged particles in the thermosphere (also known as the ionosphere) and also to the extremely high temperatures in this region (up to 1500 K at 300 km). Ultra-violet radiation becomes weaker in intensity with decreasing altitude and less photodissociation and photoionisation take place leading to a drop in temperature.

1.1.2 Mesosphere

The increased density in the mesosphere leads to a greater number of molecular collisions and thereby a greater complexity of reactions. There is photodissociation as in reaction (1) but in the mesosphere atomic oxygen reacts with molecular oxygen to form ozone:



M is typically N₂ or O₂ which acts as a third body stabilising the energy rich product from the highly exothermic bimolecular reaction. The density increases with decreasing altitude, hence there is a greater probability of collisions and thus greater concentrations of ozone are produced. A steady state concentration of ozone is maintained as it is formed by reaction (3) and destroyed by reactions (4) and (5):



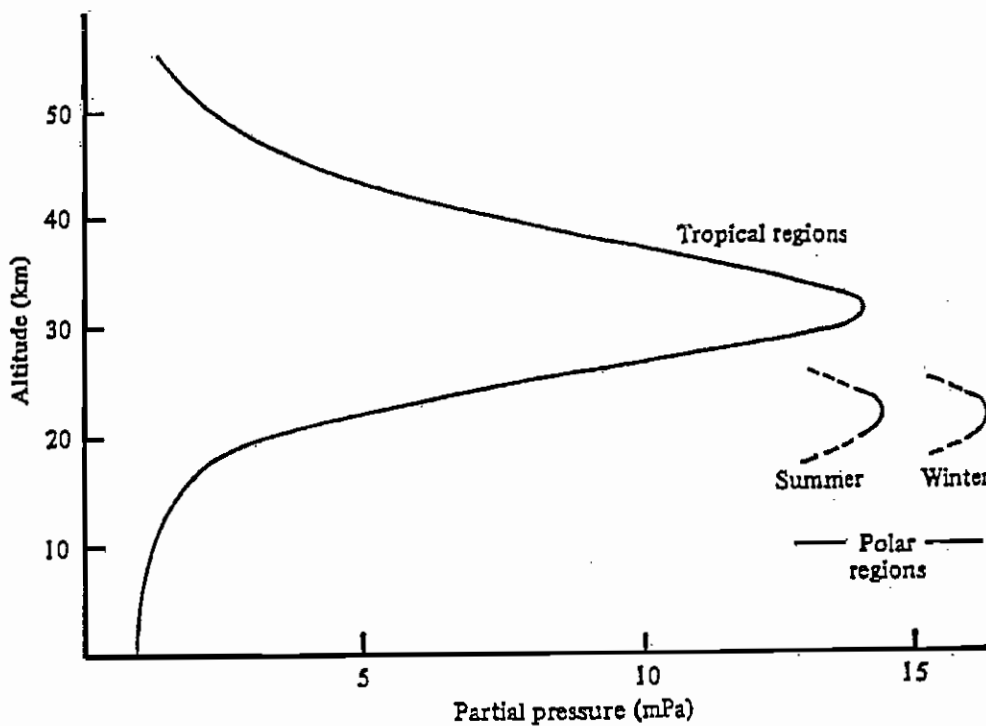
Reactions (3) and (4) are highly exothermic leading to the increase in temperature with decreasing altitude.

1.1.3 Stratosphere

The most important constituent in the stratosphere is ozone. Despite its very low concentration ozone is vital to life on earth as it prevents harmful ultra-violet radiation ($\lambda < 290\text{nm}$) from reaching the earth's surface. Ozone in the stratosphere is constantly being formed, destroyed and reformed during daylight hours through reactions (3), (4), and (5). Ozone is produced in the stratosphere because there is adequate UV-C from sunlight to dissociate some O₂ molecules and so produce oxygen atoms, most of which collide with other O₂ molecules and form ozone. The ozone in the stratosphere filters UV-B and UV-C from sunlight, but is destroyed temporarily by this process or by reaction with oxygen atoms. Ozone is not formed in this way below the stratosphere due to the lack of UV-C required to produce O atoms. Above the

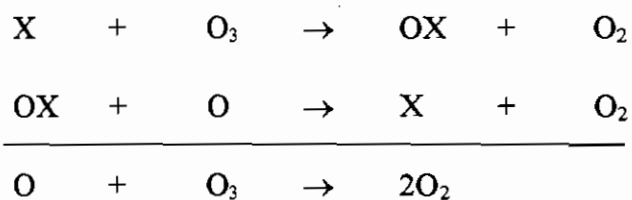
stratosphere, oxygen atoms predominate and usually collide with other oxygen atoms to form O_2 . The cyclic reaction mechanism of reactions (3), (4) and (5), involving only species derived from oxygen, was suggested by Chapman in 1930 [1] and is thus known as the Chapman cycle. As with the mesosphere, the gas density of the stratosphere increases with decreasing altitude leading to higher ozone concentrations at lower altitudes. The ozone concentration peaks at 25-30km and then falls off due to the absorption of the UV-C photons. Figure 1.2 shows a plot of the partial pressure of ozone as a function of altitude which demonstrates clearly the stratospheric ozone layer peaking at ~30km in tropical regions [2].

Figure 1.2 Plot of the partial pressure of ozone as a function of altitude for the tropical regions [2].



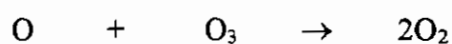
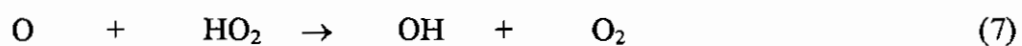
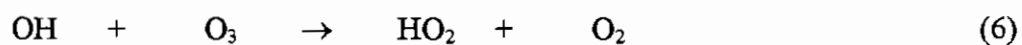
More recently it has been shown that the destruction of ozone and ozone precursors in the stratosphere is not only caused by reactions (4) and (5). The Chapman mechanism accounts for about 20% of the total natural destruction rate for stratospheric ozone.

These alternate ozone destruction schemes take the general form:

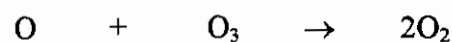
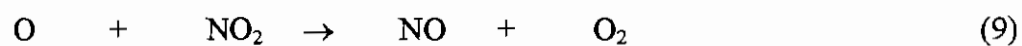
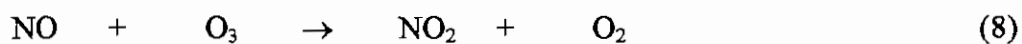


where $X = H, OH, NO, Cl$.

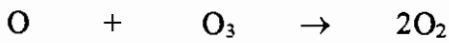
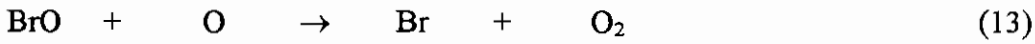
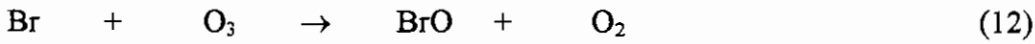
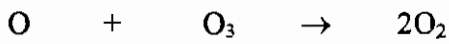
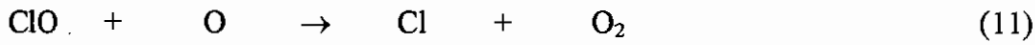
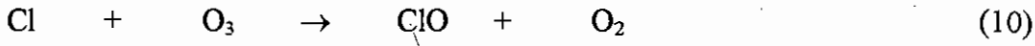
For example the reaction of ozone with hydrogen containing species (HO_x):



The oxides of nitrogen, NO and NO_2 (i.e. NO_x) provide a similar destructive process for ozone:



Compounds other than NO_x and HO_x may also cause the destruction of stratospheric ozone. Most notable of these are atomic chlorine (Cl) and atomic bromine (Br):



Different halocarbons undergo dissociation at different wavelengths and those photolysed at shorter wavelengths must reach higher altitudes in the stratosphere to be photodissociated. For example, atom for atom bromine is potentially far more destructive towards stratospheric ozone than chlorine. This is primarily due to the fact that photolysis of bromine compounds occurs lower in the atmosphere where ozone concentrations are greatest. Estimates of the catalytic activity of Br relative to that of Cl range from 10 to 50 [3]. Similarly, the chlorine compounds are photolysed at lower altitudes than fluorine compounds causing more ozone destruction.

Phase-out of production of chlorofluorocarbons (CFCs) began in 1987 with the Montreal protocol [4]. Production in 1989 of the main CFCs (CFCl_3 , CF_2Cl_2 , $\text{CF}_2\text{ClCFCl}_2$, $\text{CF}_2\text{ClCF}_2\text{Cl}$ and CF_2ClCF_3) was frozen at the 1986 level. This target was reduced further in 1994 to 80% of the 1986 level and a further reduction to 50% was

expected in 1999. However, due to increased concern over the health risks involved the production of CFCs has currently ceased in EU member states on the order of the European Union Regulation (EC) No. 3093/94. The protocol allows for substitution of halocarbons as long as the total ozone depletion potential remains unchanged. Substitution of brominated compounds for non-brominated compounds is not permitted.

In recent years there has been an increase in the use of the hydrofluorocarbons (HFCs) and hydrochlorofluorocarbons (HCFCs) as possible replacements for CFCs. As HFCs and HCFCs are still halocarbons they retain many of the desirable properties of the CFCs but because they contain hydrogen they degrade in the lower atmosphere. This results in shorter atmospheric lifetimes and reduces their contribution to global warming. However, as HCFCs have a potential for ozone depletion, they are termed "transitional substances" by the Montreal protocol and are due to be phased out by 2030. HFCs have no potential for ozone destruction as they contain no chlorine or bromine.

1.1.4 Troposphere

The troposphere is the layer of the atmosphere that is the nearest the earth's surface (0-15km). It contains the air that supports all life on earth and thus a knowledge of the chemical composition and factors that may perturb the chemical balance is of vital importance. The troposphere contains ~ 90% of the total atmospheric mass and as such contains the bulk of anthropogenic and biogenic emissions leading to a complex array of chemical transformations. The chemical composition of the natural troposphere

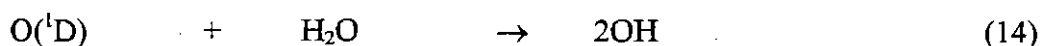
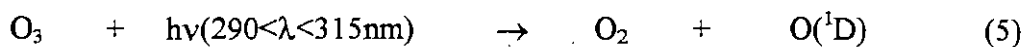
is made up almost entirely of nitrogen, oxygen, noble gases and water vapour as shown in Table 1.1.

Beneath the tropopause the natural production of ozone ceases in the absence of the ultra-violet light ($\lambda < 245\text{nm}$) required to produce atomic oxygen. While ozone in the stratosphere is vital for life on earth, its presence in the troposphere is considered a major pollutant and is used as one of the criteria for the presence of photochemical smog. The two main sources of ozone in the natural troposphere are:

- *Injection from the stratosphere.* Concentrations of stratospheric ozone are relatively high compared to tropospheric concentrations. Transport of air masses between the stratosphere and troposphere is inhibited by the temperature inversion at the tropopause. However, during unusual weather conditions this inversion may be “relaxed” as a result of *tropopause folding* and *wave driven pumping*, leading to transport of ozone from the stratospheric ozone layer.
- *Photochemical production of ozone in the presence of NO_x , CH_4 and sunlight.* Photochemical reactions in the troposphere involve mainly absorption of near UV and visible radiation ($290 < \lambda < 400\text{nm}$). The reaction that initiates daytime tropospheric chemistry is the photolysis of ozone to yield electronically excited oxygen atoms ($\text{O}({}^1\text{D})$) which react with water vapour to generate hydroxyl radicals:

Table 1.1 Average percentage of main tropospheric constituents under clean air conditions [5].

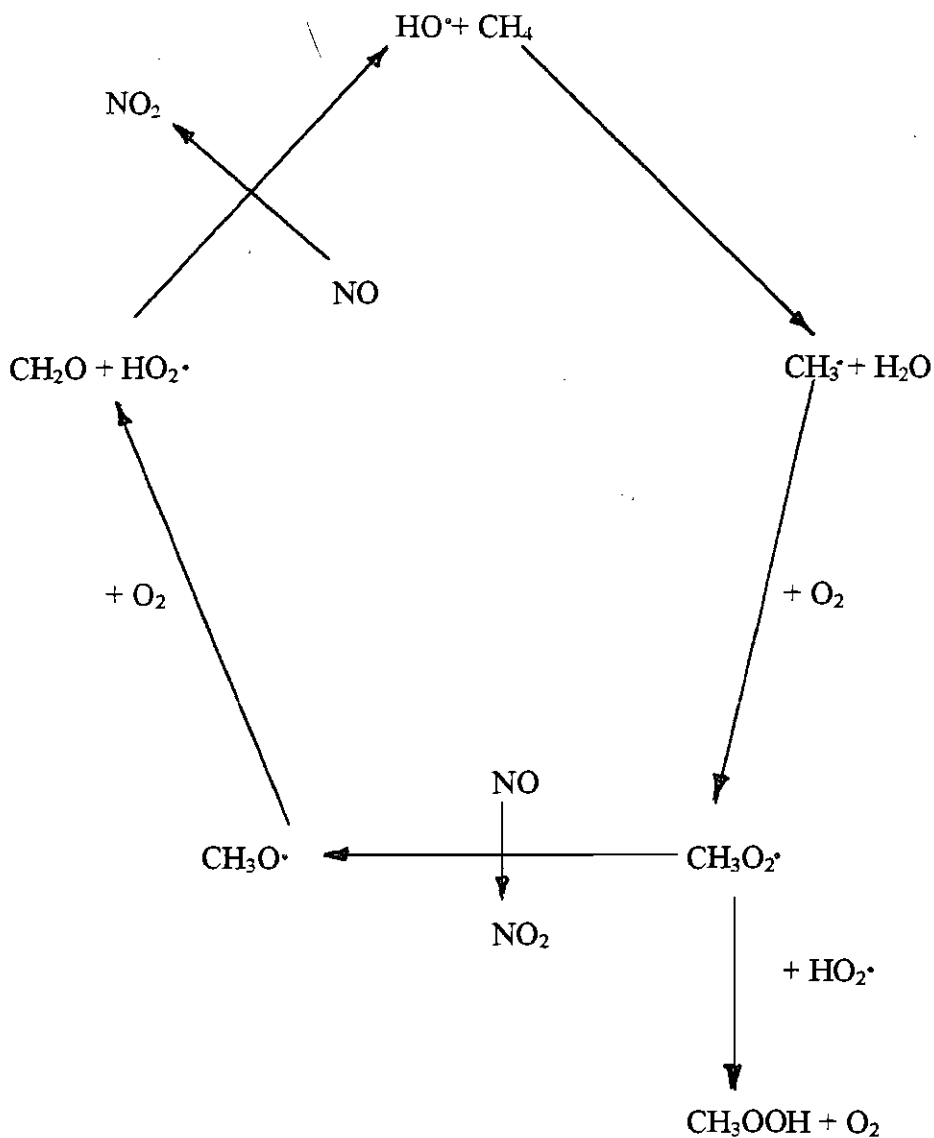
Gas	Mean percentage
Nitrogen (N ₂)	78
Oxygen (O ₂)	21
Argon (Ar) and other noble gases	0.9
Water vapour (H ₂ O)	0 – 3
Carbon dioxide (CO ₂)	0.035
Methane (CH ₄)	0.00017
Hydrogen (H ₂)	0.00006
Nitrous oxide (N ₂ O)	0.000033
Carbon monoxide (CO)	4 – 20 x 10 ⁻⁶
Ozone (O ₃)	1 – 5 x 10 ⁻⁵
Ammonia (NH ₃)	10 ⁻⁶ – 10 ⁻⁸
Sulphur dioxide (SO ₂)	10 ⁻⁵ – 10 ⁻⁷
Nitrogen oxides (NO _x)	10 ⁻⁵ – 10 ⁻⁸



Hydroxyl radicals are highly reactive towards a wide range of volatile organic compounds (VOCs), with the exception of CFC's and provide a very efficient mechanism for the scavenging of the majority of both biogenic and anthropogenic emissions to the troposphere.

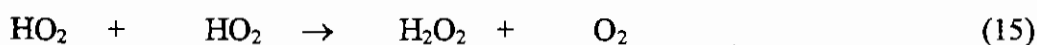
Figure 1.3 shows the cyclic mechanism for the reaction of methane with OH radicals to form formaldehyde with the consequent oxidation of NO to NO₂ and regeneration of OH. H-atom abstraction from CH₄ by OH leads to the formation of a methyl radical (CH₃) and water. Under atmospheric conditions the methyl radical reacts rapidly with molecular oxygen to form a methylperoxy radical (CH₃O₂). The fate of the methylperoxy radical depends on the ambient levels of NO_x. At NO_x concentrations ≤20ppt the chain is terminated by reaction of the methylperoxy radical with a hydroperoxy radical to form methylhydroperoxide, which undergoes wet deposition. At higher concentrations of NO_x (≥ 20ppt) the methylperoxy radical oxidises NO to NO₂ and forms a methoxy radical (CH₃O).

Figure 1.3 Reaction pathway for the oxidation of Methane in the troposphere.

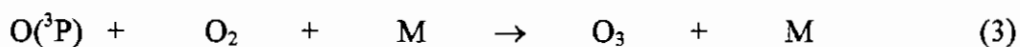
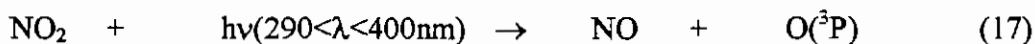


The methoxy radical reacts with molecular oxygen to form the primary oxidation product, formaldehyde, and a hydroperoxy radical (HO₂). This hydroperoxy radical oxidises another molecule of NO to NO₂ and recycles the OH radical. The main fate of formaldehyde is photolysis to form CO and HO₂ radicals with a small fraction undergoing a similar oxidation pathway to that described above after reaction with OH.

This chain reaction may be terminated by:



As in the stratosphere and mesosphere NO_x is of central importance to the chemistry of the troposphere. Photolysis of NO₂ (reaction 17) followed by reaction (3) is the only known anthropogenic source of ozone in the troposphere:



Consequently, any increase in ozone precursor emissions i.e. VOCs and NO_x is of major concern since it will result in enhanced levels of photochemical oxidants.

1.2 THE POLLUTED TROPOSPHERE

Over the past 50 years there has been growing concern about increasing pollution levels and the deterioration in the condition of the earth's atmosphere. The depletion of the ozone layer and increased incidences of both sulphurous and photochemical smog have led to a greater awareness about chemical air pollution. This has resulted in a more widespread interest in research on the physical and chemical transformations of pollutants in the atmosphere.

One of the main classes of pollutants emitted to the atmosphere are VOCs which are important precursors in the photochemical production of tropospheric ozone. A strict definition of a VOC is any organic compound that may exist in the vapour phase at atmospheric temperatures, but in general the term VOC refers to any gaseous organic compound in the atmosphere. VOC emissions arise from both natural (biogenic) and man-made (anthropogenic) sources. Estimates of ~100 million tonnes per year of anthropogenic VOCs are released into the atmosphere with ~ 1000 million tonnes per year from biogenic sources [5,6]. Listed in Table 1.2 are the total VOC (excluding methane) emissions for the 15 member states of the EU for the years 1985, 1990 and 1994 [7]. The data shows a reduction in VOC emissions in most European countries, with the exception of Greece, Italy and Portugal, between 1990 and 1994 with a consequent reduction in total European emissions over the same period.

Anthropogenic sources of VOCs include vehicle exhaust emissions, evaporation of petrol and diesel fuels, solvent evaporation and emissions from industrial processes and oil refining. Biogenic sources include the emissions from plants, trees, animals and

anaerobic processes in bogs and marshes. VOCs and their reaction products are increasingly regarded as posing an unacceptable risk to public health as well as to the biological and physical environments.

Extensive research has been carried out on the behaviour of selected VOCs in the body after oral, dermal or inhalatory exposure together with the toxic effects caused via the different routes [8 and references therein]. These studies have identified high risk VOCs responsible for both short and long term toxicity in humans such as carcinogenicity, genotoxicity, reproductive toxicity, and affects on the nervous, immune, cardiovascular and endocrine systems.

Once emitted VOCs may undergo several different processes in the atmosphere:

- **Dispersion** accounts for all diffusion and transport processes caused by turbulence and circulation of air masses and may be responsible for substantial dilution of emissions.
- *Physical transformations such as condensation into particles, adsorption onto surfaces or solution into water droplets i.e. any process that removes the VOC from the gaseous phase.*
- **Deposition** is the process that transfers VOCs into soils etc. (dry deposition) or waters (wet deposition) by sedimentation.
- **Chemical reactions** which convert VOCs into organic and/or inorganic products which in turn may undergo any of the above processes.

Table 1.2 VOC emissions by country in kTonnes for the member states of the EU in 1985, 1990 and 1994 [7].

Country	1985	1990	1994
Austria	400	418	358
Belgium	407	332	320
Denmark	198	175	156
Finland	210	209	190
France	2393	2393	2308
Germany	3290	3155	2153
Greece	155	293	362
Ireland	102	102	93
Italy	1850	2080	2239
Luxembourg	20	19	17
Netherlands	463	420	375
Portugal	199	202	227
Spain	1265	1051	1120
Sweden	553	526	459
UK	2439	2623	2354
Total	13944	13998	12731

In recent years evidence has surfaced to suggest that concentrations of tropospheric ozone are influenced by human activity. Pittcock [9] observed that concentrations of ozone are greater at mid-latitudes of the northern hemisphere than at corresponding latitudes in the southern hemisphere. Similarly, Logan [10] has shown that the major source of ozone in both Europe and North America is from anthropogenic sources. These observed increases over the relatively more industrialised areas compared to the less industrialised areas of Africa, Asia and South America is believed to be due to increased emissions of the ozone precursors NO_x and VOCs.

Ozone plays an important role in controlling the chemical composition of the troposphere since it is the source of hydroxyl radicals, the major daytime scavengers of trace species in the troposphere. An increase in ozone concentration is significant for a number of reasons:

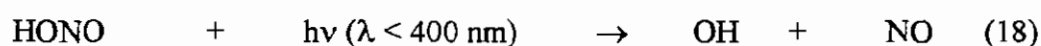
- (i) Ozone is important in maintaining the climate of the troposphere. A doubling of tropospheric ozone may lead to an increase in surface temperatures of $\sim 0.9 \text{ K}$ [11].
- (ii) Ozone is known to induce changes in cells and fluids of the respiratory tract causing alterations in the mechanical functions of the lungs. This leads to coughing, shortness of breath and respiratory pains in humans [12].
- (iii) Field studies have shown that yields of agricultural crops decrease as tropospheric ozone increases with reductions of 6 – 8 % per 10ppb of ozone [13].
- (iv) Increased levels of tropospheric ozone may have contributed to the observed forest decline in Europe and the U.S. [14].

The detrimental effects of ozone as listed above were initially observed in Los Angeles in the mid-twentieth century. Once the precursors of ozone had been identified, possible control strategies and air quality standards for these precursors (primary pollutants) and ozone itself (a secondary pollutant) were devised. In 1992 the European Union introduced emission reduction targets for VOCs and NO_x of a 30% reduction by the year 2000 from the 1990 emission levels in order to reduce tropospheric ozone concentrations. The health effects of ozone on both plants and animals has led to very stringent air quality standards by both the EU and the World Health Organisation (WHO). The ozone thresholds from the European Council directive 92/72/EEC and WHO air quality guidelines are given in Table 1.3.

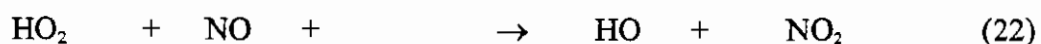
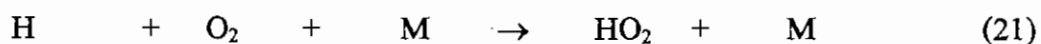
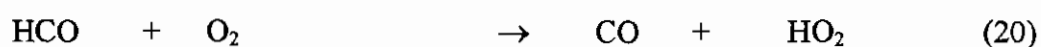
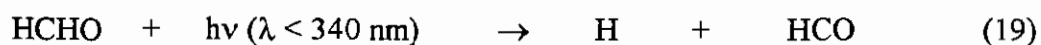
Table 1.3 European Union and World Health Organisation population information and vegetation concentration thresholds for Ozone.

Parameter	Threshold ($\mu\text{g}/\text{m}^3$)
1 hour average EU population information	180
1 hour average EU vegetation protection	200
1 hour average EU population warning	360
Fixed 8 hour EU health protection	110
24 hour average EU vegetation protection	65
8 hour average WHO health protection guideline	120

When VOCs are mixed with nitrogen oxides and irradiated with sunlight ($290 < \lambda < 400\text{nm}$) a complex chain of free radical reactions leads to the formation of secondary photochemical pollutants, e.g. ozone, aldehydes, hydrogen peroxide, peroxyacetyl nitrate (PAN), organic and inorganic acids and fine particles, collectively known as photochemical smog. The oxidation sequence for non-methane hydrocarbons (NMHCs) parallels that of methane in the clean troposphere. Oxidation begins by reaction with OH radicals which are generated by photolysis of ozone (reaction 5) followed by reaction with water vapour (reaction 14). Other sources of OH radicals in the polluted troposphere include the photolysis of nitrous acid (HONO):



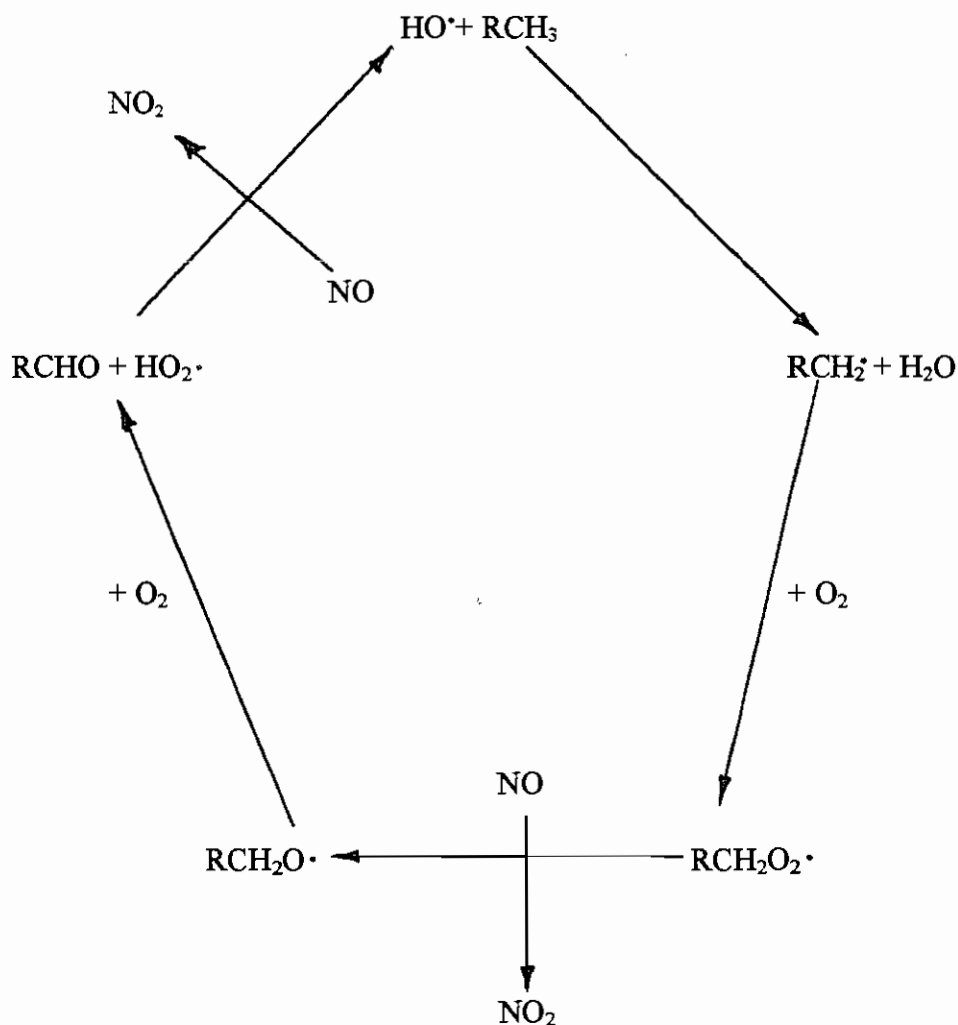
and photolysis of formaldehyde (HCHO):



The reaction pathway for the oxidation of saturated VOCs by OH radicals is summarised in Figure 1.4 where RCH_3 denotes any saturated organic with an abstractable hydrogen. Oxidation begins with abstraction of a H-atom by OH radicals to form water and an alkyl radical (RCH_2). The alkyl radical then reacts with molecular oxygen to form the peroxy radical (RCH_2O_2). At the concentrations of NO_x present in

the polluted atmosphere peroxy radicals react rapidly with NO to form NO₂ and an alkoxy radical (RCH₂O). The alkoxy radical again reacts with molecular oxygen to form the primary oxidation product, a carbonyl compound and a hydroperoxy radical (HO₂).

Figure 1.4 Generalised scheme for reaction of OH radicals with saturated VOCs (RCH₃) in the troposphere.



Finally the hydroperoxy radical oxidises NO to NO₂ with regeneration of OH. The NO₂ formed in this reaction sequence may then form ozone via reactions (17) and (3). The net result of this cycle is that for every molecule of organic reacted, two molecules of NO are oxidised to NO₂, and hence two O₃ molecules formed. The carbonyl compound formed will undergo further oxidation by OH and/or photolysis leading to further NO oxidation. The peroxy radicals formed easily convert NO to NO₂ at ambient concentrations where the thermal oxidation of NO by O₂ is negligible. The atmospheric relevance of this reaction sequence is that there is a mechanism for oxidation of NO to NO₂ which does not involve the loss of ozone during daylight hours.

1.3 PHOTOCHEMICAL OZONE CREATION POTENTIAL (POCP)

It has been established in *Section 1.2* that all VOCs (with the exception of CFCs) in the presence of NO_x and ultra-violet light produce ozone. However, not all VOCs emitted to the atmosphere contribute equally to ozone formation. Each hydrocarbon has to compete against other hydrocarbons for OH radicals to form the peroxy radicals which are necessary to create ozone. The potential that each VOC has for ozone production depends on two key steps in the reaction mechanism shown in Figure 1.4. The first step determines how fast the peroxy radical is formed after reaction of OH with the VOC. This is determined by the intrinsic reactivity of the VOC towards OH, a parameter which can be experimentally measured. The second series of steps relate to the number of molecules of NO oxidised to NO_2 per molecule of VOC reacted which may be affected by the presence of sinks for NO_x such as the formation of organic nitrates and peroxy acetyl nitrate (PAN) as well as other reaction channels for the alkoxy radical such as decomposition and isomerisation.

In recent years a number of studies have been carried out to quantify the photochemical ozone creation potentials of various VOCs. Hough and Derwent [15] have used computer model simulations to determine the contribution of 37 VOCs to ozone formation. Carter and Atkinson have developed an incremental reactivity scale for VOCs with respect to ozone formation based on both experimental studies [16] and computer model simulations [17]. The incremental reactivity is defined as the amount of ozone formed per unit VOC added or subtracted from the VOC mixture in a given air mass. The incremental reactivity scale has been further refined by Carter [18,19] and Bowman and Seinfeld [20,21].

Derwent and Jenkin [22] have also formulated a reactivity scale which describes the ozone forming potential of each VOC per unit mass emission; known as the Photochemical Ozone Creation Potential or POCP. Derwent and Jenkin [22] define the POCP by subtracting the emissions of a particular VOC from a 69 component mixture using photochemical model calculations and then expressing the POCP as the change in ozone concentration when the emissions of that particular VOC are set to zero in the photochemical model calculation. The POCP values of the 69 VOCs are stated relative to ethene (ethylene) which is used as a reference due to its medium reactivity with the OH radical. The POCP scale has been further developed by Andersson-Skold *et al* [23] and Derwent *et al* [24].

Table 1.4 presents the POCP of each VOC from the trajectory model of Derwent and Jenkin [22]. Each value is normalised relative to the corresponding value for ethene, which is assigned a value of 100. In general, the POCP values for alkanes lie between 30-50 except for methane and ethane which are considerably lower. The apparent lack of a positive correlation between POCP value and reactivity towards OH would suggest that the POCP value is not simply a function of the OH radical rate constant. The branching in the higher alkanes appears to be significant and Derwent [22] states that the more stable intermediates formed in the degradation pathway of branched alkanes will reduce the potential to form ozone as it will reduce the number of peroxy radicals available to oxidise NO to NO₂.

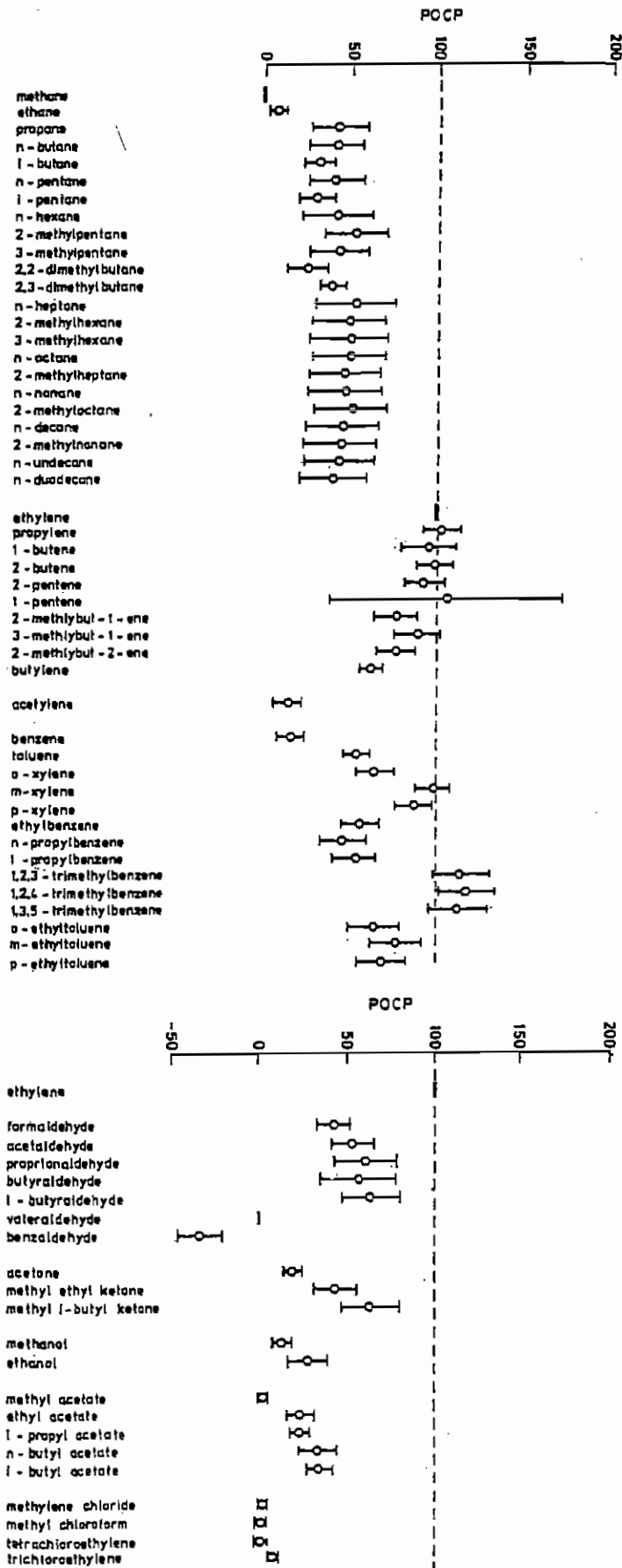
The POCPs of the alkenes are within the range 60-110 but show a tendency to decrease with increasing carbon number, in contrast to their reactivity towards OH radicals. The decrease in POCP with increasing size of the alkene can be attributed to

the increase in stability of the aldehydes and ketones formed in the degradation pathway. Relative to formaldehyde, formed from ethylene, longer chain aldehydes and ketones photolyse more slowly while reaction with OH becomes more important. Whereas reaction of OH with aldehydes or ketones maintains the number of free radicals, photolysis increases the steady state free radical concentration and therefore stimulates ozone production.

The POCPs of aromatic hydrocarbons lie within the range 50-120, with the exception of benzene which has a POCP of 20 due to its relatively low reactivity towards the OH radical. Alkylation of the benzene ring with methyl groups greatly enhances the reactivity towards OH and therefore has a dramatic influence on the POCP with the trimethylbenzenes displaying the highest POCPs. The presence of longer chain alkyl substituents such as ethyl and n-propyl result in significantly lower POCPs due to increasing stability of the α -dicarbonyls formed in aromatic degradation.

The aldehydes have similar POCPs to the corresponding alkanes and lie in the range 40-70. These relatively low POCPs, in contrast to their high OH reactivities, derives from the fact that OH oxidation is in competition with photolysis. Photolysis acts as a source of free radicals which stimulates ozone production, whereas OH oxidation forms PAN via the peroxyacyl radical. PAN acts as a sink for NO_x and hence reduces ozone formation. While this competition is relevant to the aliphatic aldehydes, benzaldehyde does not undergo photolysis and as a result has a negative POCP. The three ketones show a wide range of POCPs, 20-70, and are also similar in magnitude to the corresponding alkanes.

Table 1.4 The POCPs for the 69 VOCs studied by Derwent and Jenkin [22] showing the mean and standard deviation for each VOC relative to ethene.



The two alcohols studied have very low POCPs reflecting the relatively low reactivity of alcohols with OH. The OH oxidation products (formaldehyde from methane and acetaldehyde from ethane) are readily photolysed to produce free radicals but this does not significantly increase the POCPs of the alcohols due to their low reactivities. The esters have similar POCPs to the alcohols with values in the range 20-45. Finally the chlorocarbons have POCP values close to zero as they are extremely unreactive towards the OH radical. However, low reactivity with the OH radical means that the chlorocarbons may be transported to the stratosphere where they have high stratospheric ozone depletion potentials.

In subsequent work Derwent et al [24] used the POCP concept in computer simulations to assess the contribution of certain organics to ozone formation in Europe in 1995. Table 1.5 shows UK emissions by solvent type coupled with their POCP-weighted emissions. Aromatics appear to be the most important class of ozone producing compounds, despite having a lower emission total *than the alkanes*. Halocarbons show the least capacity to produce ozone despite having a substantial total mass emission.

These POCP results are designed to help in the construction of targeted hydrocarbon control strategies with respect to ozone formation and the values obtained in these studies indicate that aromatic compounds are the most important class of hydrocarbon precursors to ozone formation. The halocarbons have the lowest POCP but the stratospheric ozone depletion potentials of halocarbons restricts their large scale use as solvents. The oxygenated solvents (alcohols and ethers) appear to offer an acceptable

atmospheric alternative to aromatics due to their relatively low POCP values and hence have been the subject of considerable interest in industry in recent years.

Table 1.5 Emissions and POCP-weighted emissions for each hydrocarbon type [24].

Hydrocarbon type	Emission (kT yr ⁻¹)	POCP-weighted emission (kT yr ⁻¹)
Aromatics	195	185
Alkanes	220	137
Ketones	74	43
Alcohols and Ethers	142	78
Esters	35	14
Halocarbons	79	3

Table 1.6 provides the total emissions and POCP-weighted emissions for each of the source categories of VOCs. Although solvent usage has the largest total emission of any source category it has only the fourth largest POCP-weighted emission. This is because motor vehicle exhaust emissions are more reactive, contributing relatively more to ozone formation per unit mass emitted.

Table 1.6 Emissions and POCP-weighted emissions for the main source categories of hydrocarbons in the atmosphere [24].

Source Category	Emission (kT yr ⁻¹)	POCP-weighted emission (kT yr ⁻¹)
Petrol exhaust	652	78
Petroleum refining	134	62
Petrol evaporation	143	61
Solvent usage	787	59
Stationary combustion	56	49
Diesel exhaust	175	44
Industrial and residential waste	3	28
Natural gas leakage	34	26
Chemical processes	200	21

In summary, aromatic compounds are important precursors to ozone formation and are also known to play a significant role in the formation of secondary organic aerosol. The reactivity of aromatics in the atmosphere combined with an understanding of their oxidation mechanisms has long been cited as critical for modelling of chemical transformations in the troposphere.

2.0 INTRODUCTION TO AROMATIC COMPOUNDS

2.1 AROMATIC COMPOUNDS

2.1.1 Aromatics in Fuel

A large source of aromatic compounds in urban air comes from petrol through both evaporation and exhaust emissions. Consequently the high POCP values for aromatics lead to the high POCP weighted emission for petrol exhausts as shown in Table 1.6. Petrol contains a variety of hydrocarbons depending on legislation and engine requirements, both of which are discussed in greater detail below. A typical hydrocarbon composition of petrol is given in Table 2.1, which shows aromatics making up 35% of the hydrocarbon content.

Table 2.1 Typical % hydrocarbon composition of petrol [25].

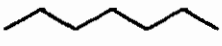
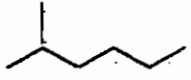
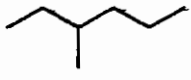
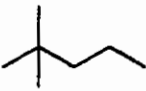
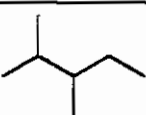
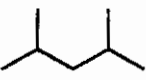
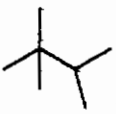
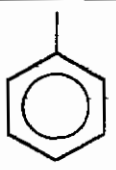
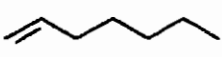
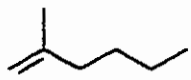
Hydrocarbon	Typical % hydrocarbon composition
n-alkanes	15
<i>Iso</i> -alkanes	30
Cycloalkanes	12
Aromatics	35
Olefins	8

The formulation of petrol has developed over the past century with the problem of engine knock (detrimental effects to the pistons and cylinder head) and engine performance having the greatest effect on motor fuel composition. When fuels were formulated to raise the engine compression ratio in order to increase performance and fuel economy,

knocking tendency increased. In 1926 Graham Edgar developed the octane scale which determined the knock intensity of organics in a standard engine. Using two reference fuels, n-heptane (octane quality zero) and isooctane (octane quality 100) Edgar determined octane numbers for a series of organic compounds in petrol. A list of hydrocarbons containing 7 carbon atoms and their research octane numbers (R.O.N.) are shown in Table 2.2, where it is clear that molecular structure of the compound has a definite affect on the octane number.

The octane rating of the fuel reflects the ability of the unburnt end gases to spontaneously ignite under specified test conditions. During the oxidation of a hydrocarbon fuel, hydrogen atoms are abstracted from the molecule by radical species. Straight chain alkanes like n-heptane have secondary C-H bonds which are much easier to break than the primary C-H bonds of isooctane and aromatic C-H bonds. Hence, branched aliphatic and aromatic hydrocarbons are more resistant to oxidation and therefore have higher octane numbers. As a result these branched hydrocarbons, and particularly aromatics, became highly desirable in motor fuels. However, as outlined in the *General Introduction*, the high POCP values of C₇ to C₁₀ aromatics has resulted in high levels in fuel becoming unacceptable for environmental reasons. Combined with this is the concern over the presence of benzene, a known carcinogen. EU directive 98/70/EC proposes a decrease in the benzene content of petrol from 5%(v/v) to 2%(v/v) and a reduction in the total aromatic content from 45% to 42% by the 1st January 2000, with a view to a further possible reduction to 35% by the year 2005.

Table 2.2 Structures and Research Octane Numbers (R.O.N.) for a series of hydrocarbons containing 7-carbon atoms [26].

Hydrocarbon	Structure	Research Octane Number (R.O.N.)
n-heptane		0.0
2-methylhexane		42.4
3-methylhexane		52.0
2,2-dimethylpentane		92.8
2,3-dimethylpentane		91.1
2,4-dimethylpentane		83.1
2,2,3-trimethylbutane		112.0
toluene		120
1-heptene		54.5
2-methyl-1-hexene		90.7

As an alternative to aromatics in motor fuel much research has focused on the use of oxygenates (in particular alcohols and ethers) which have high octane numbers, as shown in Table 2.3 for the more commonly used oxygenates, but considerably lower POCP values. Besides the low POCP values and high octane numbers, the presence of an oxygen atom in the molecule means alcohols and ethers have a low inherent tendency to form smoke which makes them highly desirable fuel additives. However, both methanol and ethanol are miscible in water and may be lost in the combustion product, hence the higher molecular weight alcohols and ethers are more desirable.

Table 2.3 Structures and Research Octane Numbers (R.O.N.) of the most frequently used oxygenates in motor fuel [26].

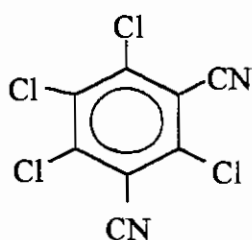
Oxygenate	Structure	Research Octane Number (R.O.N.)
Methanol	$\text{CH}_3\text{—OH}$	122
Ethanol	$\text{CH}_3\text{—CH}_2\text{—OH}$	121
t-butanol	$\begin{array}{c} \text{CH}_3 \\ \\ \text{CH}_3\text{—C—OH} \\ \\ \text{CH}_3 \end{array}$	106
methyl t-butyl ether (MTBE)	$\begin{array}{c} \text{CH}_3 \\ \\ \text{CH}_3\text{—C—O—CH}_3 \\ \\ \text{CH}_3 \end{array}$	115
t-amyl methyl ether (TAME)	$\begin{array}{c} \text{CH}_3 \\ \\ \text{CH}_3\text{—C—CH}_2\text{—O—CH}_3 \\ \\ \text{CH}_3 \end{array}$	108

Combined with the high POCP values of aromatics is the fact that the aromatic fraction of petrol contains benzene, a known carcinogen. It is estimated that the overall benzene concentration in leaded petrol is ~2.7% (v/v) with unleaded being slightly higher at 3.3% (v/v) and super unleaded close to 5% (v/v) [27]. Results published by the UK Transport Committee in 1994 showed that a catalytic converter virtually eliminates all traces of benzene from the exhaust gas when using unleaded petrol, while it was also stated that using unleaded petrol in a car not fitted with a catalytic converter resulted in higher benzene emissions than those using leaded fuel [28]. European legislation requires that all cars manufactured since 1995 must be fitted with a catalytic converter, and that the sale of leaded petrol be eliminated by the end of the century.

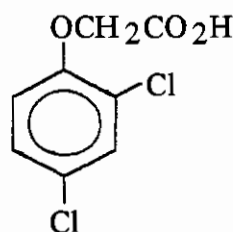
2.1.2 Aromatics in Industry

Alkylated aromatics e.g. toluene and the xylenes are widely used as industrial solvents while halogenated aromatics are used in several areas of the chemical and pharmaceutical industry. For example, benzyl chloride is a raw material in the synthesis of phenobarbital, benzedrine and demerol. Organohalogens (particularly organochlorines) are widely used in crop protection by 90% of grain farmers in the EU and US.

Examples include:



Daconil (fungicide)



2,4-Dichlorophenoxyacetic acid (herbicide)

Aromatic fluorine intermediates (AFIs) are widely used in chemical synthesis due the mobile nature of the fluorine atom in synthetic reactions.

Although considerable research has been carried out on the atmospheric chemistry of alkylated aromatics [29] the chemistry of halogenated aromatics in the atmosphere is relatively unknown and their presence in ambient air may be a cause for concern.

2.1.3 Toxicology of Aromatics

Benzene is a known carcinogen and its toxicity involves both bone marrow depression and leukemogenesis caused by damage to multiple classes of hematopoietic cell functions.

Study of the relationship between the metabolism and toxicity of benzene indicates that several metabolites of benzene play significant roles in generating benzene toxicity.

Benzene is metabolised, primarily in the liver, to a variety of hydroxylated and ring-opened products, (shown in Figure 2.1) that are transported to the bone marrow. As benzene is

more fat than water soluble it is further metabolised in the fatty tissue of the bone marrow.

Initially benzene is oxidised by cytochrome P450 which is found in both the liver and the bone marrow. The intermediate product is benzene oxide which either rearranges

spontaneously to phenol or can be hydrolysed enzymatically to benzene dihydrodiol, a precursor of catechol which can either form the ring cleavage product trans,trans-

mucanaldehyde and then trans,trans-muconic acid or be excreted in the urine. Phenol is

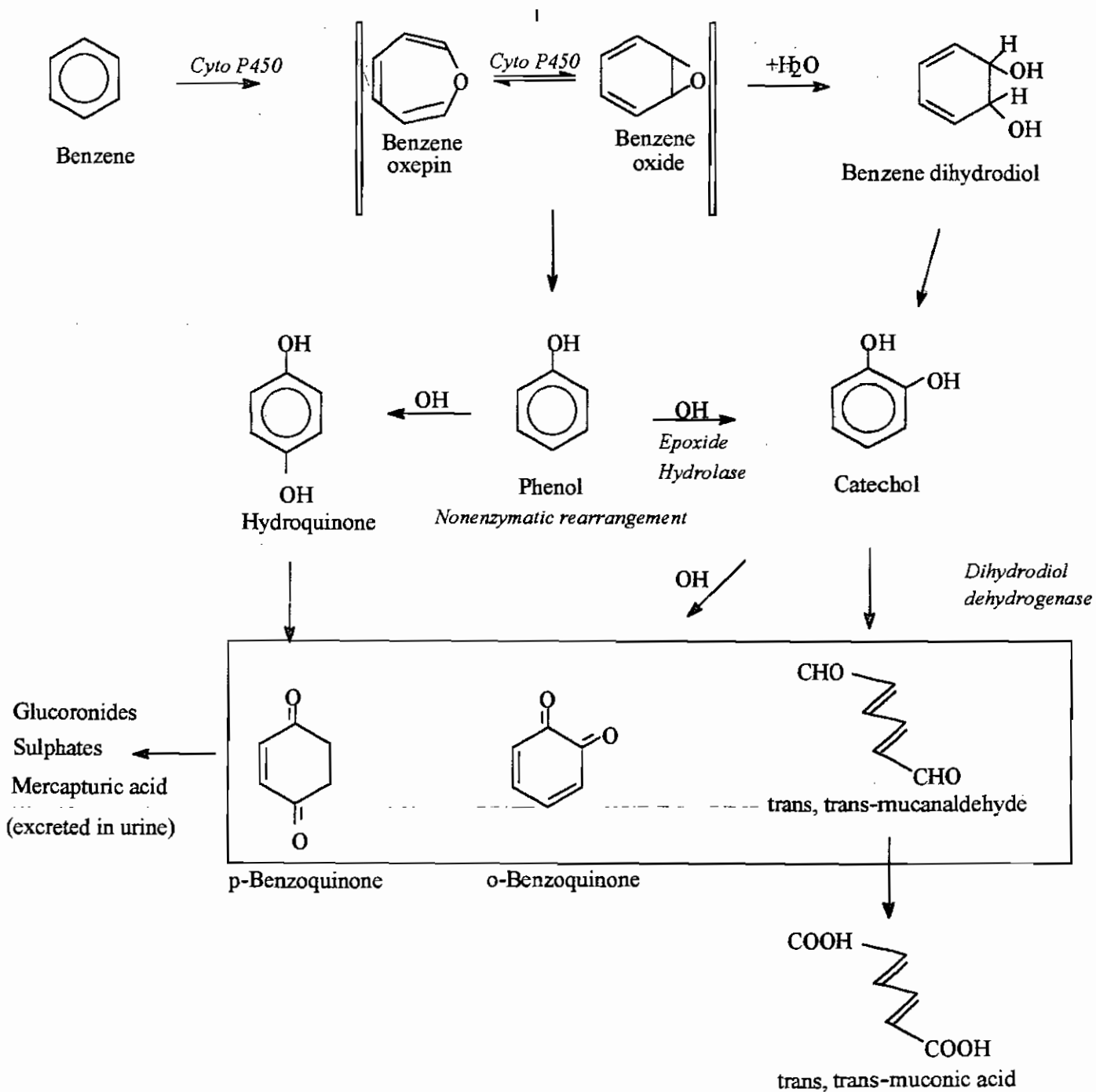
either excreted as water soluble sulphate or glucoronide conjugates in urine or, to a lesser

extent, further oxidised to the electrophilic compounds p-benzoquinone and o-

benzoquinone via the corresponding hydroquinones and semiquinones. The metabolism of benzene to phenol and the subsequent formation of water soluble phenyl conjugates (i.e. glucoronides, sulphates and mercapturic acid) is considered to be a detoxification pathway. The metabolism of dihydroxybenzenes, their oxidation to semiquinones and quinones and the ring opening reactions of benzenedihydrodiol to the reactive trans,trans-muconaldehyde are considered to be the toxic pathways.

The high POCPs of aromatics combined with their ability to form benzene by dealkylation in the combustion process and the presence of benzene in the fuel are not the only concerns. Several experiments have been carried out on animals to determine the adverse effects caused by a variety of VOCs including aromatics [30 and references therein]. As well as being a known carcinogen benzene has displayed toxic effects on animal foetuses [31] while toluene [32], styrene [33], the xylenes [34], phenol [35], chlorobenzenes [36] and chlorophenols [37] have all shown adverse effects on the central nervous system. Styrene [38] has also demonstrated some mutagenic properties and phenol [39] has known detrimental effects to the cardio-vascular system. While all of these experiments have been carried out on animals they demonstrate the potential for toxic effects in humans.

Figure 2.1 The toxicological pathway for Benzene in the body [30].



2.2 ATMOSPHERIC CHEMISTRY OF AROMATICS

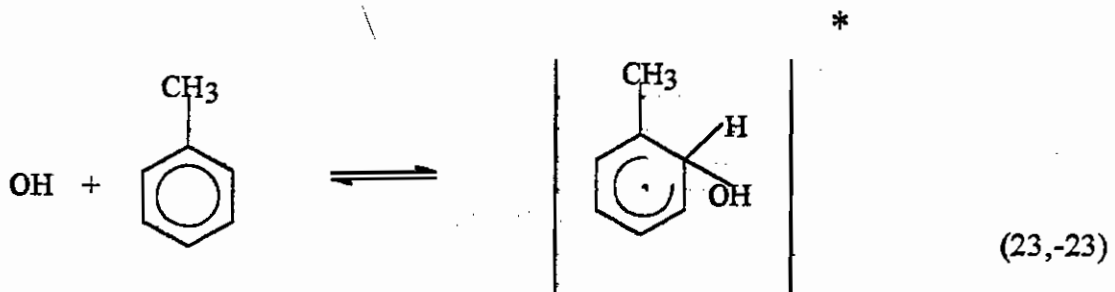
The main loss process for aromatics in the troposphere is by reaction with the OH radical, with room temperature rate constants ranging from $1.72 \times 10^{-13} \text{ cm}^3 \text{ molecule}^{-1} \text{ s}^{-1}$ [29] for hexafluorobenzene to 5.73×10^{-11} for 1,3,5-trimethylbenzene [29] and hence atmospheric lifetimes in the range 67 days to 5 hours (assuming $[\text{OH}] = 1 \times 10^6 \text{ molecules cm}^{-3}$). While reaction with the OH radical is important during the day, the dominant night-time loss process for many VOCs, particularly unsaturated organics, is via reaction with nitrate radicals (NO_3) [40]. Typical NO_3 rate constants for alkylated aromatics, relevant to atmospheric conditions, cover the range $\sim 10^{-17}$ to $10^{-15} \text{ cm}^3 \text{ molecule}^{-1} \text{ s}^{-1}$ [40] resulting in lifetimes of many months to years (assuming $[\text{NO}_3] = 2.4 \times 10^8 \text{ molecules cm}^{-3}$) showing that reaction with NO_3 is not a significant loss process for these compounds. Aromatics are reactive towards chlorine atoms with rate constants of the order of $\sim 10^{-10} - 10^{-13} \text{ cm}^3 \text{ molecule}^{-1} \text{ s}^{-1}$ [41] at 298K, but such reactions are only significant in marine air masses where there is sufficient Cl atom production. Ozone may react but only very slowly with aromatics with rate constants typically $< 10^{-20} \text{ cm}^3 \text{ molecule}^{-1} \text{ s}^{-1}$ [42] and hence, this loss process is of negligible atmospheric importance.

2.2.1 Reactions of Aromatic compounds with OH radicals

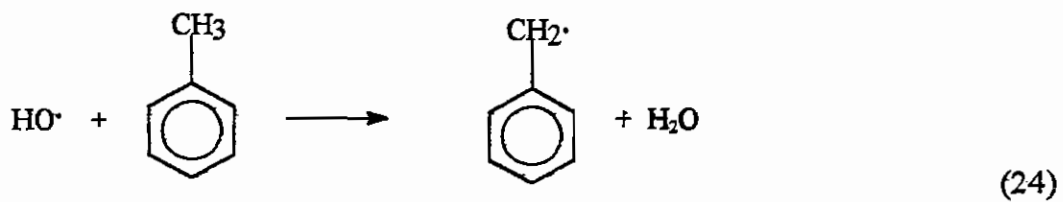
The high electron density of the aromatic ring means that addition of the electrophilic OH radical is possible as well as hydrogen atom abstraction. Hence, there are four possible pathways for reaction of OH radicals with alkyl substituted aromatics.

Using toluene as an example:

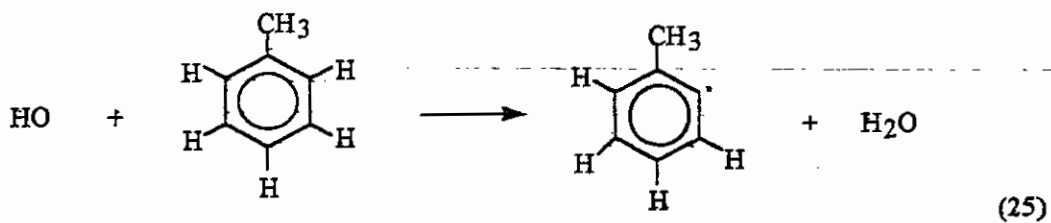
- Reversible OH radical addition to the electron rich aromatic ring:



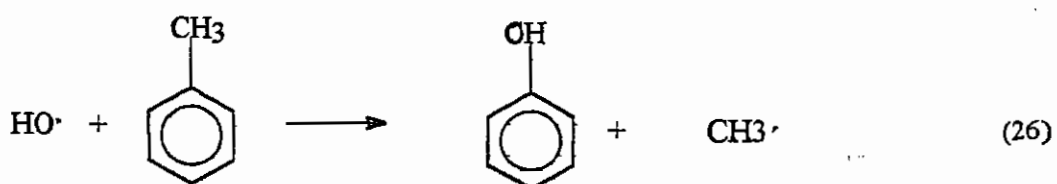
- Hydrogen atom abstraction from the alkyl side chain:



- Hydrogen atom abstraction from the aromatic ring



- Substituent group (including H-atom) elimination:



Hydrogen atom abstraction from the aromatic ring (reaction 25) is thermodynamically unfavourable compared to aliphatic hydrocarbons due to the relative bond energies of an alkyl C-H bond ($\sim 355 \text{ kJ mol}^{-1}$) and an aromatic ring C-H bond ($\sim 460 \text{ kJ mol}^{-1}$) so the contribution of this channel to the overall reaction is expected to be negligible. Reaction (26) does not appear to be of any significance since phenol has not been observed as a product of the OH-toluene reaction [43,44]. This leaves two possible pathways for OH radical attack: OH addition to the aromatic ring (reaction 23) and H-atom abstraction from the alkyl side chain (reaction 24). H-atom abstraction from the alkyl substituent leads to the formation of a benzyl radical and water. This radical undergoes atmospheric oxidation by a similar pathway to that of a saturated hydrocarbon leading to the formation of benzaldehyde and nitrotoluene as shown in Figure 2.2, and discussed in greater detail in the next section.

OH addition results in the formation of an energy rich alkylhydroxycyclohexadienyl radical adduct. Collisional stabilisation of this adduct results in the formation of a variety of ring retaining products, including phenols, nitro-aromatics, and ring cleavage products such as α -dicarbonyls, as shown in Figure 2.3 and discussed in greater detail in the next section.

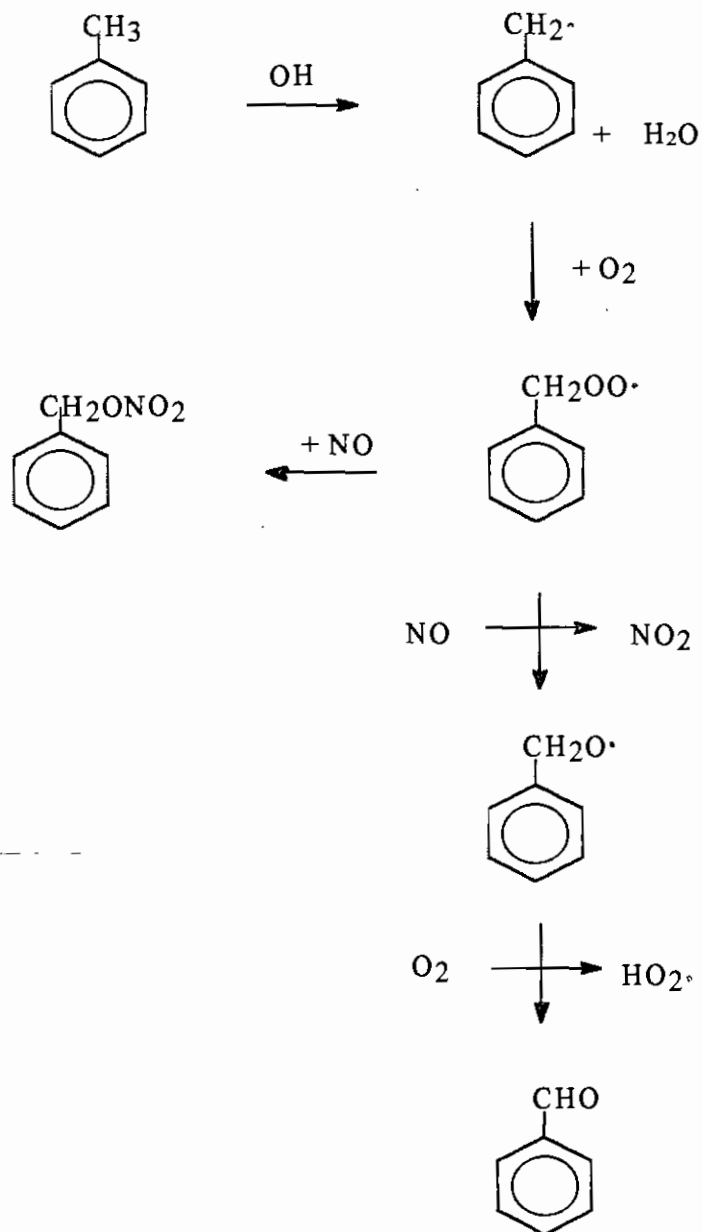
In order to determine the relative contributions of the addition and abstraction pathways to the overall OH radical reaction the temperature dependence of the rate constant and product studies have been conducted. The results of temperature dependant studies (discussed in more detail in *Section 2.4.2*) show that there are three distinct temperature regimes for the overall reaction:

- Below 325K there is insufficient energy for H-atom abstraction from the alkyl substituent to occur so OH addition to the ring predominates.
- Above 450K thermal back-decomposition of the OH-aromatic adduct becomes so rapid that only H-atom abstraction (H-atom and halogen atom elimination for benzene and halogenated benzenes respectively) is observed.
- In the temperature range 325-450K both pathways occur and their relative contribution to the overall rate constant varies with temperature.

2.2.2 Product studies

Under tropospheric conditions the reactions subsequent to H-atom abstraction from the alkyl side chain are reasonably well understood and are shown in Figure 2.2. The sole fate of the benzyl radical under atmospheric conditions is addition of O₂ to generate a benzylperoxy radical. The subsequent reactions of the benzylperoxy radical in the presence of NO lead to the formation of benzaldehyde and benzyl nitrate. The fraction of benzyl nitrate formed from this reaction is ~0.1 at room temperature and atmospheric pressure [45]. A similar reaction pathway accounts for the formation of tolualdehydes and methylbenzyl nitrates from the xylenes isomers [46], while an analogous reaction mechanism is expected for other alkyl substituted benzenes.

Figure 2.2 Reaction pathway following H-atom abstraction from toluene by OH radicals in the presence of NO_x [47].

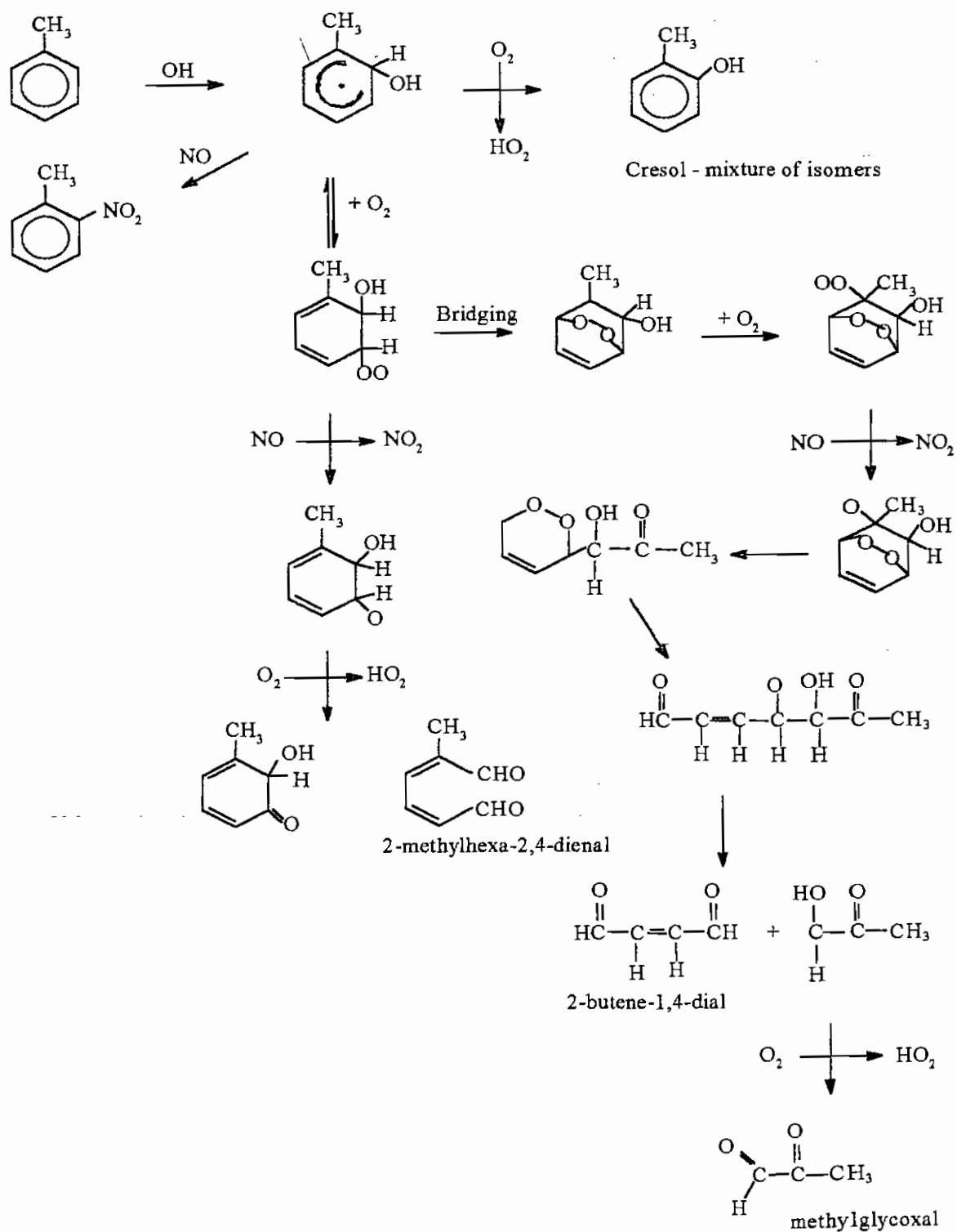


The reversible addition pathway is less well understood with a variety of ring retaining and ring cleavage products observed. Furthermore, product studies to date have only quantitatively accounted for 60-70% of the mass balance for the reacted carbon in the OH initiated oxidation of toluene [42 and references therein]. Addition of the OH radical to the aromatic ring leads to the formation of an alkylhydroxycyclohexadienyl radical adduct as shown in Figure 2.3. This adduct is collisionally stabilised under tropospheric conditions (high pressure limit above ~ 100 Torr) and may react with O₂ to form phenolic compounds (cresols from toluene) or with NO to form nitrotoluenes. Product yields from studies on some of the more common aromatics (benzene, toluene and the xylenes) and their products have been reported [42 and references therein]. For toluene ~10% of the overall reaction is by H-atom abstraction from the alkyl substituent to form, in the presence of NO, benzaldehyde and benzyl nitrate. The cresols, which are the major addition products, account for a further ~ 25% of the reacted carbon. The ring cleaved α -dicarbonyls, glyoxal and methylglyoxal, and their co-products make up another ~25% of the reaction. The remaining 40% of the reacted carbon is made up of compounds that are not quantitatively known but contain a variety of ring retaining and ring cleavage products.

Studies subsequent to the review of Atkinson [42] have attempted to identify/quantify the unknown products of the OH-aromatic addition reaction. Forstner *et al* [48] have examined the formation of secondary organic aerosols from the photooxidation of aromatics and found that unsaturated anhydrides (furanones) are predominant components of aerosol from all aromatics studied. Saturated anhydrides were also detected in significant quantities and it is predicted that these are formed from

Figure 2.3 Reaction pathway following OH addition to Toluene in the presence of NO_x

[47].



hydrogenation of the furandiones in the particle phase. Yu *et al* [49] have conducted smog chamber studies to attempt to comprehensively determine all carbonyl products from the OH initiated degradation of toluene, the xylenes, 1,2,3- and 1,2,4-trimethylbenzene. A range of carbonyl products were identified including aromatic aldehydes, quinones, di-unsaturated 1,6-dicarbonyls, unsaturated 1,4-dicarbonyls, saturated dicarbonyls, hydroxy dicarbonyls, glycoaldehyde, hydroxy acetone, triones and epoxy carbonyls. Yu and Jeffries [50] have also presented experimental evidence for the formation of epoxide intermediates in the reactions of the same set of aromatics, consistent with theoretical calculations performed by Bartolotti and Edney [51]. These epoxide intermediates are important because they are potentially toxic and mutagenic.

Atkinson and Aschmann [52] have examined the effect of NO_2 concentration on the product yields from the reaction of OH with toluene, o-xylene and 1,2,3-trimethylbenzene. The results of this study show that under typical tropospheric conditions the hydroxycyclohexadienyl-type radicals formed from benzene, toluene, the xylenes and trimethylbenzenes react primarily with O_2 over NO_2 . Similarly, Moschonas *et al* [53] have investigated the effect of O_2 and NO_2 on the ring retaining reactions of OH and benzene. The main products were phenol and a peroxy radical which decomposed to a series of ring cleavage products. However, in the presence of NO_2 , nitrobenzene is also formed in yields linear to the initial NO_2 concentration and vanishing as $[\text{NO}_2]$ approaches zero. Smith *et al* [54] have determined a primary product distribution from the reaction of OH with toluene at concentrations of NO_x similar to atmospheric conditions i.e. ppb NO_x

mixing ratios. The major primary products detected (as a fraction of the reacted aromatic) were glyoxal (0.238), methylglyoxal (0.167), o-cresol (0.120), benzaldehyde (0.06), 4-oxo-2-pentenal (0.03). Six other ring cleavage products were detected at yields below 3%. It was also found that the yield of cresol isomers was invariant of the NO₂ concentration indicating that under atmospheric conditions the reaction of the hydroxycyclohexadienyl radical with NO₂ is of minor importance.

Lay *et al* [55] have carried out quantum calculations on the thermodynamics of the OH-benzene adduct (hydroxy-2,4-cyclohexadienyl) using a quantum version of Rice-Ramsperger-Kassel theory (QRRK). The results of these calculations have provided evidence for the possible formation of a bicyclic intermediate in the reaction.

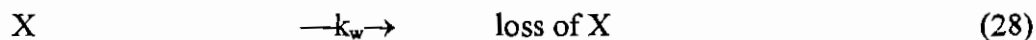
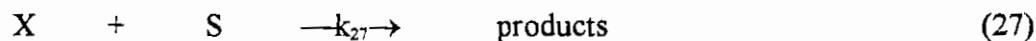
It is now well established from product studies that, at room temperature and atmospheric pressure, addition of the OH radical to the aromatic ring accounts for ~90% of the overall reaction for toluene while hydrogen atom abstraction from the methyl substituent accounts for the remainder. This is in agreement with the figure found by extrapolating kinetic data from > 380K back to room temperature. Further experimental evidence that OH addition to the ring is the dominant reaction channel under atmospheric conditions comes from comparing the reactivity of toluene h₈ and toluene-d₈ with OH radicals, where there is no significant difference in the recommended rate constants [29]. The absence of a measureable kinetic isotope effect is consistent with the predominance of the addition pathway.

2.3 EXPERIMENTAL TECHNIQUES

The bimolecular rate constant for the gas phase reaction between a substrate, S, and a reactive species, X (atom or radical), may be determined by either *absolute* or *relative rate* methods.

2.3.1 Absolute methods

The gas phase reactions studied are usually bimolecular of the type:



where X is either OH or NO₃ radicals, Cl atoms or O₃, etc. and S is an organic or inorganic substrate. Pseudo-first-order conditions are generally used regardless of the absolute experimental technique employed. Usually, small concentrations of X are monitored in the presence of a large excess of S. The rate of loss of X may be expressed as:

$$-d[X] / dt = k_{27}[X][S] + k_w[X] \quad \text{I}$$

$$= (k_{27}[S] + k_w)[X] \quad \text{II}$$

where k_{27} is the bimolecular rate constant for reaction of X with S and k_w is a correction for other losses of X. If the initial concentration of substrate, $[S]_0$ is present in large excess over the initial concentration of reactive species, $[X]_0$, i.e. $[S]_0 \geq 10[X]_0$ then the concentration of S remains essentially unchanged during the reaction. And X will decay exponentially with time as in a first order reaction. Thus equation II may be expressed as:

$$-d[X]/dt = k[X] \quad \text{III}$$

$$\text{where } k' = k_{27}[S]_0 + k_w.$$

Rearranging:

$$-d[X]/[X] = -d \ln[X] = k' dt \quad \text{IV}$$

Integrating:

$$\ln([X]/[X]_0) = -k' t$$

or

$$\ln [X] = -k' t + \ln [X]_0 \quad \text{V}$$

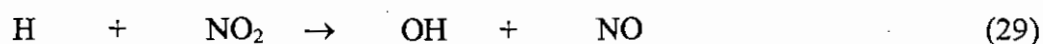
A plot of $\ln[X]$ versus time should be linear with k' obtained from the slope. A series of reactions at varying $[S]_0$ leads to a set of corresponding k' values after correction for wall loss. Hence, a plot of k' versus $[S]_0$ should be linear with slope equal to k_{27} , the bimolecular rate constant. Pseudo-first order conditions obviates the necessity for measurement of absolute concentrations of X since any physical property proportional to

same value of k . Accurate absolute concentrations of S are, however, required.

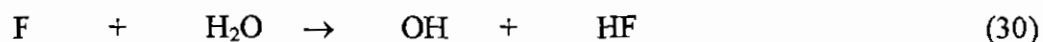
In experiments relevant to the atmospheric chemistry of aromatics the techniques most routinely employed are *fast flow discharge systems (FFDS)* and *flash photolysis (FP)*. In fast flow discharge an excess of inert gas (typically He or Ar) is mixed with the reactants X and S in a flow tube typically 2-5cm in diameter and 1 meter in length. As the mixture travels down the flow tube at relatively high linear flow speeds ($\sim 1000 \text{ cm s}^{-1}$), reactive species X reacts with the substrate S. The decay of X along the tube is monitored and applied to equation V to obtain the rate constant. The term *fast flow* comes from the high flow speeds while the *discharge* term is comes from the use of microwave discharge to generate the reactive species X.

The technique employed in fast flow discharge systems depends on the reaction under investigation. One approach is to inject X at a fixed point at the upstream end of the tube where it mixes with S. The decay of X is then monitored using a detector which moves along the length of the flow tube. However, if variation of the reaction times is required, one of the reactants enters at the upstream end of the flow tube and the second reactant is added through a moveable inlet. In this case the detector is fixed at the downstream end of the flow tube and the reaction time is varied by moving the mixing point for X and S using a moveable injector and fixed detector.

Hydroxyl radicals may be generated by:



or



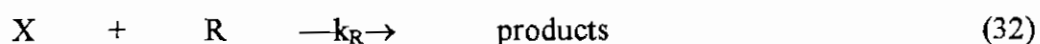
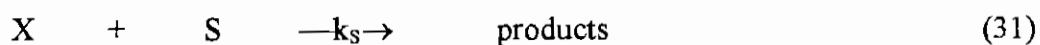
with H and F atoms being generated from microwave discharge of the parent diatomic gases H₂ and F₂ respectively. Most FFDS studies have employed reaction (29) as the source of OH radicals which, under the experimental conditions used, is free of interference from vibrationally excited OH radicals.

The detection systems used to monitor OH in fast flow discharge systems may be resonance fluorescence (RF), laser induced fluorescence (LIF) and mass spectrometry (MS). Resonance fluorescence is usually used for atomic species (e.g. H, O, Cl) but may also be used for certain diatomics such as the OH radical. Laser induced fluorescence is used more often for molecular species as it offers more sensitivity and wider applications but with greater complexity.

The *flash photolysis* technique, developed by Norrish and Porter [56] in the late 1940s relies on a flash of light to generate the reactive species X. The flash lamp is triggered and the pulse of light dissociates a parent molecule, producing the reactive species X on a millisecond timescale. The light source has now been replaced by high-powered lasers with pulse duration down to the nanosecond range with high repetition rate. Following the photolytic flash the time decay of the reactive species is monitored by resonance fluorescence or laser induced fluorescence similar to that described for FFDS.

2.3.2 Relative rate method

If the absolute rate constant for reaction of the reactive species, X, with a reference compound, R, has been well established by one or more of the absolute techniques previously described, then the rate constant for reaction of X with the substrate, S, can be determined by monitoring the competitive loss of R and S in the presence of X. The experimental technique involves observing the competitive reactions of R and S with the reactive species X in the same reaction vessel:



Assuming that the only loss process for S and R is by reaction with X and providing dilution due to sampling is negligible, then the rate of decay of S and R may be expressed mathematically as:

$$-d[S]/dt = k_S[X][S]$$

$$-d[R]/dt = k_R[X][R]$$

Hence

$$-d[S]/[S] = -d \ln[S] = k_S[X]dt$$

$$-d[R]/[R] = -d \ln[R] = k_R[X]dt$$

Combining these equations and eliminating X leads to the expression:

$$d\ln[S]/dt = k_S/k_R d\ln[R]/dt \quad \text{VI}$$

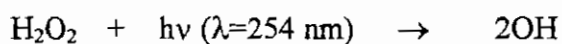
Integrating from $t=0$ to t gives:

$$\ln([S]_0/[S]_t) = k_S/k_R \ln([R]_0/[R]_t) \quad \text{VII}$$

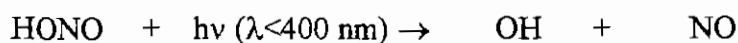
A plot of $\ln([S]_0/[S]_t)$ versus $\ln([R]_0/[R]_t)$ should yield a straight line of slope k_1/k_2 and zero intercept. Since the rate constant for the reference reaction k_R is known, k_S can be calculated from the slope.

A variety of photolytic and non-photolytic sources of OH radicals have been used in relative rate studies. The major photolytic sources of OH radicals used in early studies were:

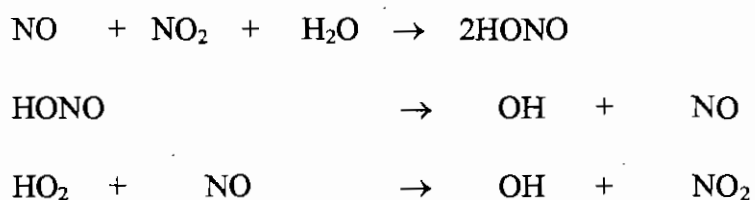
Photolysis of hydrogen peroxide (H_2O_2) [57]:



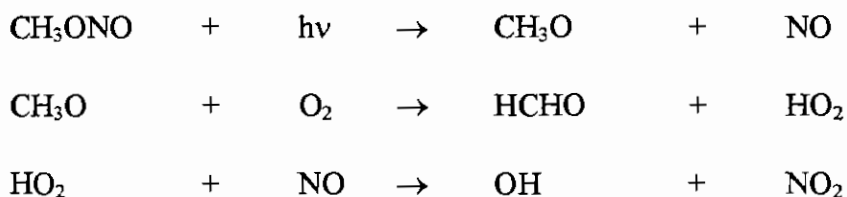
Photolysis of nitrous acid (HONO) [58]:



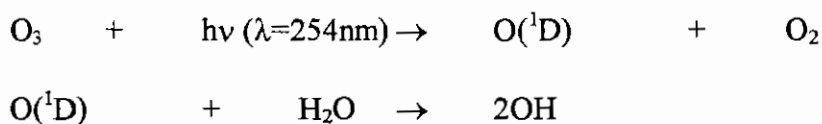
Photolysis of NO_x -organic-air mixtures [59], where the major sources of OH were probably the reactions:



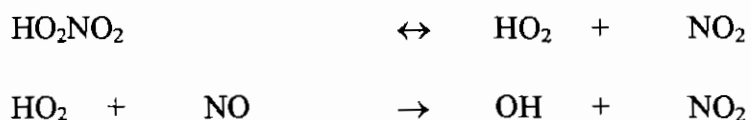
Photolysis of methyl nitrite in air has been widely employed as an OH source over the past two decades[60]:



More recently, photolysis of ozone/water vapour mixtures has been used to generate OH in relative rate studies[61]:



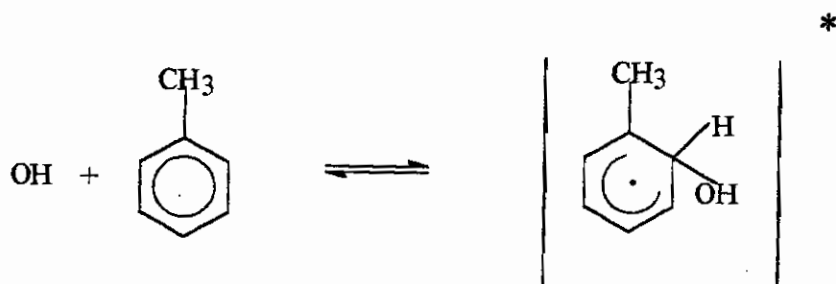
Three different non-photolytic sources of OH radicals have also been used. The formation of OH from the reaction of hydrazine (N_2H_4) with ozone (O_3) has been utilised despite the fact that the reaction mechanism is not fully understood [62]. The thermal decomposition of HO_2NO_2 in the presence of NO in air has been used by Barnes *et al* [63] to generate OH radicals:



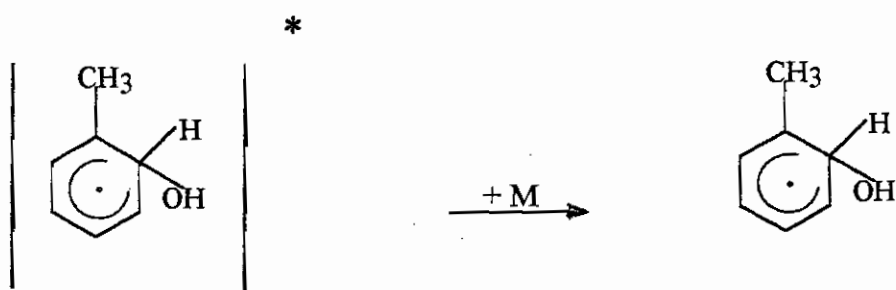
2.4 PREVIOUSLY REPORTED RATE DATA

2.4.1 Room temperature rate data

The dominant reaction channel at room temperature is OH addition to the aromatic ring to form an energy-rich OH-aromatic adduct:



This energy-rich adduct can either decompose back to reactants or be collisionally stabilised by a third body (M):



Kinetic studies on the pressure dependence of the reaction of OH radicals with benzene in argon [46,64-66] and in helium [46,67] show that, at room temperature, the rate constant is in the fall-off region between second and third order kinetics below ~25-50 Torr total pressure of diluent gas, while similar studies on the OH + toluene reaction reveal a pressure independent rate constant above ~100 Torr of argon [68,69]. Ravishankara *et al* [70] have demonstrated that the rate constants for the reaction of OH with the xylene isomers reach their high pressure limit at ~20 Torr of argon at 298K.

The available room temperature rate data for reaction of OH radicals with alkyl substituted and halogenated aromatics at, or close to, the high pressure limit are listed in Table 2.4. Due to the large number of kinetic studies to date, the table includes the rate constants recommended after an extensive literature review by Atkinson [29] in 1989 (which takes all previous work into account) and rate data reported since this review. For compounds where insufficient work has been carried out to date for a recommended value to be stated with confidence, all rate data are included.

In general there is good agreement between the recommended room temperature rate constant of Atkinson [29] and the more recent determinations for toluene [71,72], m-xylene [71] and 1,3,5-trimethylbenzene [71]. Kramp and Paulson [71] also set out to reduce the degree of uncertainty in the rate constants previously reported for reaction of OH with m-xylene and 1,3,5-trimethylbenzene which showed a scatter of $\pm 25\%$ and $\pm 35\%$ respectively. These investigators carried out a series of relative rate measurements using ten different reference compounds and the resultant rate constants are in excellent agreement with those recommended by Atkinson[29].

Kinetic studies on the reaction of OH radicals with halogenated aromatics are more limited. Recommended rate constants exist only for the monohalobenzenes, hexafluorobenzene and benzyl chloride, while p-dichlorobenzene [73,74] is the only otherhalogenated aromatic for which more than one study exists.

The data in Table 2.4 clearly demonstrates that increasing the number of alkyl substituents on the aromatic ring leads to greater reactivity towards the electrophilic OH radical.

Since the dominant reaction channel under these conditions is addition of the electrophilic OH radical to the aromatic ring, this trend can be rationalised in terms of an increase in the electron density of the aromatic ring with increase in the number of electron donating alkyl groups. For example, $k(\text{OH} + \text{toluene})$ is about a factor of 4 greater than $k(\text{OH} + \text{benzene})$. $k(\text{OH} + \text{xylenes})$ are approximately an order of magnitude greater than $k(\text{OH} + \text{benzenes})$ while $k(\text{OH} + \text{trimethylbenzenes})$ are about 4 orders of magnitude larger than $k(\text{OH} + \text{benzene})$. Rate data for reaction of OH with the tetramethylbenzene isomers have not been previously reported.

The rate of OH radical addition is also influenced by the position of alkyl substituents on the ring, i.e. the reactivity differs for the different isomers. The recommended rate constants for $k(\text{OH} + \text{xylenes})$ are in the order: $k(\text{OH} + \text{m-xylene}) > k(\text{OH} + \text{o-xylene}) \approx k(\text{OH} + \text{p-xylene})$. A similar trend is observed for the ethyltoluene isomers. The trimethylbenzene isomers also show significantly different OH radical rate constants with $k(\text{OH} + 1,3,5\text{-trimethylbenzene}) > k(\text{OH} + 1,2,3\text{-trimethylbenzene}) \approx k(\text{OH} + 1,2,4\text{-trimethylbenzene})$.


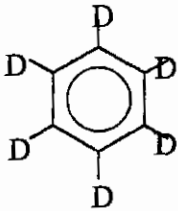
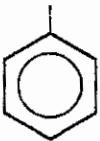
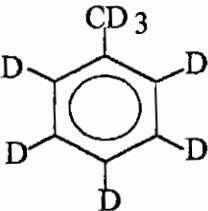
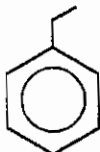
The recommended rate constants for the monosubstituted alkyl benzenes are, within the error limits, equal to that for toluene suggesting that increasing size of the alkyl substituent has a negligible effect on the electron density of the aromatic ring; the decrease in reactivity for t-butylbenzene being possibly due to steric hindrance to OH attack at the ortho position. Kinetic studies carried out on monosubstituted alkylbenzenes by Ohta and Ohyama [75], Ravishankara *et al* [70] and Lloyd *et al* [76] have concluded that all monosubstituted alkylbenzenes have essentially the same reactivity with the OH radical. This is

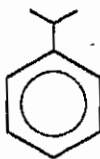
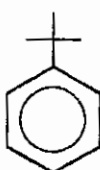
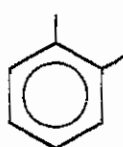
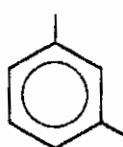
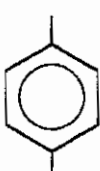
somewhat surprising since one might expect that, as with straight chain alkanes, increasing the length of the alkyl group should enhance the importance of the abstraction pathway and hence lead to an increase in the overall reaction rate.

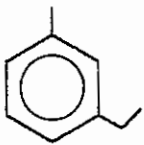
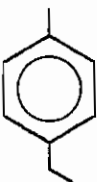
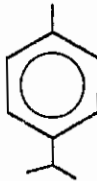
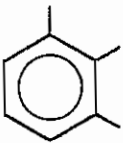
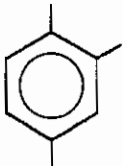
Aromatic compounds with saturated cyclic substituents, namely indane and tetralin, would be expected to exhibit the same reactivity towards OH as the ortho-dialkylsubstituted benzenes, o-xylene ($13.7 \times 10^{-12} \text{ cm}^3 \text{ molecule}^{-1} \text{ s}^{-1}$) [29] and o-ethyltoluene ($12.3 \times 10^{-12} \text{ cm}^3 \text{ molecule}^{-1} \text{ s}^{-1}$) [29]. The low pressure room temperature rate constant reported by Baulch *et al* [77] for indane ($9.2 \pm 1.3 \times 10^{-12} \text{ cm}^3 \text{ molecule}^{-1} \text{ s}^{-1}$) is reasonably close to that expected for OH addition to the aromatic ring. However, the rate constant determined by Atkinson and Aschmann [78] for reaction of OH with tetralin ($34.3 \pm 0.6 \times 10^{-12} \text{ cm}^3 \text{ molecule}^{-1} \text{ s}^{-1}$) at 298K and atmospheric pressure appears unexpectedly high compared to indane, suggesting greatly enhanced OH addition to the aromatic ring and/or H-atom abstraction from the saturated ring. It is difficult to reconcile these rate data given that the only differences between the two compounds is a small degree of ring strain in the five membered ring and the presence of an additional $-\text{CH}_2-$ group in tetralin.

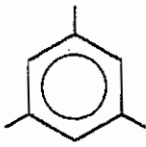
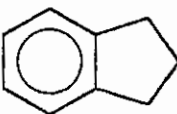
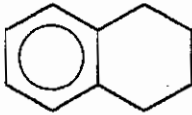
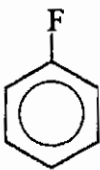
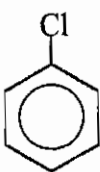
The presence of a halogen substituent on the benzene ring leads to a decrease in reactivity towards OH radicals compared to benzene, presumably due to the negative inductive effect of the halogen reducing the electron density of the ring. The reactivity of the mono-halobenzenes is consistent with the trend in electronegativity values of the halogen substituents : $k(\text{OH} + \text{fluorobenzene}) < k(\text{OH} + \text{chlorobenzene}) < k(\text{OH} + \text{bromobenzene}) < k(\text{OH} + \text{iodobenzene})$.

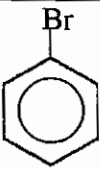
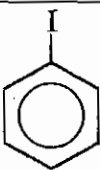
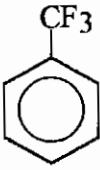

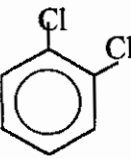
Table 2.4 Rate constants for the reaction of OH radicals with aromatic compounds at Room temperature and at, or close to, the high pressure limit.

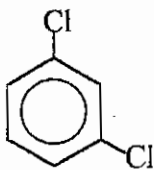
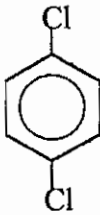
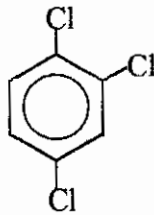
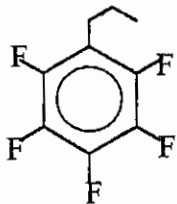
Aromatic	$k_{OH} \times 10^{12}$ $\text{cm}^3 \text{ molecule}^{-1} \text{ s}^{-1}$	Technique	Literature reference
 benzene	1.23	E	Atkinson [29]
 benzene-d ₆	1.14	E	Atkinson [29]
 toluene	5.96 5.5 ± 0.5 5.9 ± 1.5 5.8 ± 1.5	E RR RR RR	Atkinson [29] Kramp + Paulson [71] Anderson + Hites [72] Anderson + Hites [72]
 toluene-d ₈	6.31	E	Atkinson [29]
 ethylbenzene	7.1	E	Atkinson [29]

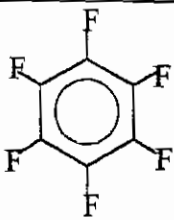
Aromatic	$k_{OH} \times 10^{12}$ $\text{cm}^3 \text{ molecule}^{-1} \text{ s}^{-1}$	Technique	Literature reference
 <i>iso</i> -propylbenzene	6.5	E	Atkinson [29]
 <i>tert</i> -butylbenzene	4.60 ± 0.45	RR	Ohta + Ohyama [75]
 <i>o</i> -xylene	13.7	E	Atkinson [29]
 <i>m</i> -xylene	23.6 22.0 ± 2.7	E RR	Atkinson [29] Kramp + Paulson [71]
 <i>p</i> -xylene	14.3	E	Atkinson [29]

Aromatic	$k_{OH} \times 10^{12}$ $\text{cm}^3 \text{ molecule}^{-1} \text{ s}^{-1}$	Technique	Literature reference
 m-ethyltoluene	19.2	E	Atkinson [29]
 p-ethyltoluene	12.1	E	Atkinson [29]
 p-cymene	15.1 ± 0.41	RR	Corchnoy + Atkinson [79]
 1,2,3- trimethylbenzene	32.7	E	Atkinson [29]
 1,2,4- trimethylbenzene	32.5	E	Atkinson [29]

Aromatic	$k_{OH} \times 10^{12}$ $\text{cm}^3 \text{ molecule}^{-1} \text{ s}^{-1}$	Technique	Literature reference
 1,3,5- trimethylbenzene	57.5 57.3 ± 5.3	E RR	Atkinson [29] Kramp + Paulson [71]
 indane	9.2 ^a	DF-RF	Baulch <i>et al</i> [77]
 tetralin	34.3 ± 0.6	RR	Atkinson + Aschmann [78]
 fluorobenzene	0.69	E	Atkinson [29]
 chlorobenzene	0.77	E	Atkinson [29]

Aromatic	$k_{OH} \times 10^{12}$ $\text{cm}^3 \text{ molecule}^{-1} \text{ s}^{-1}$	Technique	Literature reference
 bromobenzene	0.77	E	Atkinson [29]
 iodobenzene	1.1	E	Atkinson [29]
 benzotrifluoride	0.46 ± 0.12	RR	Atkinson <i>et al</i> [80]
 4-chloro- benzotrifluoride	0.24 ± 0.08	RR	Atkinson <i>et al</i> [80]
 o-dichlorobenzene	0.42 ± 0.02	FP-RF	Wahner + Zetzsch [73]

Aromatic	$k_{OH} \times 10^{12}$ $\text{cm}^3 \text{ molecule}^{-1} \text{ s}^{-1}$	Technique	Literature reference
 m-dichlorobenzene	0.72 ± 0.02	FP-RF	Wahner + Zetzsch [73]
 p-dichlorobenzene	0.32 ± 0.02 0.43 ± 0.09	FP-RF RR	Wahner + Zetzsch [73] Arnts <i>et al</i> [74]
 1,2,4- trichlorobenzene	0.50 ± 0.10	FP-RF	Rinke + Zetzsch [82]
 n-propyl- pentafluorobenzene	3.06 ± 0.24	FP-RF	Ravishankara <i>et al</i> [70]

 <p>hexafluorobenzene</p>	0.172	E	Atkinson [29]
--	-------	---	---------------

a 0.32 and 1.3 Torr total pressure.

E Evaluated rate constant based on extensive literature review.

RR Relative rate method.

DF-RF Discharge Flow-Resonance Fluorescence technique.

FP-RF Flash Photolysis-Resonance Fluorescence technique.

2.4.2 Temperature dependant rate data

As outlined in *Section 2.2* the reaction of OH radicals with aromatic compounds proceeds via two alternate pathways: (i) abstraction of a H-atom from the alkyl group (except for benzene) and (ii) OH addition to the aromatic ring. Previous studies have shown that the relative contribution of the addition and abstraction pathways is temperature dependant [46,70]. At temperatures <325K there is insufficient energy for H-atom abstraction to occur to any great extent and OH addition predominates. At temperatures >325K H-atom abstraction is feasible but the OH-aromatic adduct formed in the addition pathway becomes less stable and tends to decompose back to reactants due to the excess energy ($\sim 75\text{kJ mol}^{-1}$) which the addition adduct contains from the exothermicity of the forward reaction. As the temperature is increased the rate of decomposition of the adduct increases and, above 450K decomposition occurs so fast that only the abstraction pathway is

observed experimentally. At ambient conditions of temperature and pressure addition predominates with abstraction being of the order of 2-14% depending on the individual aromatic [29].

There have been relatively few temperature studies on OH-aromatic reactions, Table 2.5. The reported data of Perry *et al* [81], Tully *et al* [46], Lorenz and Zellner [65], Witte *et al* [82] and Wallington *et al* [83] have been included in the evaluated expression ($T < 325\text{K}$) of Atkinson [29]. More recently, Semandeni *et al* [84] have derived Arrhenius parameters using previously reported data, the data of Knispel *et al* [85] and his own work. The evaluated expressions ($T < 325\text{K}$) of Atkinson [29] and Semandeni *et al* [84] for benzene and toluene are in very good agreement: The only temperature dependant studies subsequent to this are those of Anderson and Hites [72] for reaction of OH with toluene.

All previous studies ($T < 363\text{K}$) on the reaction of OH with benzene [46,65,82,84], with the exception of Knispel *et al* [85], have reported a small positive temperature dependence over the range 234-354K, while $k(\text{OH} + \text{toluene})$ [46,80] exhibits a small negative temperature dependence over the same temperature range. $k(\text{OH} + \text{xylenes})$, based on the work of Perry *et al* [81] and Nicovich *et al* [86], is independent of temperature over the range 296-320K. Similarly, the studies of Perry *et al* [81] on the trimethylbenzene isomers reveal a temperature independent rate constant over the range 295-325K. Wallington *et al* [83] have found the monohalogenated benzenes to exhibit a zero temperature dependence over the range 234-303K, however Witte *et al* [66] observed a slight temperature dependence for the OH-bromobenzene reaction with a small positive activation energy

similar to that of benzene as has Rinke and Zetzsch [82] for $k(\text{OH} + 1,2,4\text{-trichlorobenzene})$ and Wallington *et al* [83] for $k(\text{OH} + \text{hexafluorobenzene})$.

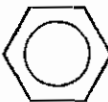
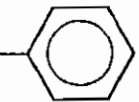
In summary, the reaction of benzene and some of the less reactive aromatics with OH have small positive activation energies whereas toluene and the more reactive aromatics tend to have small negative activation energies, or activation energies close to zero.

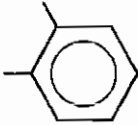
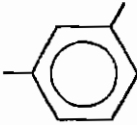
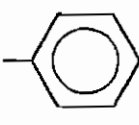
2.4.3 Aims of this work

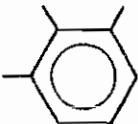
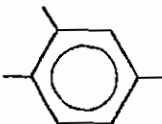
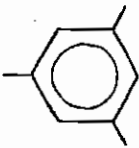
The main objectives of this study were :

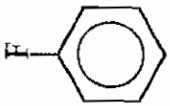
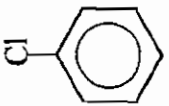
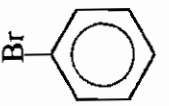
- (i) To measure relative rate constants for the reaction of OH radicals with selected aromatic compounds using a novel source of OH radicals in a NO_x – free environment, namely photolysis of ozone in the presence of molecular hydrogen.
- (ii) To conduct a systematic study on the reaction of OH radicals with a series of monoalkyl substituted benzenes in order to establish what affect, if any, increasing the length of the alkyl side chain has on the reactivity.
- (iii) To extend the kinetic database for reaction of OH radicals with tetramethylbenzenes.
- (iv) To resolve the apparent discrepancy in the reported rate data for reaction of OH radicals with indane and tetralin.
- (v) To extend the kinetic database for reaction of OH radicals with halogenated aromatics, in particular chlorotoluenes and fluorotoluenes.

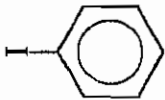
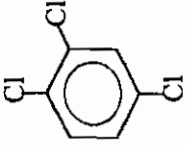
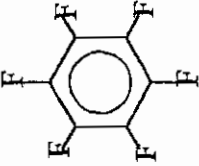
Table 2.5 Temperature dependant parameters $k = A \exp(-B/T)$ for the reaction of OH radicals with Aromatic compounds.

Aromatic	$A \times 10^{12}$ $\text{cm}^3 \text{molecule}^{-1} \text{s}^{-1}$	B K	Temp. range K	Technique	Reference
 benzene	2.47	207	243 – 354	E	Atkinson [29]
	-	-	297 – 327	FP-RF	Perry <i>et al</i> [81]
	3.1 ± 2.6	270 ± 220	250 – 298	FP-RF	Tully <i>et al</i> [46]
	6.3 ± 1.7	500 ± 50	244 – 298	FP-RF	Lorenz and Zellner [65]
	2.3	190 ± 60	239 – 354	FP-RF	Witte <i>et al</i> [66]
	-	-	234 – 296	FP-RF	Wallington <i>et al</i> [83]
	0.39	-311	298 – 354	FP-RF	Knispel <i>et al</i> [85]
	2.58	231 ± 84	274 – 363	RR	Semandeni <i>et al</i> [84]
	1.97	150 ± 105	234 – 363	E	Semandeni <i>et al</i> [84]
	 toluene	1.81	-355	213 – 324	E
-		-	298 – 328	FP-RF	Perry <i>et al</i> [81]
3.8 ± 2.5		-180 ± 170	213 – 298	FP-RF	Tully <i>et al</i> [46]
-		-	299 – 340	FP-RF	Knispel <i>et al</i> [85]
0.79		-614 ± 114	284 – 363	RR	Semandeni <i>et al</i> [84]
1.59		-396 ± 105	213 – 363	E	Semandeni <i>et al</i> [84]
-		-	276 – 397	RR	Anderson and Hites [72]

Aromatic	$A \times 10^{12}$ $\text{cm}^3 \text{molecule}^{-1} \text{s}^{-1}$	B K	Temp range K	Technique	Reference
 o-xylene	13.7 - -	0 - -	298 – 320 298 – 432 290 – 320	E FP-RF FP-RF	Atkinson [29] Perry <i>et al</i> [81] Nicovich <i>et al</i> [86]
 m-xylene	23.6 - -	0 - -	<325 298 – 320 250 – 298	E FP-RF FP-RF	Atkinson [29] Perry <i>et al</i> [81] Nicovich <i>et al</i> [86]
 p-xylene	14.3 - -	0 - -	297 – 320 298 – 320 250 – 298	E FP-RF FP-RF	Atkinson [29] Perry <i>et al</i> [81] Nicovich <i>et al</i> [86]

Aromatic	$A \times 10^{12}$ $\text{cm}^2 \text{ molecule}^{-1} \text{ s}^{-1}$	B K	Temp. range K	Technique	Reference
 1,2,3-trimethylbenzene	-	0	297 - 325	FP-RF	Perry <i>et al</i> [81]
 1,2,4-trimethylbenzene	-	0	298 - 323	FP-RF	Perry <i>et al</i> [81]
 1,3,5-trimethylbenzene		0	298 - 318	FP-RF	Perry <i>et al</i> [81]

Aromatic	$A \times 10^{12}$ ($\text{cm}^3 \text{ molecule}^{-1} \text{ s}^{-1}$)	B (K)	Temp range (K)	Technique	Reference
 fluorobenzene	1.29	0	234 - 303	FP-RF	Wallington <i>et al</i> [83]
 chlorobenzene	0.63	0	234 - 296	FP-RF	Wallington <i>et al</i> [83]
 bromobenzene	0.74 1.3	0 180 ± 60	234 - 296 245 - 362	FP-RF FP-RF	Wallington <i>et al</i> [83] Witte <i>et al</i> [66]

Aromatic	$A \times 10^{12}$ ($\text{cm}^2 \text{ molecule}^{-1} \text{ s}^{-1}$)	B (K)	Temp. range (K)	Technique	Reference
 iodobenzene	1.32	0	263 - 296	FP-RF	Wallington <i>et al</i> [83]
 1,2,4-trichlorobenzene	2.3 ± 1.0	429 ± 125	273 - 368	FP-RF	Rinke and Zetzsch [82]
 hexafluorobenzene	1.46 1.3 ± 0.3	638 610 ± 80	234 - 438 234 - 438	E FP-RF	Atkinson [29] Wallington <i>et al</i> [83]

3.0 EXPERIMENTAL

3.1 MATERIALS

The materials used, their stated purity and manufacturers are listed below:

Zero grade air, used as diluent gas, was purchased from Air Products Ltd. Nitrogen, air and hydrogen for the gas chromatograph and high purity oxygen (99.999%) used as diluent gas, were purchased from BOC Ltd.

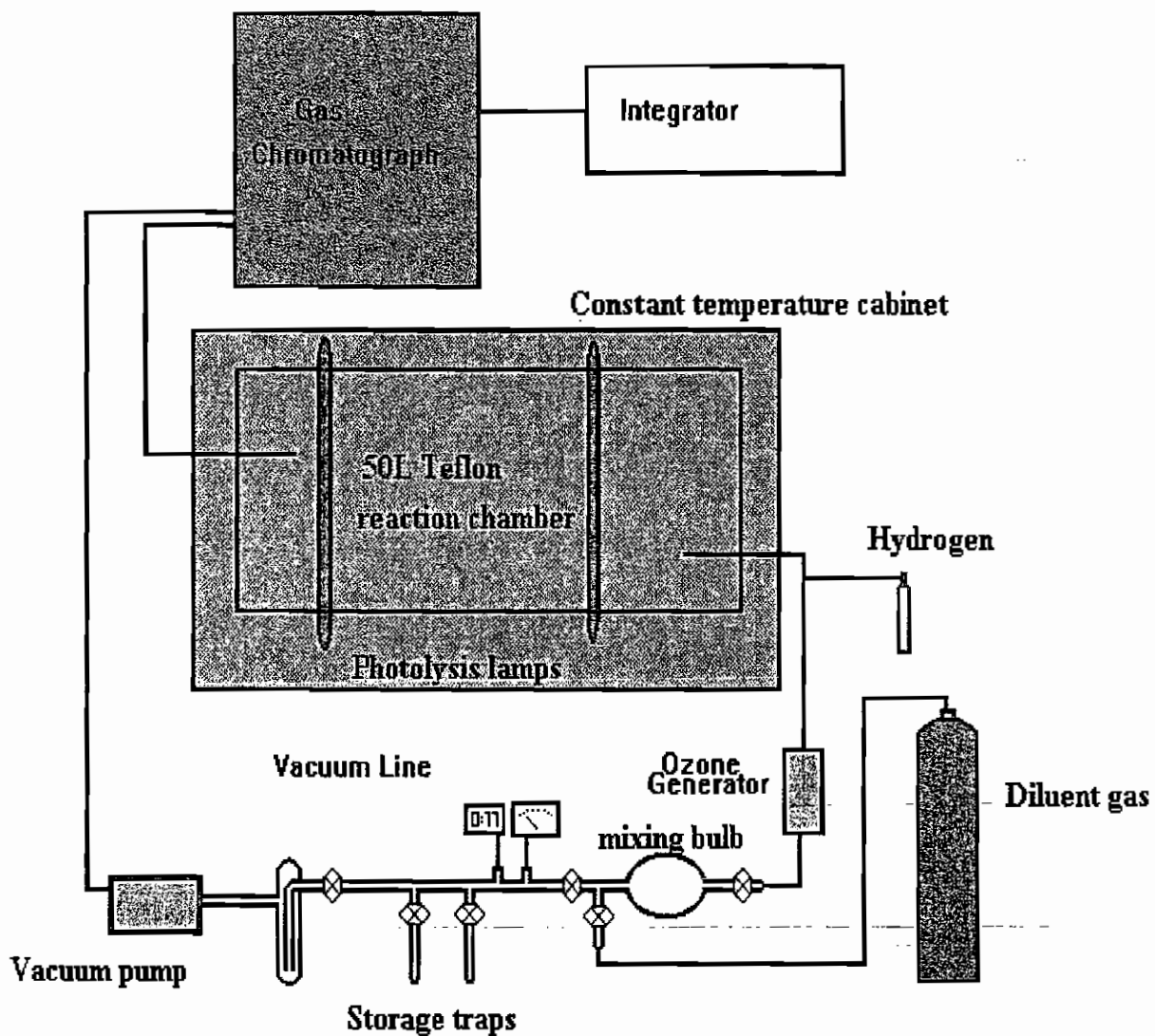
Hydrogen (99.99+%) and chlorine (99.5%) reactant gases were purchased from Aldrich Chemical Co. Ltd.

Cyclohexane (99.7%), toluene (99.8 %), toluene- d_8 (100% atom D), ethylbenzene (99.8%), n-propylbenzene (98%), n-butylbenzene (99+%), 1,2,4,5-tetramethylbenzene (98%), 1,3,5-trimethylbenzene (98%), 2-fluorotoluene (99+%), 3-fluorotoluene (99%), 4-fluorotoluene (97%), 2-chlorotoluene (99%), 3-chlorotoluene (98%), 4-chlorotoluene (98%), 1,2-diethylbenzene (>99%), indane (97%) and tetralin (99%) were purchased from Aldrich Chemical Co. Ltd.

3.2 APPARATUS

A block diagram of the experimental apparatus is shown in Figure 3.1. The apparatus consisted of a vacuum line and associated vacuum equipment, a Teflon reaction chamber surrounded by photolysis lamps and housed in a constant temperature cabinet, a gas

Figure 3.1 Schematic diagram of experimental apparatus.



chromatograph and computing integrator. The vacuum line was a conventional mercury-free Pyrex line with greaseless stopcocks. The vacuum was maintained by an Edwards two-stage rotary pump (model E2M2) in combination with a cryogenic trap and monitored with a vacuum gauge (Edwards Speedivac-Gauge model B5). Reactant vapour pressures were measured using a Chell 10 Torr pressure gauge coupled with a CPD 1A pressure readout unit. The reactants were swept into the reaction chamber with diluent gas via a 1/8" o.d. Teflon tube and all flow rates were monitored by an Aalborg mass flow meter (model GFM 1700). The flow of molecular hydrogen into the reaction chamber was monitored by an Alltech digital flow meter (model 4700).

The reaction chamber was a 50 litre FEP Teflon bag housed in a constant temperature cabinet and surrounded by two banks of photolysis lamps. Germicidal lamps (Philips TUV 15W, $\lambda = 254\text{nm}$) were used to generate OH radicals by photolysing ozone in the presence of molecular hydrogen while white lamps (Thorn 40W, $290 < \lambda < 400\text{nm}$) were used to generate chlorine atoms from photolysis of molecular chlorine. Heat, when required, was supplied by a hot air blower with temperatures maintained within $\pm 2\text{K}$ and monitored with a DeltaOhm temperature probe (model HD 8501 H).

3.3 PROCEDURE

Zero-grade air was passed through an ozone generator (Monitor Labs) for 10 minutes at a flow rate of 3 litres/min giving a final ozone mixing ratio of ~ 1000 ppm. Hydrogen was then passed directly into the reaction chamber from a lecture bottle at 0.5 litres/min. for 1 minute to give a final mixing ratio of $\sim 10,000$ ppm. The reference organic was degassed

using liquid nitrogen before a known quantity of the vapour was allowed into a calibrated bulb (121 cm³). The vapour in the remainder of the vacuum line was condensed into its storage trap using liquid nitrogen. The contents of the calibrated bulb were then flushed into the reaction chamber by a stream of zero-grade air. This procedure was repeated for the substrate aromatic resulting in mixing ratios in the range 5 – 20 ppm for the substrate and reference organic. The reaction chamber was covered with an opaque cover to prevent pre-photolysis of the reactants. After ~30 minutes a gas chromatographic analysis was carried out in triplicate to ensure that the reactant aromatic and reference organic were uniformly mixed. The reactants were then irradiated for ~20 second periods between which gas chromatographic analyses were carried out in duplicate to determine the loss of both substrate aromatic and reference organic.

3.4 ANALYSIS

Concentrations of the substrate aromatic and reference organic were measured by gas chromatography (Shimadzu GC 8A or Ai Cambridge model GC94), with flame ionisation detection. Samples of the reaction mixture were drawn through a 2 cm³ Teflon coated stainless steel sample loop using a rotary pump. On-column injection of gas samples was carried out using a six port Valco gas sampling valve connected in series with the GC carrier gas flow circuit. Chromatograms were recorded and stored on a computing integrator (Spectra-Physics Data Jet). Concentrations of aromatic substrate and reference organic were determined by measuring peak heights and peak areas. Table 3.1 shows the reference organics and analytical conditions used for each aromatic substrate.

Table 3.1 Substrate aromatics, reference organics and gas chromatographic conditions used in this work.

Aromatic Substrate	Reference Organic	Column type	Column length/m	Column i.d./mm	Column temp/°C	Detector temp /°C	N ₂ carrier flow /ml min ⁻¹
toluene	cyclohexane	DB-5	30	0.53	60	90	10
Toluene-d ₈	cyclohexane	DB-5	30	0.53	60	90	10
Ethylbenzene	cyclohexane	DB-5	30	0.53	70	90	10
n-propylbenzene	cyclohexane	DB-5	30	0.53	70	90	10
n-butylbenzene	cyclohexane	DB-5	30	0.53	80	100	10
o-diethylbenzene	cyclohexane	DB-5	30	0.53	100	120	10
indane	cyclohexane	DB-5	30	0.53	100	160	10
tetralin	cyclohexane	DB-5	30	0.53	100	160	10
1,2,4,5-tetramethylbenzene	1,3,5-trimethylbenzene	DB-5	30	0.53	100	120	10
2-fluorotoluene	cyclohexane	DB-5	30	0.53	80	100	10
3-fluorotoluene	cyclohexane	DB-5	30	0.53	80	100	10
4-fluorotoluene	cyclohexane	DB-5	30	0.53	80	100	10
2-chlorotoluene	cyclohexane	DB-5	30	0.53	80	100	10
3-chlorotoluene	cyclohexane	DB-5	30	0.53	80	100	10
4-chlorotoluene	cyclohexane	DB-5	30	0.53	80	100	10

The experimental procedure for the temperature dependant studies was similar to that outlined for the room temperature experiments. Reactions were carried out at a number of temperatures over the range 243 – 323 K.

A set of experiments was also carried out at room temperature using toluene as the substrate, cyclohexane as the reference and photolysis of ozone in the presence of water vapour as the source of OH radicals. The same procedure was followed for introducing the substrate, reference and ozone. In place of hydrogen liquid water ($\sim 0.5 \text{ cm}^3$) was injected into a heated reservoir, vaporised and flushed into the reaction chamber in a stream of zero grade air to give a final mixing ratio of $\sim 10,000$ ppm.

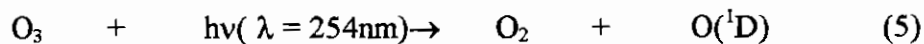
The reactivity of two aromatics (indane and tetralin) with chlorine atoms was also investigated. The experimental procedure for introducing the substrate and reference was similar to that described previously for the hydroxyl radical reactions. A known pressure of molecular chlorine was placed in a calibrated bulb. The chlorine in the remainder of the vacuum line was condensed into its storage bulb using liquid nitrogen. The contents of the calibrated bulb were then flushed into the reaction chamber with zero grade air to give a final mixing ratio of 100 ppm. After uniform mixing the reactants were irradiated by two banks of fluorescent lamps (Thorn 40W) for 2 minute periods between which gas chromatographic analyses were carried out in duplicate to determine the decay of substrate aromatic and reference organic.

4.0 RESULTS

4.1 ROOM TEMPERATURE OH RADICAL REACTIONS

The kinetic investigation was carried out using a relative rate method. This method is based on monitoring the relative decay rates of two or more organics, including one whose OH radical reaction rate constant is well known.

Hydroxyl radicals were generated from the photolysis of ozone in the presence of molecular hydrogen:



In air the hydrogen atom produced reacts with molecular oxygen to form a hydroperoxy radical (reaction 34) which reacts with ozone to generate another OH radical (reaction 35):



The aromatic substrate and reference organic (cyclohexane) react with the OH radical:



Provided that the aromatic and cyclohexane are consumed solely by reactions (36) and (37) respectively and since dilution due to sampling is avoided by the use of a collapsible Teflon chamber, the loss of aromatic and cyclohexane may be expressed as:

$$\frac{-d[\text{aromatic}]}{dt} = k_{36}[\text{OH}][\text{aromatic}] \quad \text{X}$$

and

$$\frac{-d[\text{cyclohexane}]}{dt} = k_{37}[\text{OH}][\text{cyclohexane}] \quad \text{XI}$$

where k_{36} and k_{37} are the bimolecular rate constants for reactions (36) and (37) respectively. Rearranging and integrating X and XI yields the expression (described in detail in section 2.3.2):

$$\ln \frac{[\text{aromatic}]_0}{[\text{aromatic}]_t} = \frac{k_{36}}{k_{37}} \ln \frac{[\text{cyclohexane}]_0}{[\text{cyclohexane}]_t} \quad \text{XII}$$

where $[\text{aromatic}]_0$ and $[\text{cyclohexane}]_0$ are the concentrations of the aromatic and cyclohexane at time zero and $[\text{aromatic}]_t$ and $[\text{cyclohexane}]_t$ are the corresponding concentrations at time t . Thus a plot of $\ln([\text{aromatic}]_0/[\text{aromatic}]_t)$ against $\ln([\text{cyclohexane}]_0/[\text{cyclohexane}]_t)$ should yield a straight line of slope k_{36}/k_{37} and zero intercept. A knowledge of k_{37} allows k_{36} to be calculated from the slope.

When using the relative rate technique any loss of substrate and/or reference other than by reaction with the OH radical (e.g. wall loss and/or photolysis) must be taken into

account. To check for such loss processes both substrate and reference were allowed to remain in the dark over the time-scale of the experiments. No measurable loss of any of the aromatic substrates or reference was observed. Secondly, mixtures of substrate and reference were irradiated in the absence of the radical precursor. No significant loss of substrate or reference was observed for all aromatics studied. Separate mixtures of substrate and reference were irradiated in the presence of the radical precursor to check for interference from reaction products in the gas chromatographic analysis of aromatic and reference.

Plots in the form of equation XII are shown in Figures 4.1 - 4.8 for the aromatics studied in this work. The slopes of these plots k_{36}/k_{37} and the calculated bimolecular rate constants are shown in Table 4.1. These values were placed on an absolute basis using the following recommended room temperature rate constants:

$$k(\text{OH} + \text{cyclohexane}) = 7.21 \times 10^{-12} \text{ cm}^3 \text{ molecule}^{-1} \text{ s}^{-1} [87]$$

and

$$k(\text{OH} + 1,3,5\text{-trimethylbenzene}) = 57.5 \times 10^{-12} \text{ cm}^3 \text{ molecule}^{-1} \text{ s}^{-1} [29]$$

Figure 4.1 Plots in the form of equation XII for the reaction of Toluene with OH radicals using irradiated O_3/H_2O mixtures and irradiated O_3/H_2 mixtures as the source of OH radicals at $298 \pm 2K$ and 1 atm total pressure.

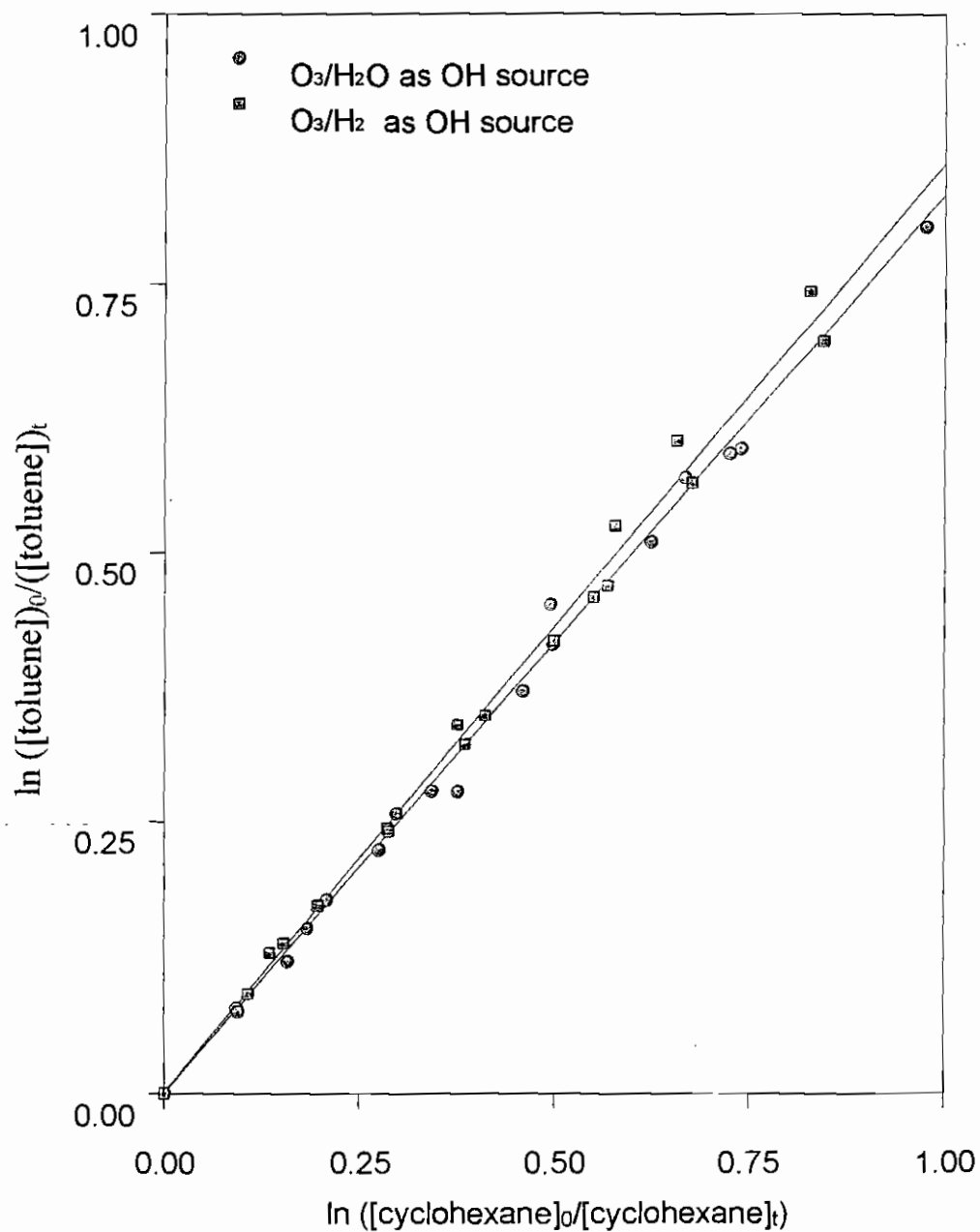


Figure 4.2 Plots in the form of equation XII for the reaction of Toluene-h₈ and Toluene-d₈ with OH radicals at 298±2K and 1 atm total pressure.

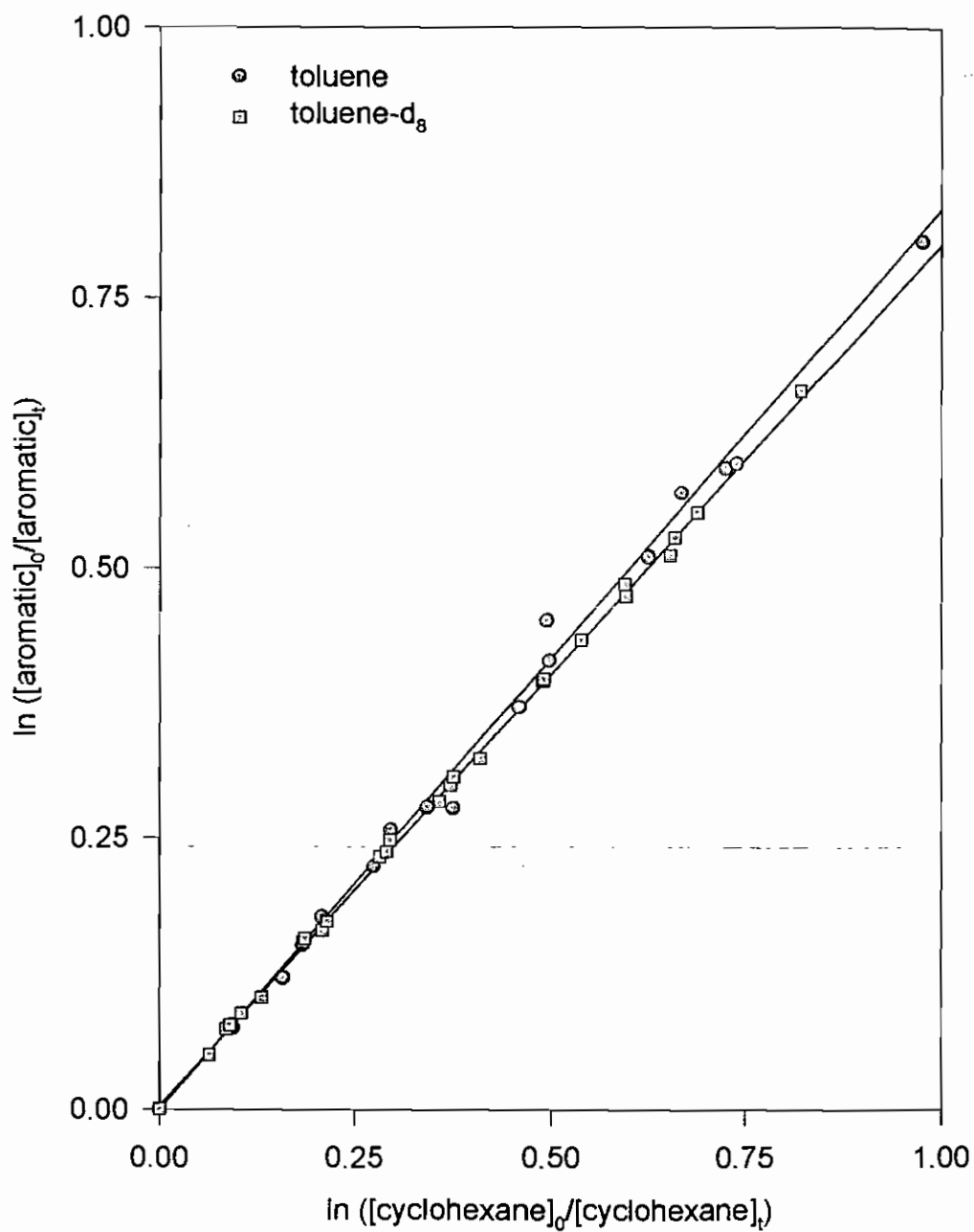


Figure 4.3 Plots in the form of equation XII for the reaction of toluene, Ethylbenzene, n-Propylbenzene and n-Butylbenzene with OH radicals at $298 \pm 2K$ and 1 atm total pressure.

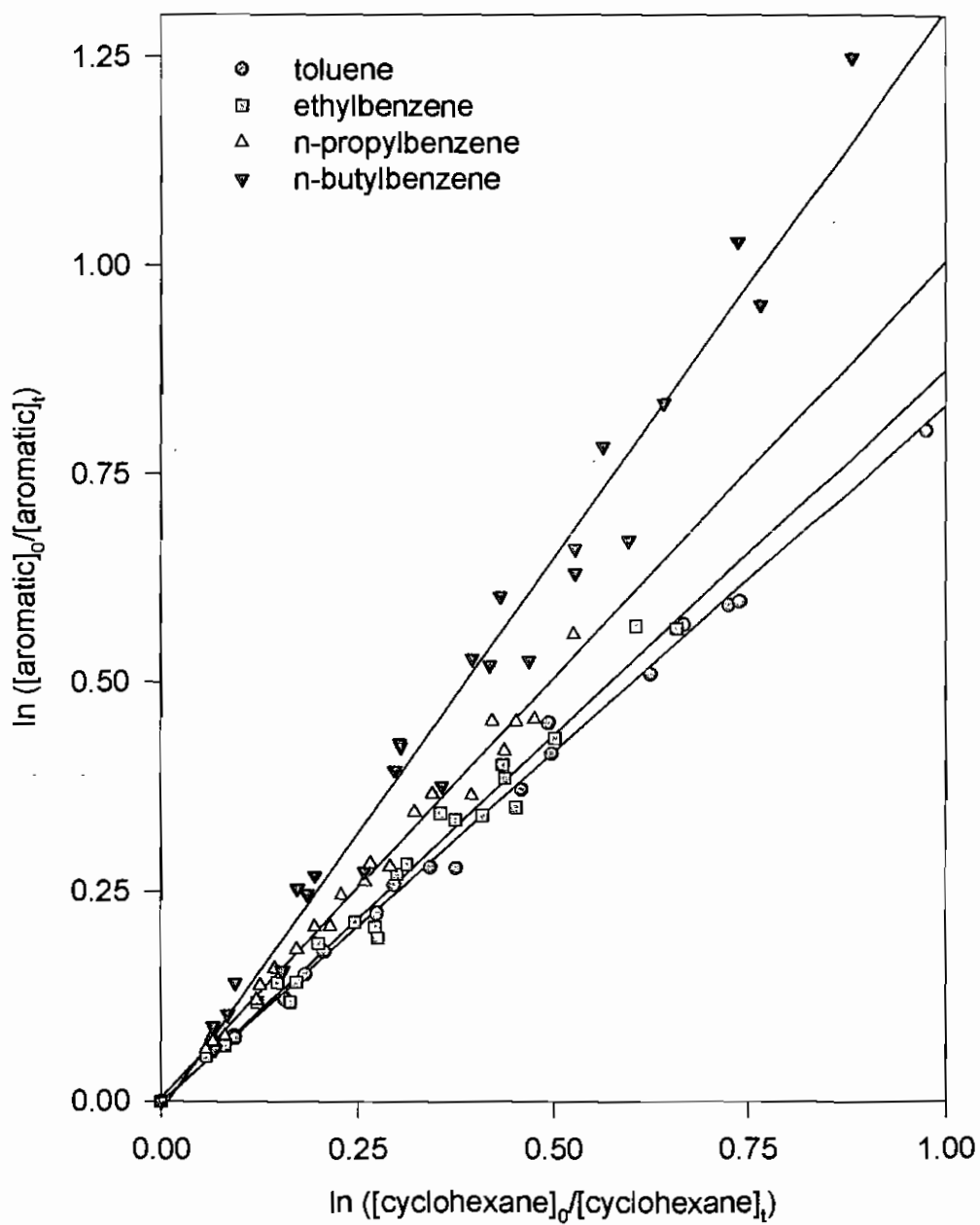


Figure 4.4 Plots in the form of equation XII for the reaction of a series of Alkylbenzenes with OH radicals at $298 \pm 2K$ and at 1 atm total pressure.

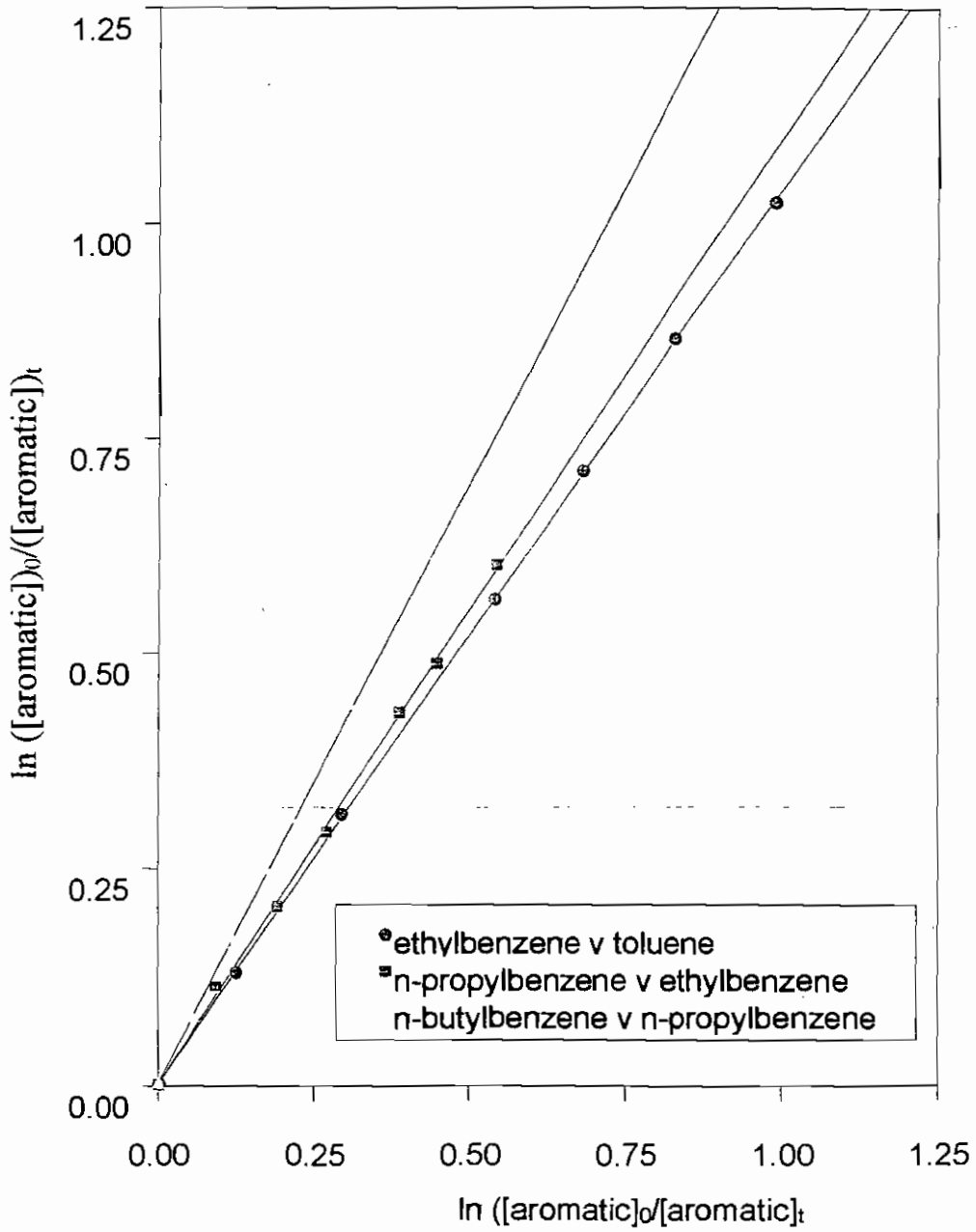


Figure 4.5 Plots in the form of equation XII for the reaction of 2-Fluorotoluene, 3-Fluorotoluene and 4-Fluorotoluene with OH radicals at $298 \pm 2K$ and 1 atm total pressure.

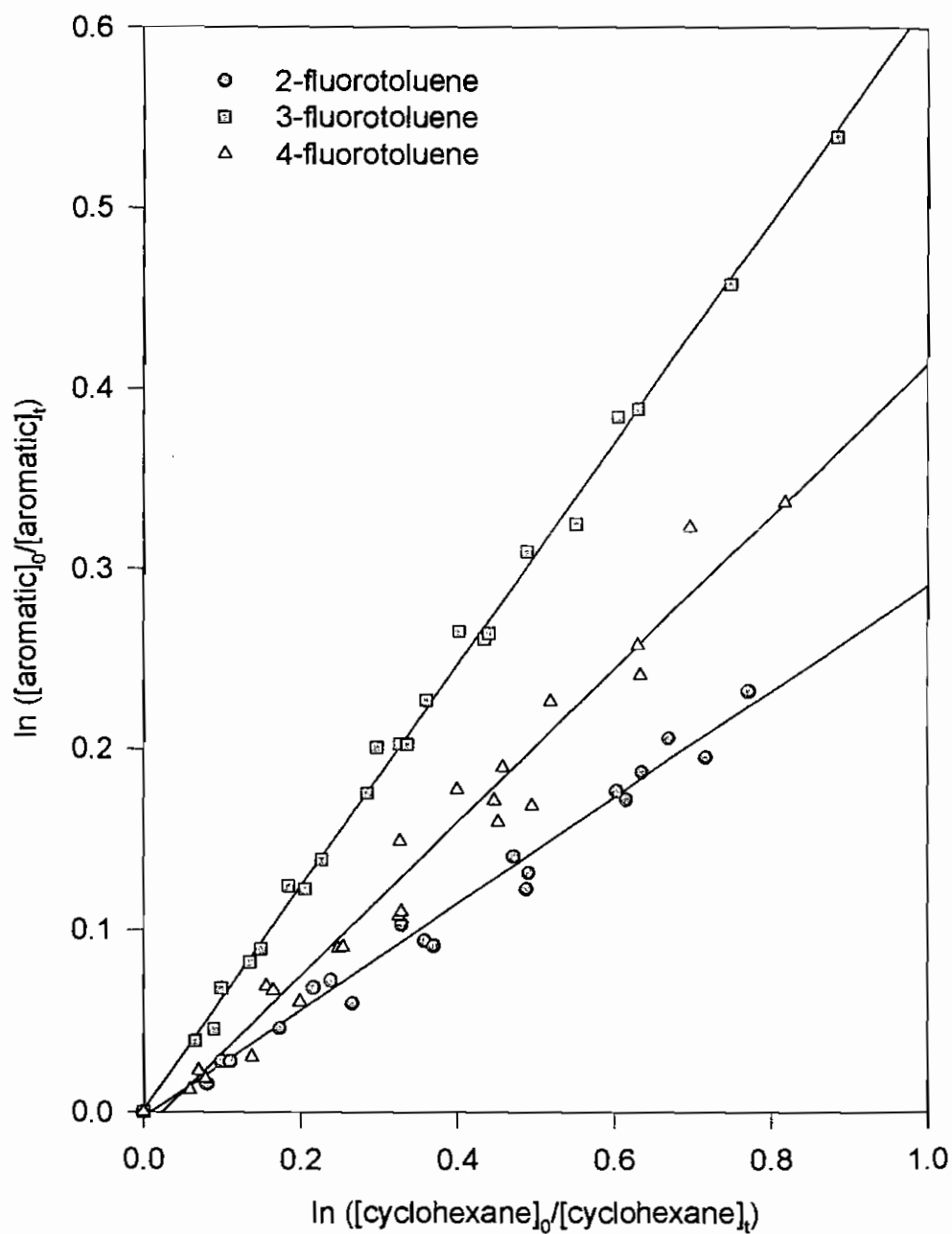


Figure 4.6 Plots in the form of equation XII for the reaction of 2-Chlorotoluene, 3-Chlorotoluene and 4-Chlorotoluene with OH radicals at $298 \pm 2K$ and 1 atm total pressure.

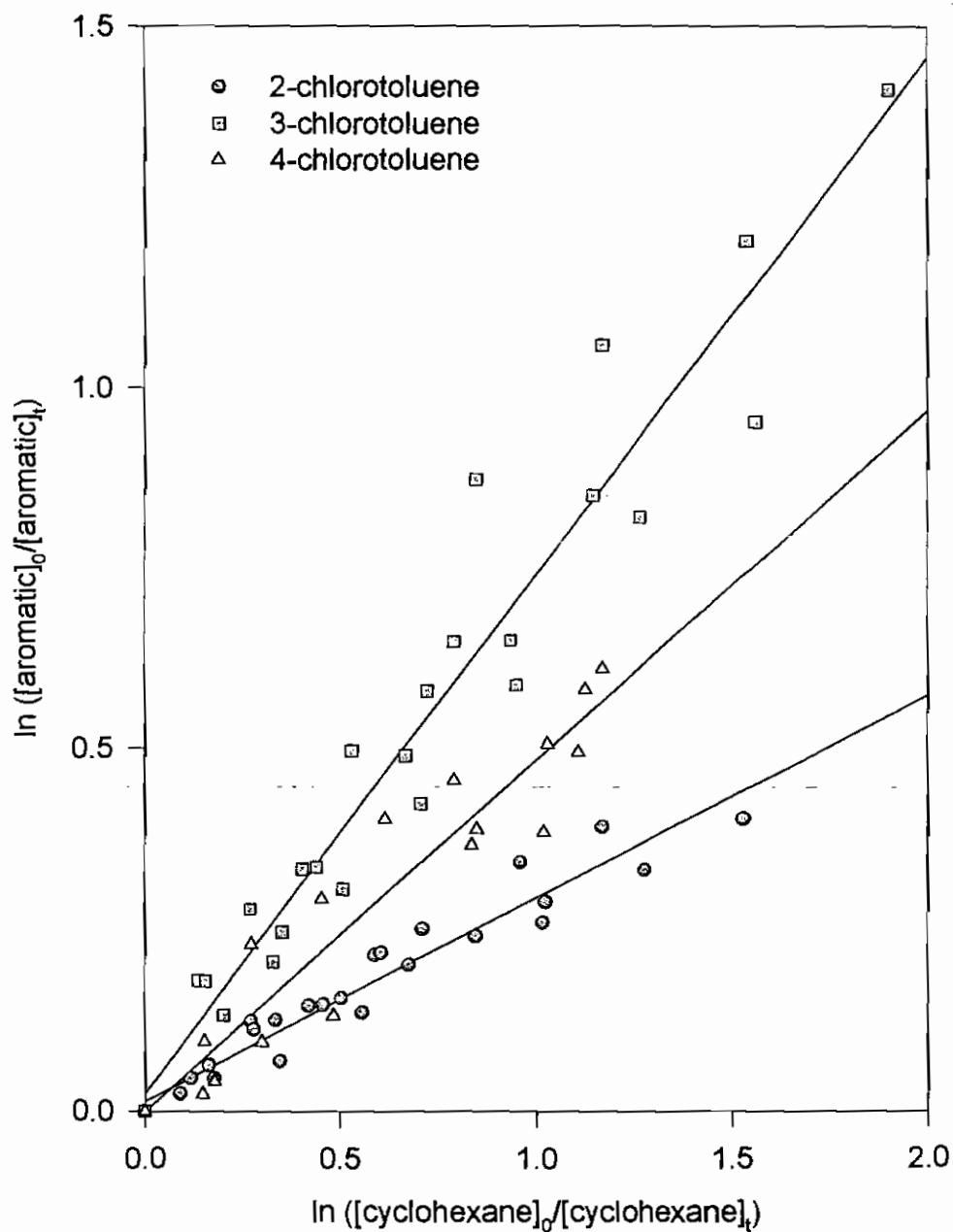


Figure 4.7 Plot in the form of equation XII for the reaction of 1,2,4,5-Tetramethylbenzene with OH radicals at $298 \pm 2K$ and 1 atm total pressure.

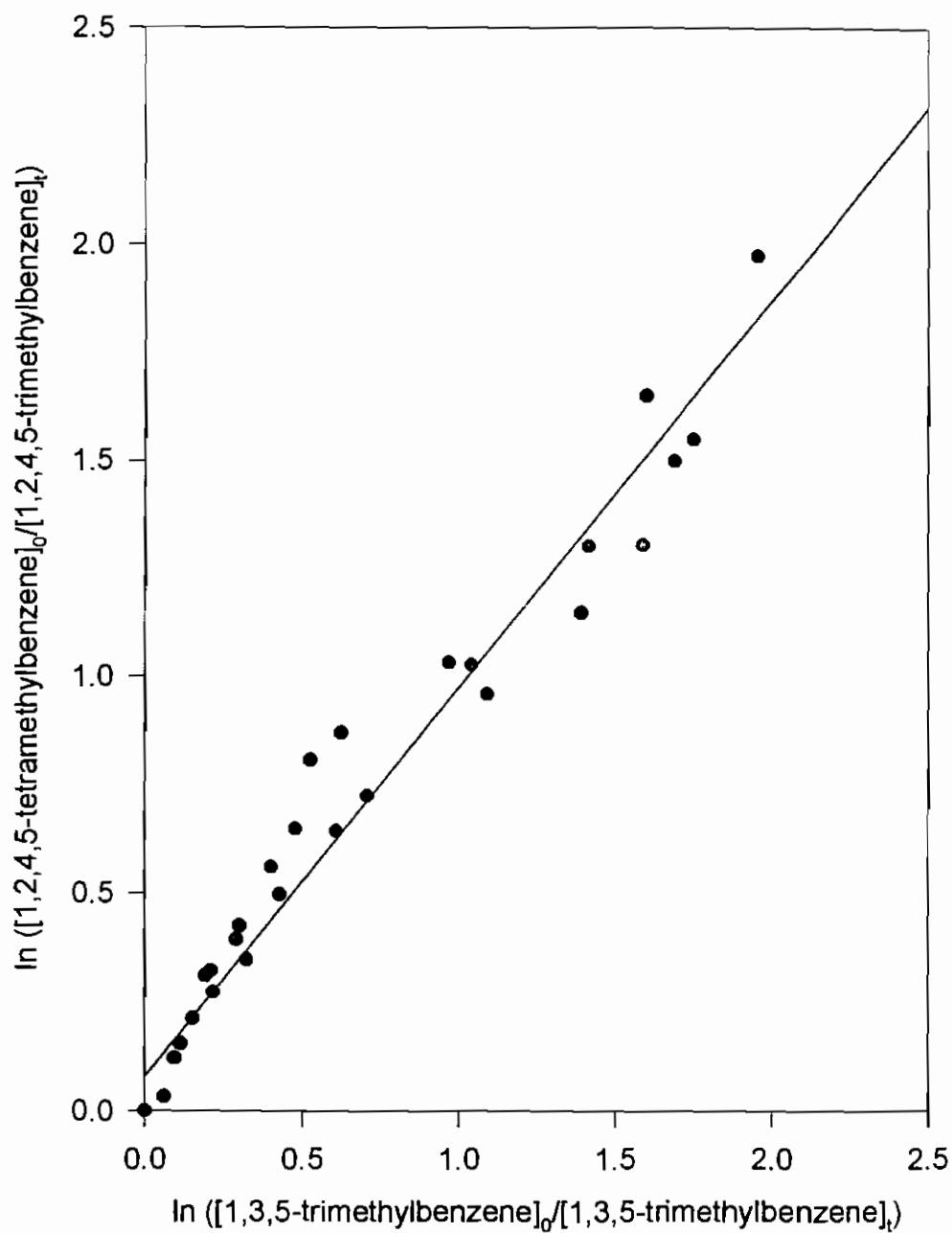


Figure 4.8 Plots in the form of equation XII for the reaction of *ortho*-Diethylbenzene, Indane and Tetralin with OH radicals at $298 \pm 2\text{K}$ and 1 atm total pressure.

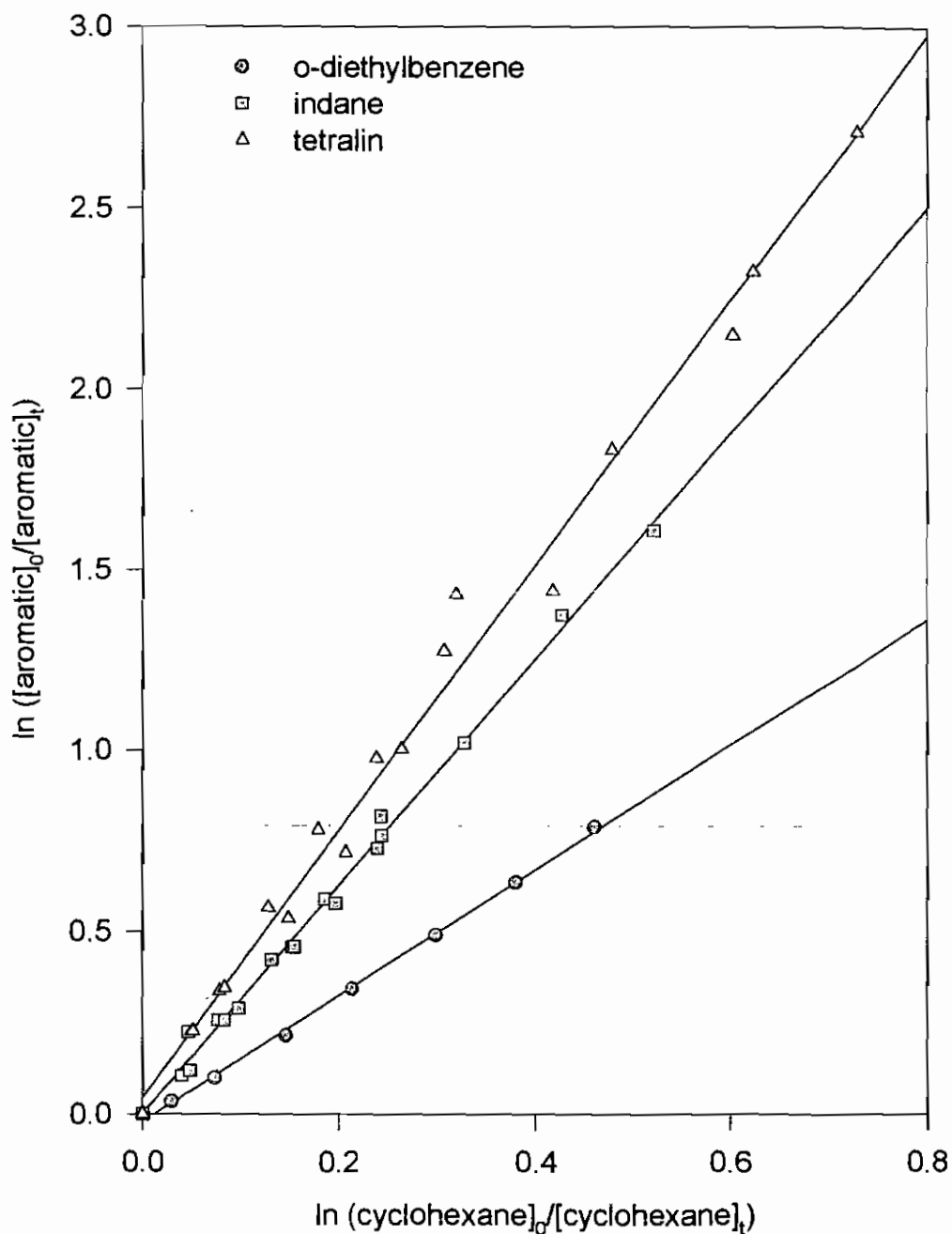


Table 4.1 Rate constant ratios, k_{36}/k_{37} , and calculated rate constants for the reaction of OH radicals with Aromatic compounds at $298 \pm 2K$ and 1 atm total pressure.

Aromatic	Slope k_{36} / k_{37}^a	$10^{12} \times k^b$ $\text{cm}^3 \text{ molecule}^{-1} \text{ s}^{-1}$
Toluene	0.82 ± 0.03	5.94 ± 0.22
Toluene-d ₈	0.80 ± 0.01	5.77 ± 0.07
Ethylbenzene	0.88 ± 0.04	6.34 ± 0.29
n-propylbenzene	1.00 ± 0.04	7.21 ± 0.29
n-butylbenzene	1.32 ± 0.07	9.52 ± 0.50
2-fluorotoluene	0.29 ± 0.01	2.09 ± 0.07
3-fluorotoluene	0.61 ± 0.01	4.40 ± 0.07
4-fluorotoluene	0.42 ± 0.02	3.03 ± 0.14
2-chlorotoluene	0.34 ± 0.03	2.45 ± 0.22
3-chlorotoluene	0.65 ± 0.07	4.72 ± 0.50
4-chlorotoluene	0.48 ± 0.06	3.46 ± 0.43
1,2,4,5-tetramethylbenzene	0.90 ± 0.06	51.6 ± 3.4
ortho-diethylbenzene	1.73 ± 0.06	12.5 ± 0.4
Indane	3.31 ± 0.26	23.9 ± 1.9
Tetralin	3.67 ± 0.18	26.5 ± 1.3

a: Errors quoted are two least-squares standard deviations of the slopes of the plots shown in Figures 4.1 – 4.8.

b: Errors quoted do not include the error in the rate constant for reaction of OH radicals with the reference organic.

4.2 TEMPERATURE DEPENDANT OH RADICAL REACTIONS

The protocol for measuring the rate constants as a function of temperature was similar to that used for the room temperature studies. Cyclohexane was used as the reference organic and relative rate constants were placed on an absolute basis using the temperature dependant $k(\text{OH} + \text{cyclohexane})$ rate expression recommended by Atkinson [87]:

$$k(\text{OH} + \text{cyclohexane}) = 2.88 \times 10^{-17} T^2 e^{(309 \pm 35/T)} \text{ cm}^3 \text{ molecule}^{-1} \text{ s}^{-1}$$

The aromatics selected for study were toluene, 3-fluorotoluene, 3-chlorotoluene, indane and tetralin. Relative rates of decay were measured at various temperatures over the range 245 - 323K and plots in the form of equation XII for each temperature are shown in Figures 4.9, 4.11, 4.13, 4.15 and 4.17. The rate constant ratios, k_{36}/k_{37} , and the calculated rate constants, k_{36} , are shown in Table 4.2 for each aromatic. Rate constants as a function of temperature, plotted in Arrhenius form, are shown in Figures 4.10, 4.12, 4.14, 4.16 and 4.18. The Arrhenius parameters obtained from these plots are shown in Table 4.3.

Figure 4.9 Plots in the form of equation XII for the reaction of Toluene with OH radicals over the temperature range 243 - 323K and at 1 atm total pressure.

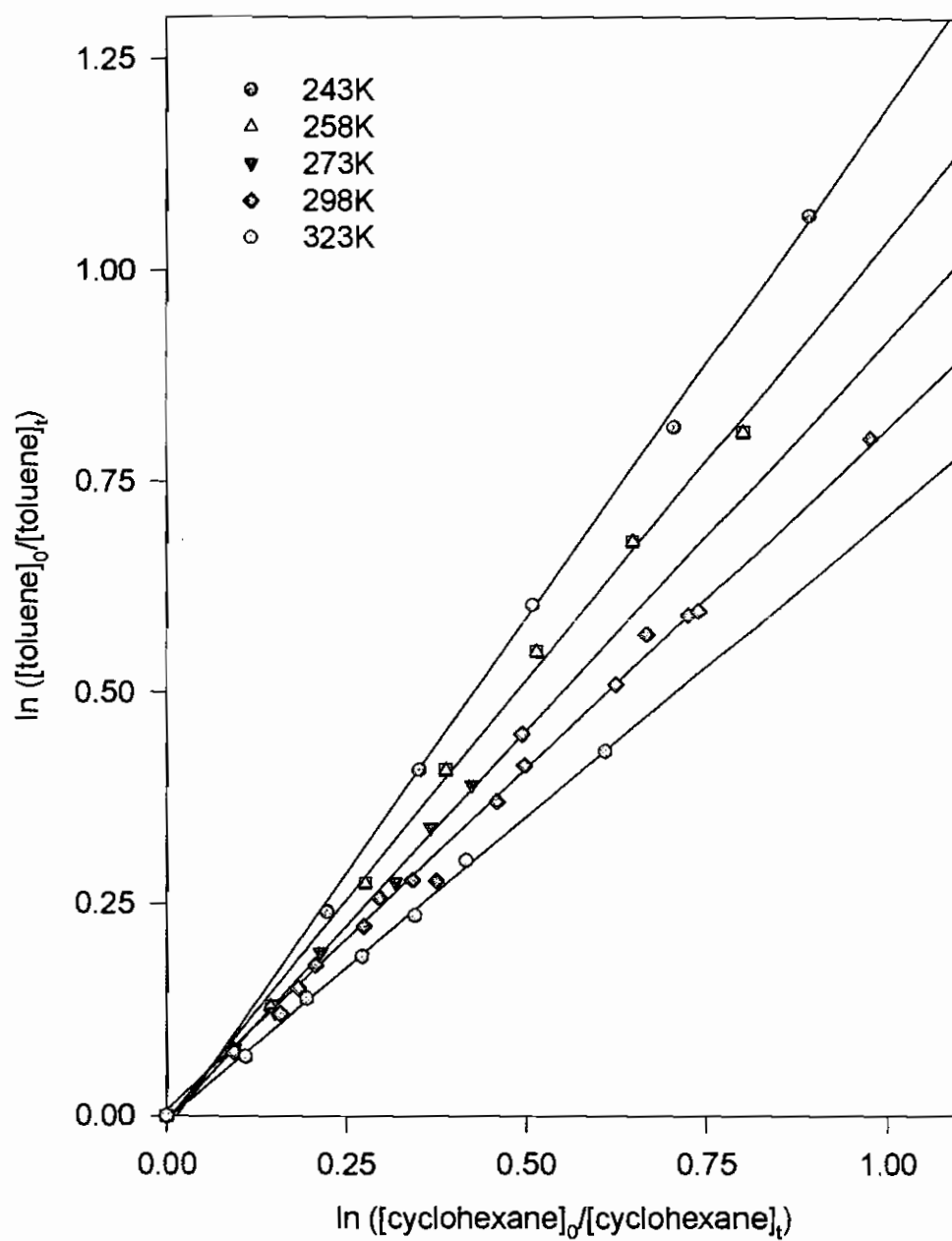


Figure 4.10 Arrhenius plot for the reaction of Toluene with OH radicals over the temperature range 243 - 323 K and at 1atm total pressure.

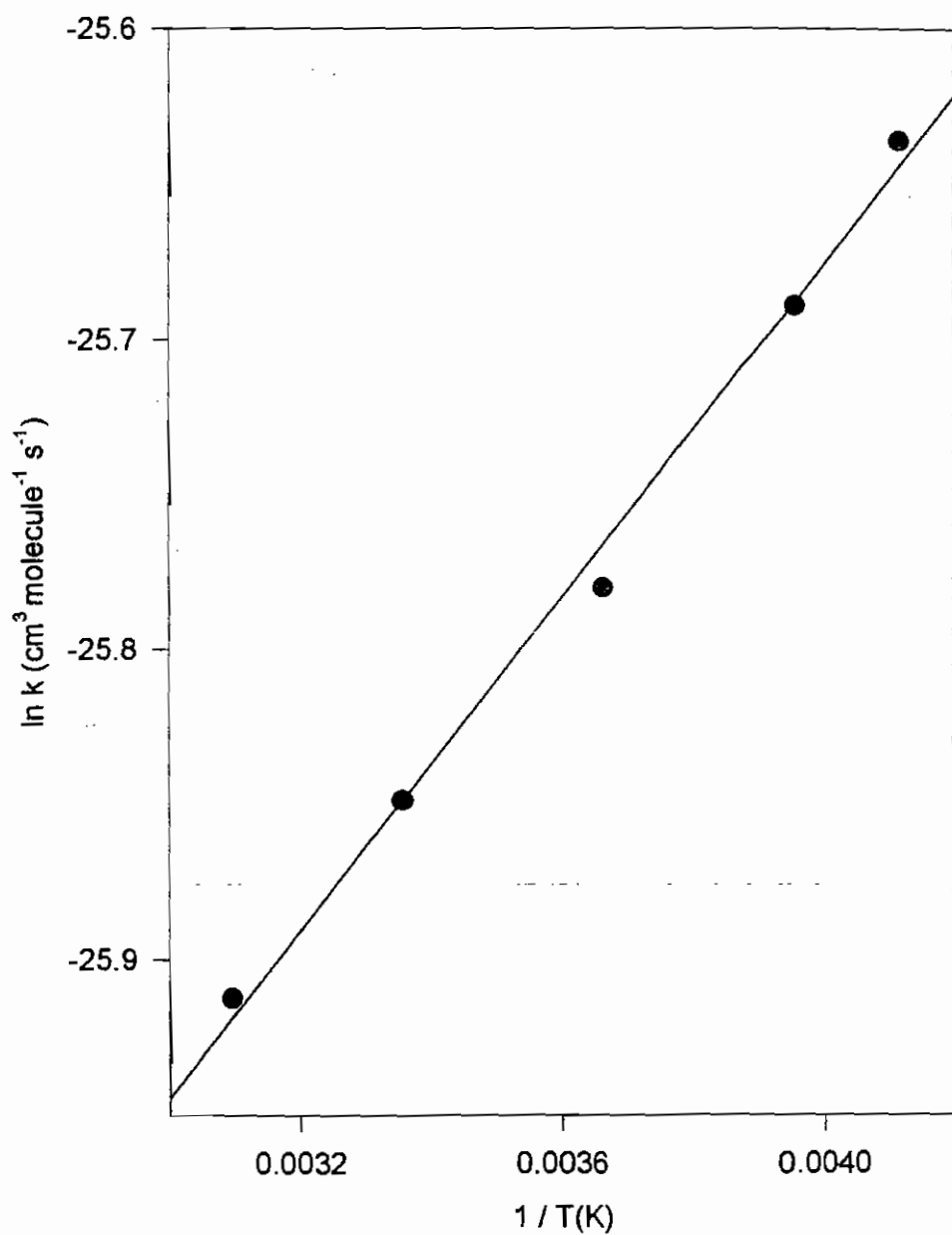


Figure 4.11 Plots in the form of equation XII for the reaction of 3-Fluorotoluene with OH radicals over the temperature range 248 - 323K and at 1 atm total pressure.

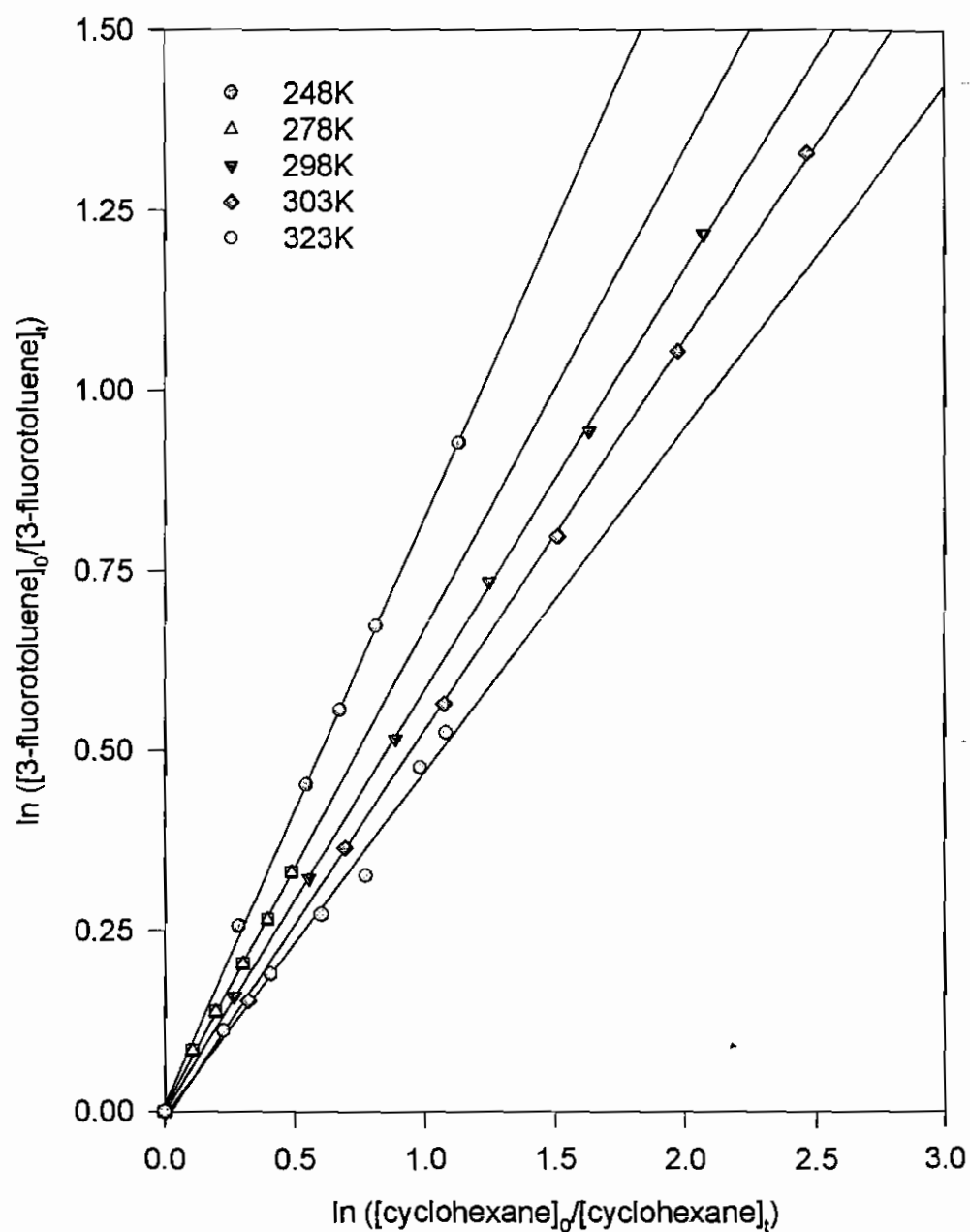


Figure 4.12 Arrhenius plot for the reaction of 3-Fluorotoluene with OH radicals over the temperature range 248 - 323 K and at 1 atm total pressure.

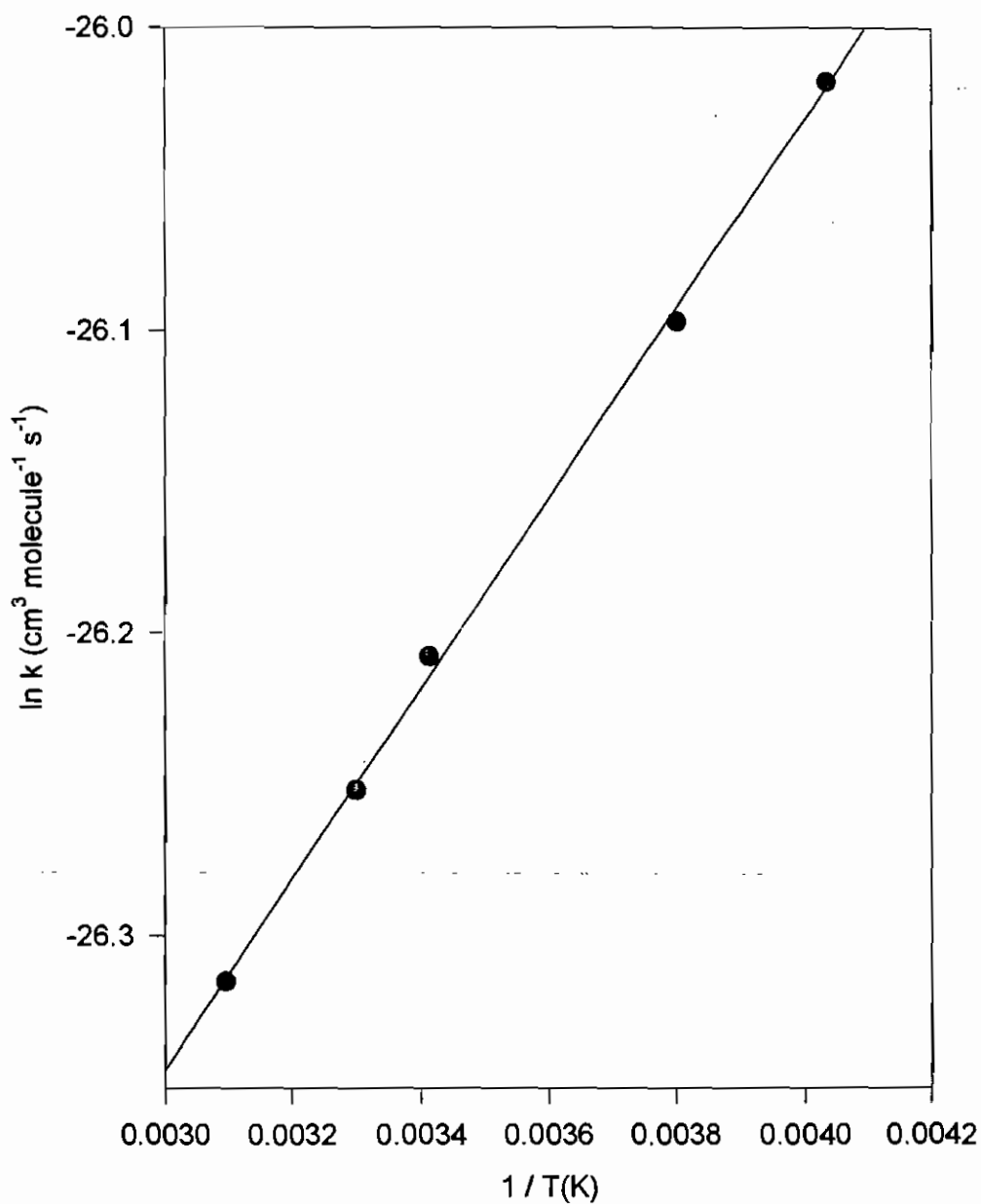


Figure 4.13 Plots in the form of equation XII for the reaction of 3-Chlorotoluene with OH radicals over the temperature range 243 - 323K and at 1 atm total pressure.

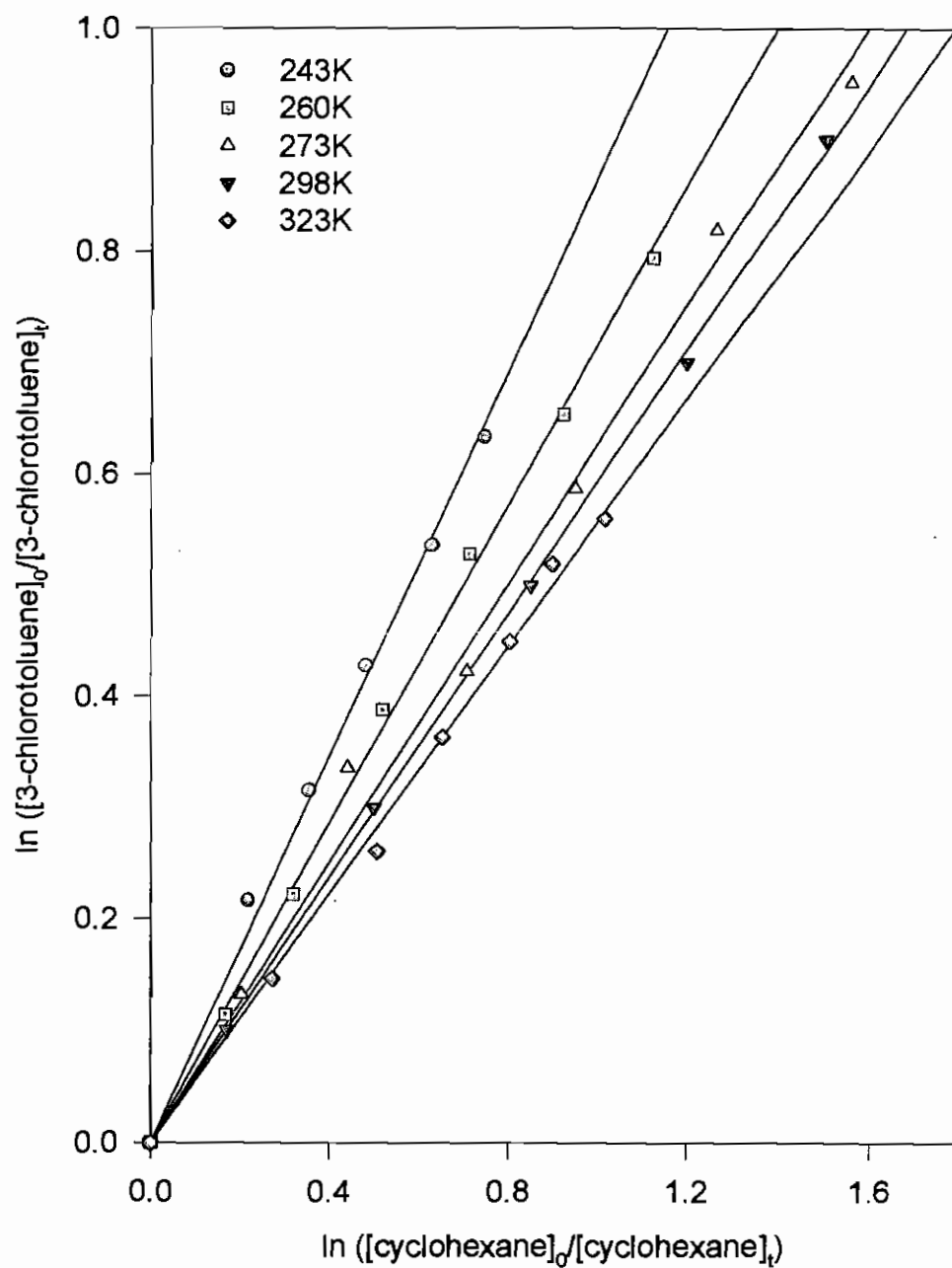


Figure 4.14 Arrhenius plot for the reaction of 3-Chlorotoluene with OH radicals over the temperature range 243 - 323 K and at 1 atm total pressure.

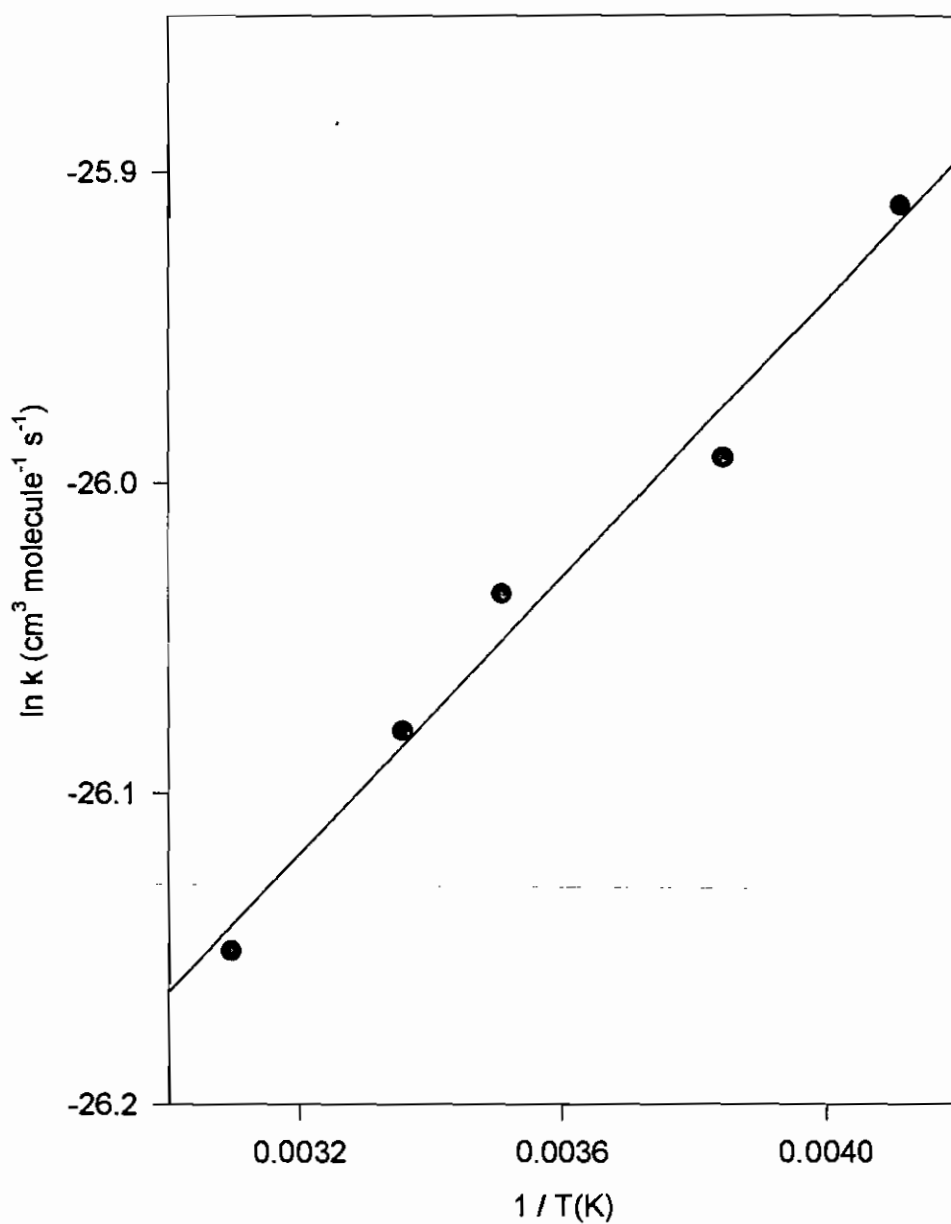


Figure 4.15 Plots in the form of equation XII for the reaction of Indane with OH radicals over the temperature range 245 - 323K and at 1 atm total pressure.

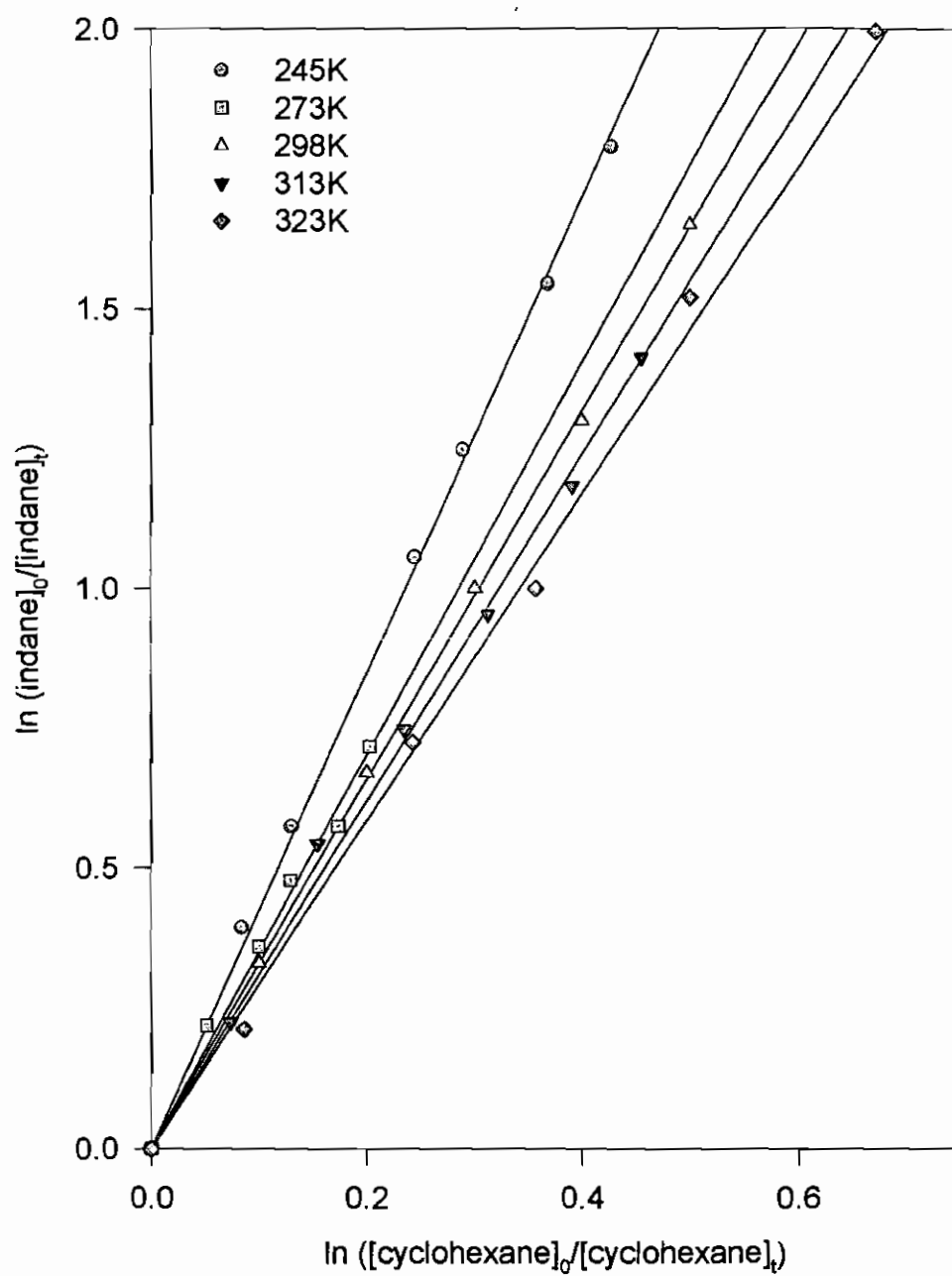


Figure 4.16 Arrhenius plot for the reaction of Indane with OH radicals over the temperature range 245 - 323 K and at 1 atm total pressure.

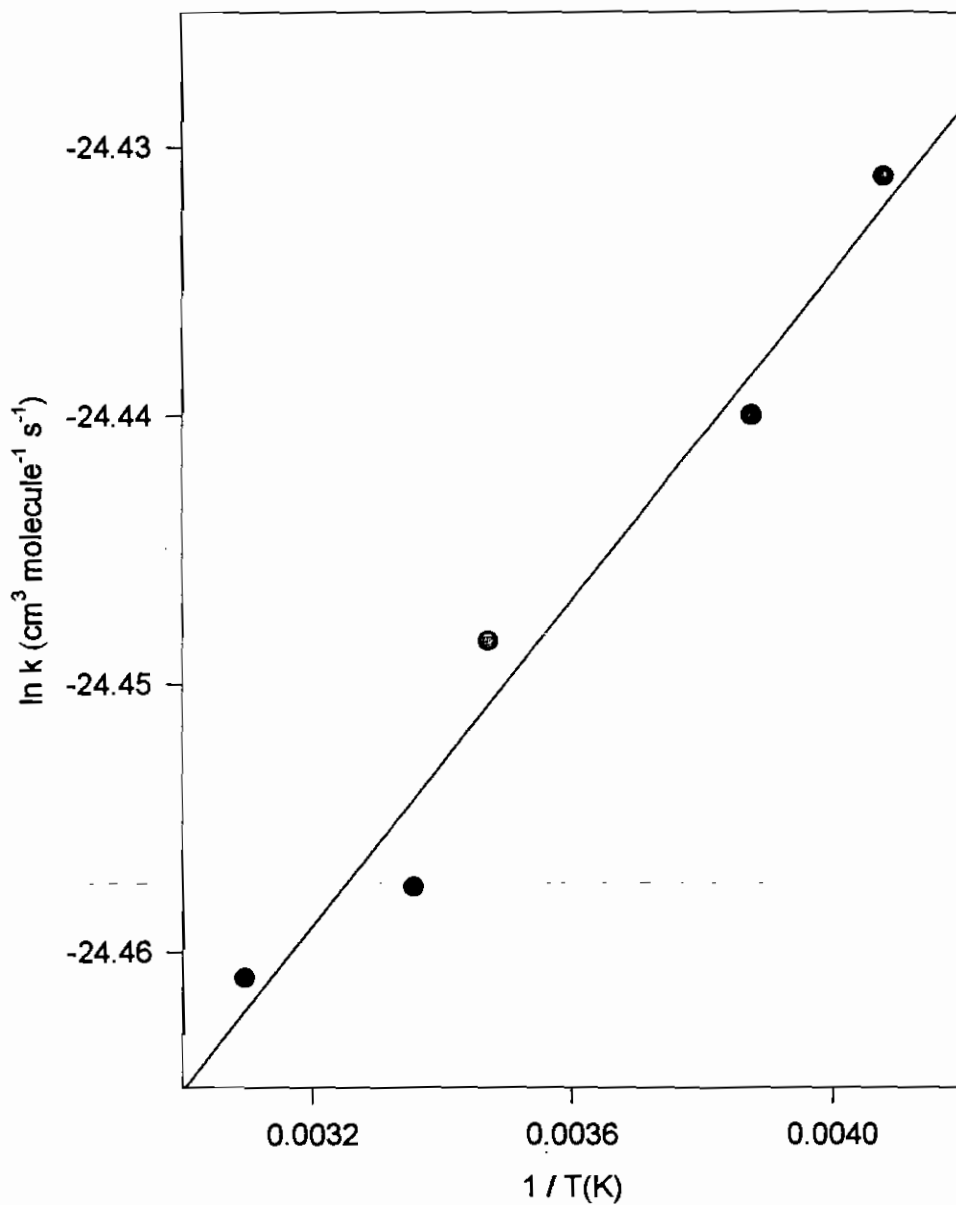


Figure 4.17 Plots in the form of equation XII for the reaction of Tetralin with OH radicals over the temperature range 243 - 323K and at 1 atm total pressure.

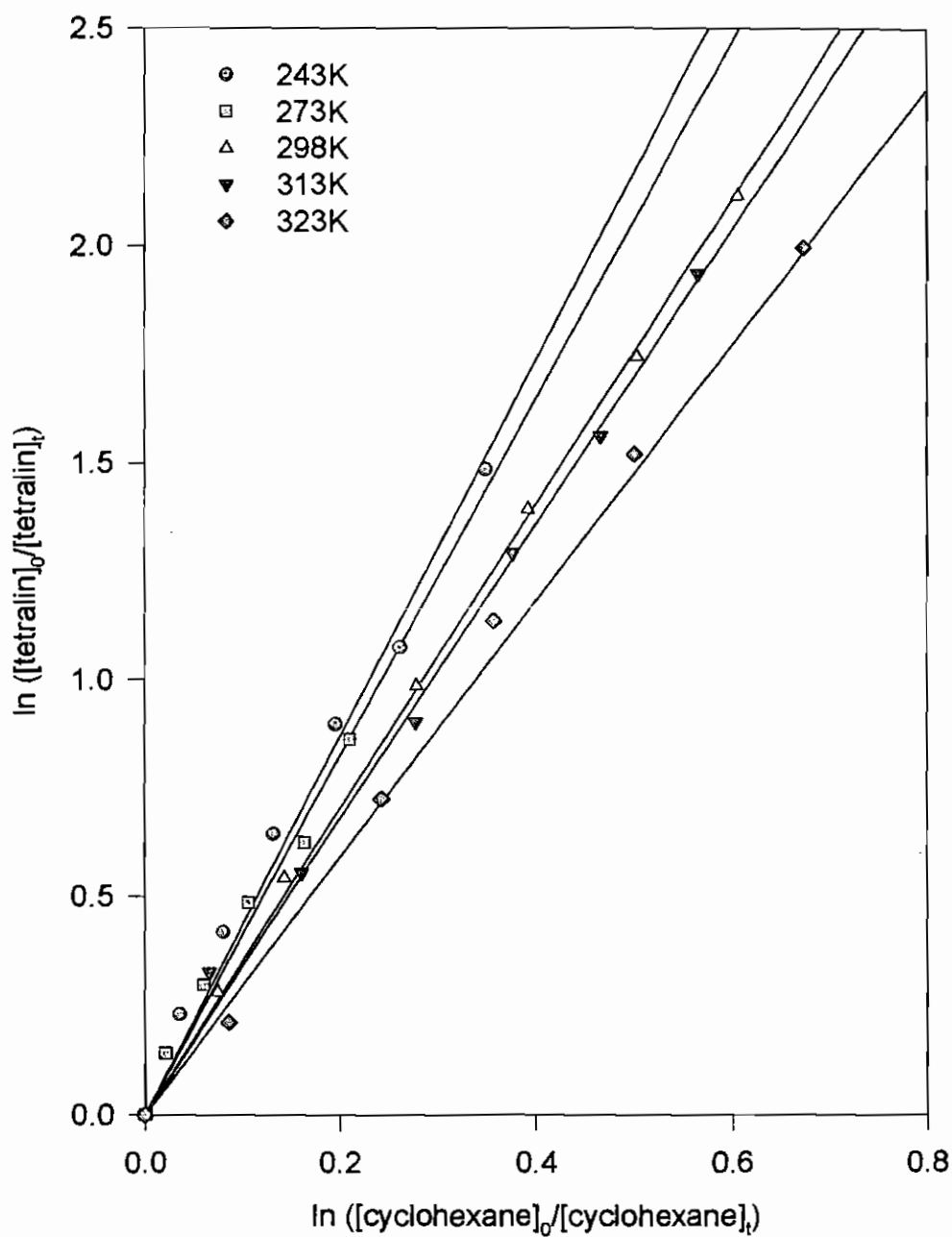


Figure 4.18 Arrhenius plot for the reaction of Tetralin with OH radicals over the temperature range 243 - 323 K and 1 atm total pressure.

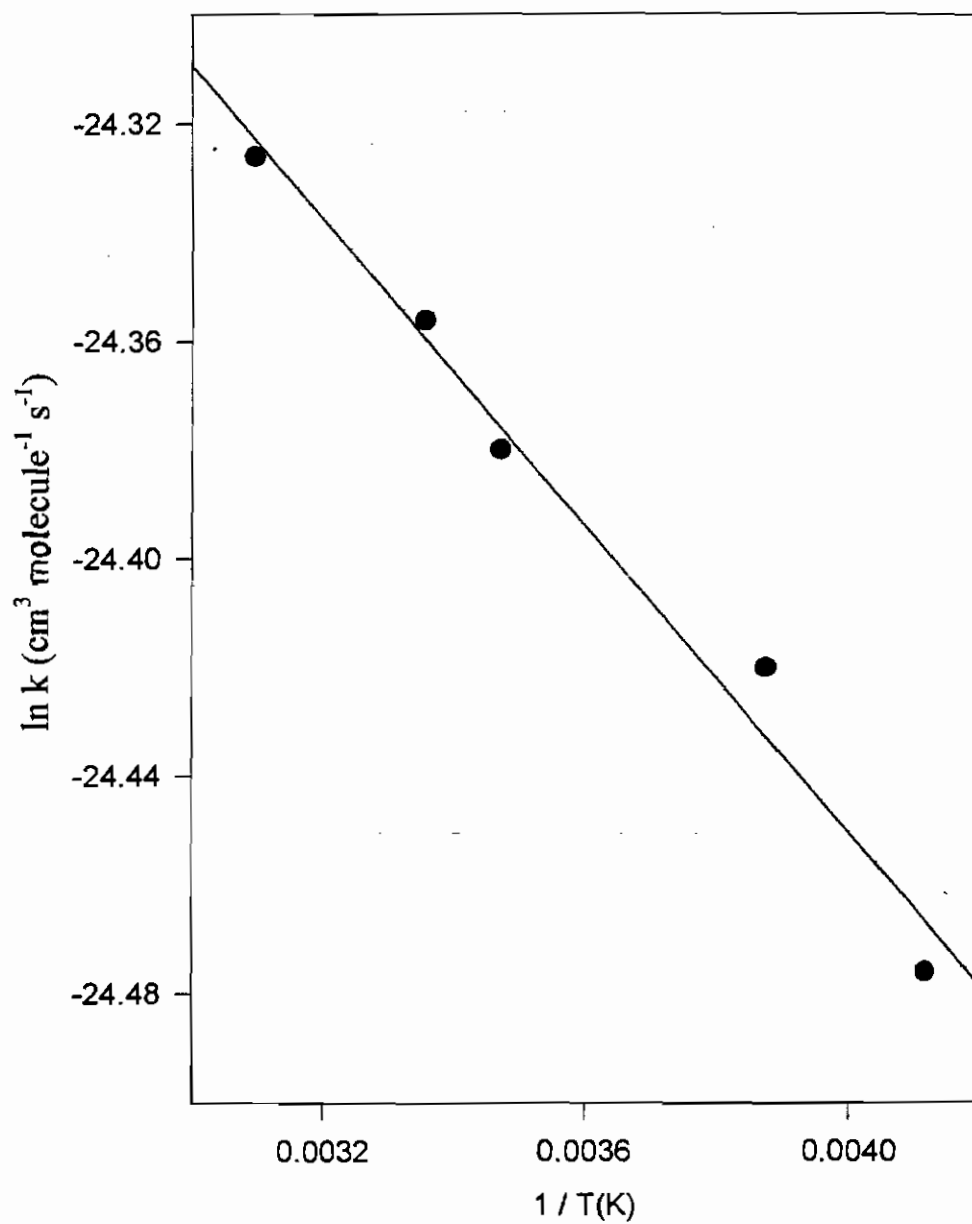


Table 4.2 Rate constant ratios, k_{36}/k_{37} , and calculated rate constants for the reaction of OH radicals with a series of Aromatic compounds over the temperature range 243 - 323K and at 1 atm total pressure.

Aromatic	Temperature K	Slope k_{36}/k_{37}	$10^{12} \times k$ $\text{cm}^3 \text{ molecule}^{-1} \text{ s}^{-1}$
Toluene	243	1.21 ± 0.02	7.35
	258	1.04 ± 0.02	6.62
	273	0.95 ± 0.01	6.34
	298	0.824 ± 0.03	5.94
	323	0.742 ± 0.02	5.80
3-fluorotoluene	248	0.82 ± 0.03	5.02
	278	0.67 ± 0.02	4.50
	298	0.61 ± 0.01	4.40
	303	0.55 ± 0.01	4.06
	323	0.48 ± 0.02	3.74
3-chlorotoluene	243	0.91 ± 0.03	5.53
	260	0.80 ± 0.04	5.11
	273	0.74 ± 0.08	4.92
	298	0.65 ± 0.07	4.72
	323	0.56 ± 0.05	4.39
Indane	245	4.02 ± 0.14	24.51
	273	3.66 ± 0.28	24.33
	298	3.31 ± 0.26	23.86
	313	3.15 ± 0.22	23.83
	323	3.04 ± 0.35	23.79
Tetralin	243	3.85 ± 0.23	23.37
	273	3.73 ± 0.11	24.82
	298	3.67 ± 0.18	26.46
	313	3.51 ± 0.16	26.57
	323	3.49 ± 0.24	27.28

Table 4.3 Arrhenius parameters for the reaction of OH radicals with selected Aromatic compounds over the temperature range 243 – 323K and at 1 atm total pressure.

Aromatic	$A \times 10^{12}$ $\text{cm}^3 \text{ molecule}^{-1} \text{ s}^{-1}$	E_a^a kJ mol^{-1}
Toluene	2.41 ± 0.96	-2236 ± 199
3-fluorotoluene	1.41 ± 0.99	-2610 ± 112
3-chlorotoluene	2.22 ± 1.21	-1845 ± 295
indane	21.6 ± 5.9	-249 ± 56
tetralin	42.5 ± 12.8	1172 ± 199

a: Errors quoted are two least-squares standard deviations of the slopes of the plots shown in Figures 4.10, 4.12, 4.14, 4.16 and 4.18.

4.3 ROOM TEMPERATURE Cl ATOM REACTIONS

The reactivity of indane and tetralin with chlorine atoms was investigated using the relative rate method. Cl atoms were generated by photolysis of molecular chlorine:



Plots in the form of equation XII for reaction of indane and tetralin with Cl atoms are shown in Figure 4.19. Rate constant ratios, k_{39}/k_{40} , and bimolecular rate constants, k_{39} , are shown in Table 4.4. Rate constants were placed on an absolute basis using:

$$k(\text{Cl} + \text{cyclohexane}) = 3.08 \times 10^{-10} \text{ cm}^3 \text{ molecule}^{-1} \text{ s}^{-1} [88]$$

Figure 4.19 Plots in the form of equation XII for the reaction of Indane and Tetralin with Cl atoms at $298 \pm 2\text{K}$ and 1 atm total pressure.

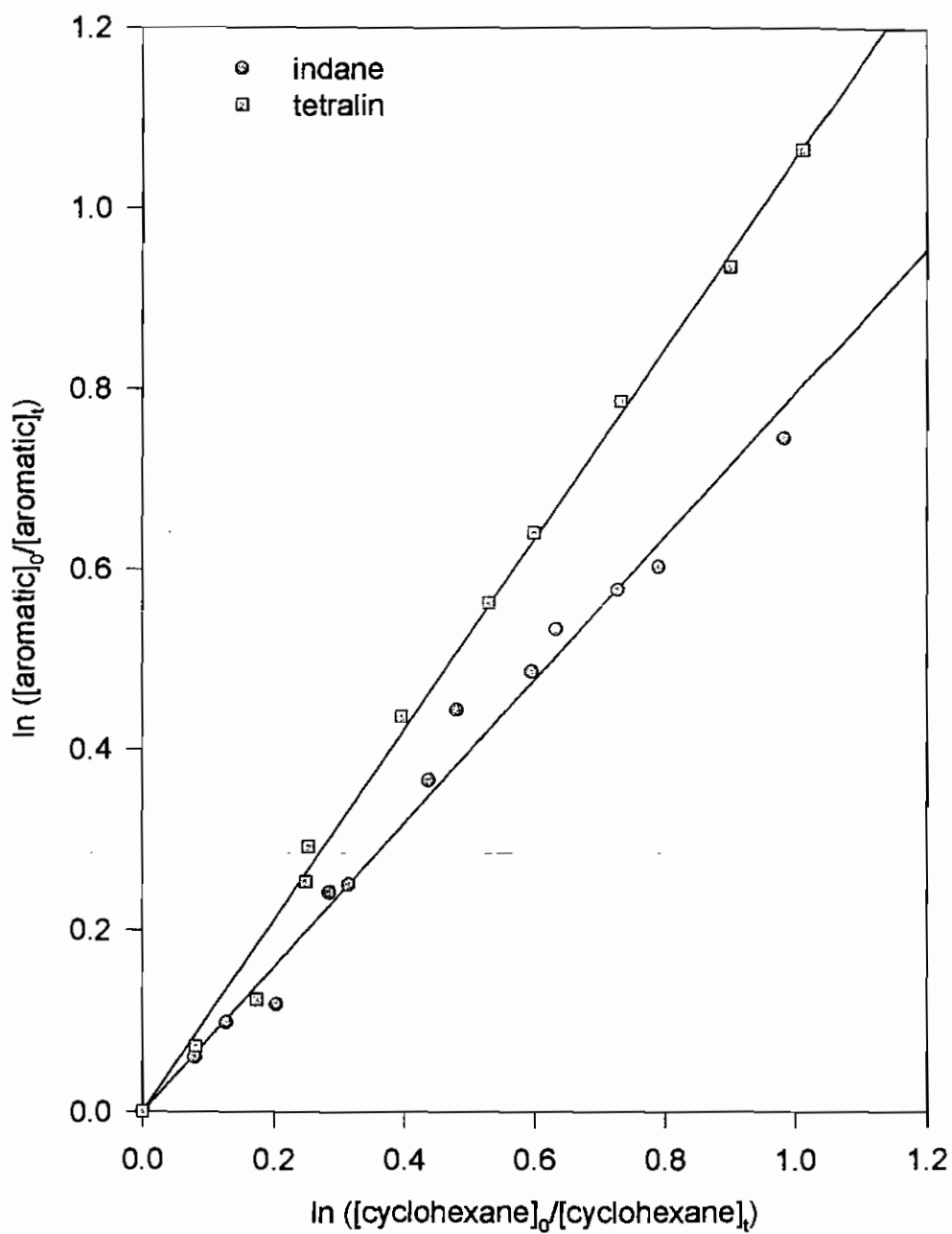


Table 4.4 Rate constant ratios, k_{39}/k_{40} , and calculated rate constants for the reaction of Cl atoms with Indane and Tetralin at $298 \pm 2K$ and 1 atm total pressure.

Aromatic	Slope k_{39}/k_{40} ^a	$10^{10} \times k$ ^b $\text{cm}^3 \text{ molecule}^{-1} \text{ s}^{-1}$
indane	0.74 ± 0.06	2.28 ± 0.18
tetralin	1.07 ± 0.04	3.30 ± 0.12

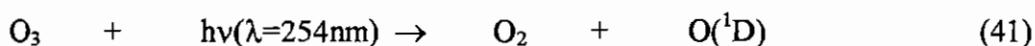
a: Errors quoted are two least-squares standard deviations of the slopes of the plots shown in Figure 4.19.

b: Errors quoted do not include the error in the rate constant for reaction of Cl atoms with the reference organic.

5.0 DISCUSSION

5.1 PHOTOLYSIS OF O₃/H₂ MIXTURES AS A SOURCE OF OH RADICALS

Photolysis of ozone in the presence of hydrogen as the precursor of OH radicals has not been previously reported in relative rate studies. Ozone was photolysed at 254 nm to yield O(¹D) and molecular oxygen:



The O(¹D) reacts rapidly with molecular hydrogen to form OH radicals:



with $k_{42} = 1.1 \times 10^{-10} \text{ cm}^3 \text{ molecule}^{-1} \text{ s}^{-1}$ [89]

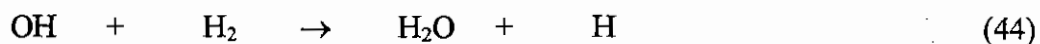
The fate of the hydrogen atom in air subsequent to reaction (42) is combination with molecular oxygen to yield HO₂ radicals:



with $k_{43} = 7.5 \times 10^{-11} \text{ cm}^3 \text{ molecule}^{-1} \text{ s}^{-1}$ [89]

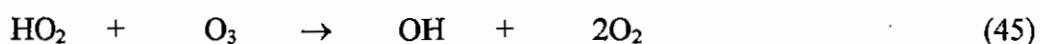
Reaction of hydrogen atoms with the substrate and/or reference organic is insignificant at the organic/oxygen concentration ratios used in this study. Baulch *et al* [89] have evaluated kinetic data for the reaction of hydrogen atoms with several aromatics and values are typically of the order of $10^{-13} \text{ cm}^3 \text{ molecule}^{-1} \text{ s}^{-1}$ at room temperature.

Reactions of OH radicals with molecular hydrogen:



with $k_{44} = 6.7 \times 10^{-15} \text{ cm}^3 \text{ molecule}^{-1} \text{ s}^{-1}$ [84]

is unimportant since OH is regenerated by reaction of HO₂ with ozone:



with $k_{45} = 2.0 \times 10^{-15} \text{ cm}^3 \text{ molecule}^{-1} \text{ s}^{-1}$ [84]

Relative rate measurements were made at $298 \pm 2\text{K}$ and in 1atm. of air using toluene as substrate and cyclohexane as reference to verify that the rate constant ratios from both the ozone/hydrogen, and the more routinely employed ozone/water OH radical precursor, were in agreement. The results of these experiments are plotted in the form of equation XII in Figure 4.1. The slopes of the plots, k_{36}/k_{37} , of 0.82 (ozone/hydrogen) and 0.81 (ozone/water) are in excellent agreement. When placed on an absolute basis using:

$$k(\text{OH} + \text{cyclohexane}) = 7.49 \times 10^{-12} \text{ cm}^3 \text{ molecule}^{-1} \text{ s}^{-1} [85]$$

the following absolute rate constants were calculated:

$$k(\text{OH} + \text{toluene}) = 5.94 \pm 0.22 \times 10^{-12} \text{ cm}^3 \text{ molecule}^{-1} \text{ s}^{-1} \text{ (ozone/hydrogen)}$$

and

$$k(\text{OH} + \text{toluene}) = 5.86 \pm 0.19 \times 10^{-12} \text{ cm}^3 \text{ molecule}^{-1} \text{ s}^{-1} \text{ (ozone/water)}$$

Both determinations are in excellent agreement with the recommended rate constant of $5.96 \times 10^{-12} \text{ cm}^3 \text{ molecule}^{-1} \text{ s}^{-1}$ [29]. The result strongly suggests that there are no complications associated with this method of OH radical generation. Hence, all rate constants reported in this study have been obtained using photolysis of O_3 in the presence of H_2 as the OH radical source.

This novel source of OH radicals has the potential to overcome some of the limitations previously encountered when using photolysis of ozone in the presence of H_2O such as:

- Interference from water vapour bands in the infrared analysis of reactants and/or reaction products.
- Limited variation in relative humidity experiments due to the large concentrations of water required.
- The inaccessibility of low temperature studies due to the relatively low vapour pressure of water.
- The potential for the occurrence of heterogeneous reactions on the walls of a “wet” reaction chamber.

5.2 ISOTOPE EFFECTS

The origin of all kinetic isotope effects lies in the changes in the quantised molecular energy levels which occur when the vibration frequencies and moments of inertia of a molecule are modified by isotopic substitution. The changes are purely mass effects, since isotopic substitution has no effect on the electron distribution or potential-energy surface for a molecule, and hence no effect on the ground-state geometry or the force constants for vibration of the molecule. In the case of a simple harmonic oscillator the vibration frequency is given by:

$$\nu = 1/2\pi (k/\mu)^{1/2}$$

and isotopic substitution alters the vibrational frequency by changing the reduced mass μ with a constant value of the force constant k .

The crucial effect of the changes in vibrational frequencies is to modify the vibrational energy levels of the molecule. The zero-point energies ($1/2 h\nu$) of the affected vibrations will change on isotopic substitution and this will change the critical energy E_0 . For example, R_3C-H and R_3C-D have zero point energies of $1/2 h\nu_0 \approx 17.2$ and 12.1 kJ mol^{-1} respectively. This gives rise to a difference in the critical energies for C-D and C-H fission of:

$$E_0(R_3C-H) - E_0(R_3C-D) = \Delta E_0 \approx 5.1 \text{ kJ mol}^{-1}$$

Hence:

$$k(\text{R}_3\text{C-H})/k(\text{R}_3\text{C-D}) = \exp(\Delta E_0/RT)$$

would give a ratio of 7.8 at 298K and 2.7 at 600K.

For example, the C-H reduced mass in toluene- h_8 is less than the C-D reduced mass in toluene- d_8 and hence has a greater zero point energy. When the C-H and C-D bonds are broken in the transition state of an abstraction reaction the activation energy difference corresponds to the difference in zero point energy of the reactants, i.e. the abstraction pathway for toluene- d_8 will have a greater energy barrier than for toluene- h_8 - called a primary isotope effect. Hence, the rate constant for D-atom abstraction will be expected to be less than that for H-atom abstraction and this difference in reactivity has been observed by Atkinson and Aschmann [78] in the reaction of toluene- h_8 and toluene- d_8 with NO_3 radicals, where H(D)-atom abstraction is the sole reaction pathway: $k(\text{NO}_3 + \text{toluene-}\text{h}_8) = 7.81 \times 10^{-17} \text{ cm}^3 \text{ molecule}^{-1} \text{ s}^{-1}$ while $k(\text{NO}_3 + \text{toluene-}\text{d}_8) = 3.43 \times 10^{-17} \text{ cm}^3 \text{ molecule}^{-1} \text{ s}^{-1}$ at 298K.

As outlined in *Section 2.2* evidence that OH addition to the aromatic ring dominates over H-atom abstraction from the alkyl substituent of toluene at room temperature is found in the absence of a primary kinetic isotope effect when H-atoms are replaced by D-atoms [46,81]. Table 5.1 shows a comparison of the room temperature rate data obtained in this work with previously reported values for the reaction of OH radicals with toluene- h_8 and

toluene-d₈. All previously reported $k(\text{OH} + \text{toluene-h}_8)$ determinations are in good agreement and the rate constant obtained in this work ($5.94 \pm 0.22 \times 10^{-12} \text{ cm}^3 \text{ molecule}^{-1} \text{ s}^{-1}$) at 298K and 1atm. is in excellent agreement with the recommended value ($5.96 \times 10^{-12} \text{ cm}^3 \text{ molecule}^{-1} \text{ s}^{-1}$)[29]. There have been only two kinetic studies to date on the reaction of OH radicals with toluene-d₈, both using absolute techniques and both in very good agreement [46,81]. The rate constant recommended by Atkinson [29] of $6.31 \times 10^{-12} \text{ cm}^3 \text{ molecule}^{-1} \text{ s}^{-1}$ (calculated from the Arrhenius parameters) for OH + toluene-d₈ represents the average of these values. The corresponding rate constant obtained from this study ($5.77 \pm 0.07 \times 10^{-12} \text{ cm}^3 \text{ molecule}^{-1} \text{ s}^{-1}$) is somewhat lower than the recommended value but more in line with that expected based on the difference between H-atom and D-atom abstraction from the methyl substituent which contributes about 10% to the overall reaction.

In truth the rate constants determined in this work for toluene-h₈ ($5.94 \pm 0.22 \times 10^{-12} \text{ cm}^3 \text{ molecule}^{-1} \text{ s}^{-1}$) and toluene-d₈ ($5.77 \pm 0.07 \times 10^{-12} \text{ cm}^3 \text{ molecule}^{-1} \text{ s}^{-1}$) do not differ within the experimental uncertainties; consistent with the predominantly addition pathway. Since the abstraction pathway only contributes ~10% to the overall reaction any decrease in reactivity due to isotopic substitution would, for these two compounds, be outside the precision of the experimental technique.

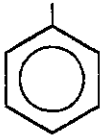
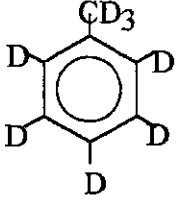
It is interesting to note that at temperatures greater than 425K (where H-atom abstraction is the dominant reaction channel) the rate constants may be expressed as:

$$k(\text{OH} + \text{toluene-}h_8) = 7.58 \times 10^{-18} T^2 \exp(11/T) \quad [29]$$

$$k(\text{OH} + \text{toluene-}d_8) = 6.85 \times 10^{-18} T^2 \exp(-276/T) \quad [29]$$

resulting in $k_H/k_D = 2.1$ at 600K. This is close to the theoretical value of 2.7, suggesting that the C-H (C-D) bond is almost fully broken at the top of the energy barrier.

Table 5.1 Rate constants for the reaction of OH radicals with Toluene-h₈ and Toluene-d₈ at room temperature and at, or close to, the high pressure limit.

Aromatic	$10^{12} \times k_{OH}$ $\text{cm}^3 \text{ molecule}^{-1} \text{ s}^{-1}$	Technique	Reference
Toluene-h ₈	6.36 ± 0.69	FP-RF	Tully <i>et al</i> [46]
	6.40 ± 0.64	FP-RF	Perry <i>et al</i> [81]
	5.5 ± 0.5	RR	Kramp and Paulson [71]
	5.9 ± 1.5	RR	Anderson and Hites [72]
	5.8 ± 1.5	RR	Anderson and Hites[72]
	6.06 ± 0.17	RR	Ohta and Ohyama[75]
	6.11 ± 0.40	FP-RF	Davis <i>et al</i> [68]
	5.78 ± 0.58	FP-RF	Hansen <i>et al</i> [90]
	5.44 ± 0.55	RR	Edney <i>et al</i> [91]
	5.96	E	Atkinson[29]
	5.94 ± 0.22^a	RR	This work
	5.86 ± 0.19^b	RR	This work
toluene-d ₈	6.40 ± 0.20	FP-RF	Tully <i>et al</i> [46]
	6.13 ± 0.63	FP-RF	Perry <i>et al</i> [81]
	6.31	E	Atkinson[29]
	5.77 ± 0.07	RR	This work

a: O₃/H₂ as OH radical source.

b: O₃/H₂O as OH radical source.

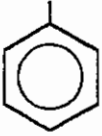
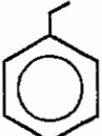
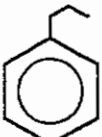
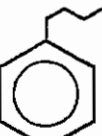
5.3 MONOALKYL SUBSTITUTED BENZENES

Included in Table 5.2 are room temperature rate constants from this work together with those previously reported [70,75,76] and the evaluations of Atkinson[29] for reaction of hydroxyl radical radicals with a series of monoalkyl substituted benzenes. In general, there is broad agreement between previously reported values for each individual aromatic where more than one study exists.

The room temperature rate coefficients obtained for reaction of OH with ethylbenzene by Ohta and Ohyama [75] and Lloyd *et al* [76], both using the relative rate method, are in very good agreement while the absolute value of Ravishankara *et al* [70] is ~15% higher. The rate constant obtained in this work ($6.34 \pm 0.29 \times 10^{-12} \text{ cm}^3 \text{ molecule}^{-1} \text{ s}^{-1}$) is lower than all previous values and hence lower than the recommended value ($7.1 \times 10^{-12} \text{ cm}^3 \text{ molecule}^{-1} \text{ s}^{-1}$) [29], but agrees within the overall experimental uncertainties.

While the rate constants reported by Lloyd *et al* [76] and Ravishankara *et al* [70] for OH + n-propylbenzene are in good agreement, the value obtained by Ohta and Ohyama [75] is 20% greater. The corresponding rate coefficient obtained in this study ($7.21 \pm 0.29 \times 10^{-12} \text{ cm}^3 \text{ molecule}^{-1} \text{ s}^{-1}$) is somewhat higher than those previously reported and almost 20% higher than the recommended value of Atkinson [29]. This study represents the first reported rate data for reaction of OH with n-butylbenzene.

Table 5.2 Rate constants for the reaction of OH radicals with a series of alkyl substituted benzenes at room temperature and at, or close to, the high pressure limit.

Aromatic	$10^{12} \times k_{OH}$ $\text{cm}^3 \text{ molecule}^{-1} \text{ s}^{-1}$	Technique	Reference
Toluene 	6.37 ± 0.17^a 5.96 5.94 ± 0.22	RR E RR	Ohta and Ohyama [75] Atkinson [29] This work
Ethylbenzene 	6.84 ± 0.30 7.95 ± 0.50^b 6.94 ± 1.39^c 7.1 6.34 ± 0.29	RR FP-RF RR E RR	Ohta and Ohyama [75] Ravishankara <i>et al</i> [70] Lloyd <i>et al</i> [76] Atkinson [29] This work
n-propylbenzene 	6.94 ± 0.24 5.86 ± 0.50^b 5.42 ± 1.09^c 6.0 7.21 ± 0.29	RR FP-RF RR E RR	Ohta and Ohyama [75] Ravishankara <i>et al</i> [70] Lloyd <i>et al</i> [76] Atkinson [29] This work
n-butylbenzene 	9.52 ± 0.50	RR	This work

- a: Experiments carried out at an unspecified temperature.
 b: Experiments carried out at 200 Torr total pressure.
 c: Experiments carried out at $305 \pm 2\text{K}$.

There has been no single systematic study to date on the reaction of OH radicals with the series of monoalkyl substituted benzenes listed in Table 5.2. Lloyd *et al* [76] reported the first rate constants for ethylbenzene ($6.94 \pm 1.39 \times 10^{-12} \text{ cm}^3 \text{ molecule}^{-1} \text{ s}^{-1}$) and n-propylbenzene ($5.42 \pm 1.09 \times 10^{-12} \text{ cm}^3 \text{ molecule}^{-1} \text{ s}^{-1}$) at 298K and atmospheric pressure using the relative rate method. Ravishankara *et al* [70] later reported room temperature rate constants for ethylbenzene ($7.95 \pm 0.50 \times 10^{-12} \text{ cm}^3 \text{ molecule}^{-1} \text{ s}^{-1}$) and n-propylbenzene ($5.86 \pm 0.50 \times 10^{-12} \text{ cm}^3 \text{ molecule}^{-1} \text{ s}^{-1}$) from flash photolysis-resonance fluorescence studies, and concluded that the increase in chain length of the alkyl substituent has no effect on reactivity towards the OH radical. This invariance of the rate constant as a function of the chain length of the substituent was rationalised by Ravishankara *et al* [70] in terms of similar Hammett constants for the alkyl substituents combined with the dominant reaction pathway being OH addition to the aromatic ring. More recently, Ohta and Ohya *et al* [75] carried out an extensive kinetic study on the reactions of OH radicals with mono-, di- and trialkyl benzenes. Their reported room temperature rate constants for toluene ($6.37 \pm 0.08 \times 10^{-12} \text{ cm}^3 \text{ molecule}^{-1} \text{ s}^{-1}$), ethylbenzene ($6.84 \pm 0.30 \times 10^{-12} \text{ cm}^3 \text{ molecule}^{-1} \text{ s}^{-1}$) and n-propylbenzene ($6.94 \pm 0.24 \times 10^{-12} \text{ cm}^3 \text{ molecule}^{-1} \text{ s}^{-1}$), while appearing to show a small increase with increasing length of the alkyl substituent, do not differ within the quoted experimental errors. From the reported OH rate data for monoalkyl substituted benzenes relevant to atmospheric conditions, Atkinson [29] concluded that the room temperature rate coefficient for toluene is reasonably applicable to the higher monoalkyl substituted benzenes.

The room temperature OH radical rate constants obtained in this systematic study for monoalkyl substituted benzenes, Table 5.2, show a small but definite increase with increasing chain length of the alkyl substituent: toluene ($5.94 \pm 0.22 \times 10^{-12} \text{ cm}^3 \text{ molecule}^{-1} \text{ s}^{-1}$) < ethylbenzene ($6.34 \pm 0.29 \times 10^{-12} \text{ cm}^3 \text{ molecule}^{-1} \text{ s}^{-1}$) < n-propylbenzene ($7.21 \pm 0.29 \times 10^{-12} \text{ cm}^3 \text{ molecule}^{-1} \text{ s}^{-1}$) < n-butylbenzene ($9.52 \pm 0.50 \times 10^{-12} \text{ cm}^3 \text{ molecule}^{-1} \text{ s}^{-1}$). These values have been obtained using a single reference (cyclohexane) and hence, the differences are believed to be outside experimental error.

Further experimental evidence from this study in support of these reactivity differences is illustrated in Figure 4.4, which shows the relative rates of disappearance of pairs of monoalkyl substituted benzenes, resulting in:

$$k(\text{OH} + \text{ethylbenzene})/k(\text{OH} + \text{toluene}) = 1.04 \pm 0.003$$

$$k(\text{OH} + \text{n-propylbenzene})/k(\text{OH} + \text{ethylbenzene}) = 1.10 \pm 0.004$$

and

$$k(\text{OH} + \text{n-butylbenzene})/k(\text{OH} + \text{n-propylbenzene}) = 1.39 \pm 0.010$$

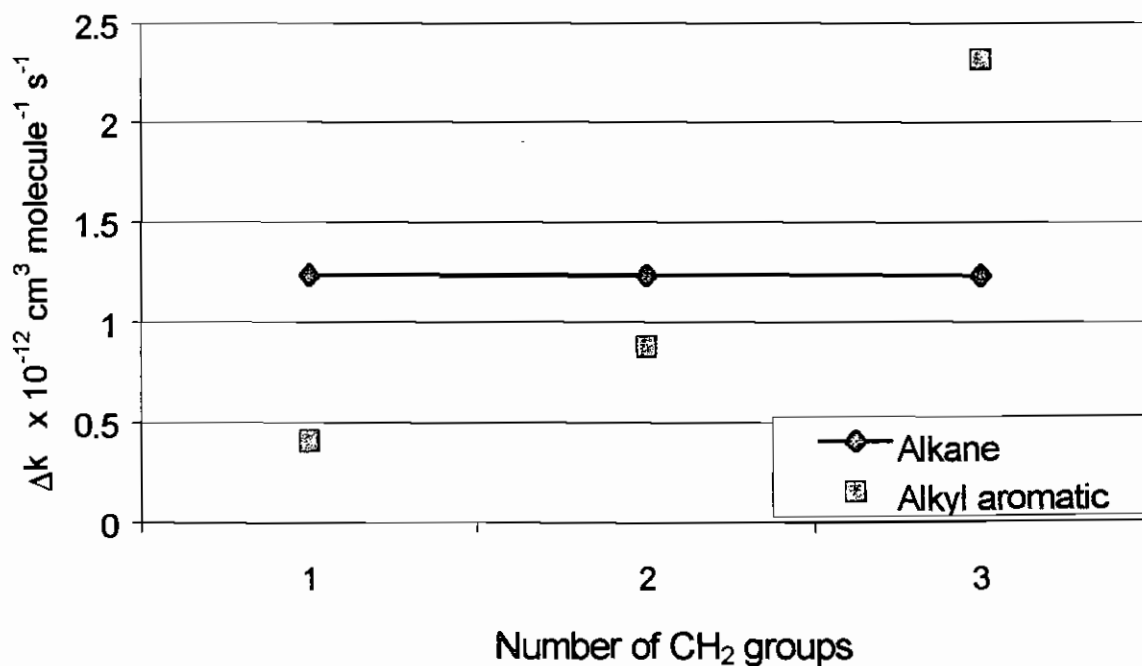
The increase in reactivity of monoalkyl substituted benzenes with increasing length of the alkyl side chain observed in this work could be due to:

- (i) An increase in the importance of the abstraction pathway with increasing number of $-\text{CH}_2-$ groups in the alkyl side chain, and/or
- (ii) Enhanced addition to the aromatic ring due to an increased inductive effect with increasing size of the alkyl substituent.

Should the observed increase in reactivity be due to an increase in the contribution of the abstraction pathway, one would expect:

- (i) abstraction from the α -CH₂ group to be more facile based on thermochemical considerations given that the benzylic C-H bond strength is 368 kJ mol⁻¹ compared to 397 kJ mol⁻¹ for secondary C-H bonds [92] and hence toluene and ethylbenzene to show the biggest difference in reactivity and
- (ii) reactivity differences (Δk) with increasing length of side chain to approach that for H-atom abstraction from a -CH₂- group in a normal alkane (1.23×10^{-12} cm³ molecule⁻¹ s⁻¹)[87]. A plot of Δk vs. number of -CH₂- groups is shown in Figure 5.3.

Figure 5.3 Plot of Δk versus number of CH₂ groups for this series of Monoalkylbenzenes.



The trend illustrated graphically in Figure 5.3 suggests that the observed reactivity differences cannot be rationalised solely in terms of an increase in the contribution of the abstraction pathway. Support for enhanced OH addition to the aromatic ring with increasing size of alkyl substituent comes from a comparison of the rate constants with the corresponding ionisation potentials for this series of compounds, Table 5.3, which show a definite increase in reactivity with decreasing ionization potential.

Table 5.3 Ionisation Potentials and room temperature OH radical rate constants for a series of monoalkyl substituted benzenes.

Aromatic	Ionisation Potential ^a eV	$10^{12} \times k_{OH}^b$ $\text{cm}^3 \text{ molecule}^{-1} \text{ s}^{-1}$
Toluene	8.821 ± 0.01	5.94
Ethylbenzene	8.76 ± 0.01	6.34
n-propylbenzene	8.72 ± 0.01	7.21
n-butylbenzene	8.69 ± 0.01	9.52

a: Rosenstock *et al* [93].

b: This work.

In conclusion, it would appear that the small but definite increase in reactivity towards OH with increasing length of the alkyl chain is probably a combination of both a greater contribution of the abstraction pathway and enhanced addition to the aromatic ring.

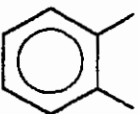
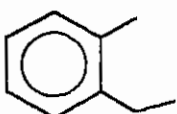
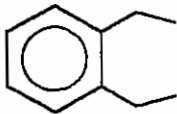
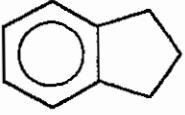
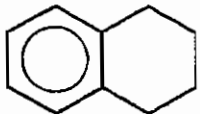
5.4 DIALKYL SUBSTITUTED BENZENES

Table 5.3 contains kinetic data at 298K and at, or close to, the high pressure limit for reaction of OH radicals with selected ortho-dialkyl substituted benzenes, previously reported and obtained in the present study. Room temperature rate constants have been reported for reaction of OH radicals with o-xylene using both absolute [70,81,86,90] and relative rate techniques [59,75,88,91,93,94]. All reported values are in good agreement resulting in a recommended limiting high-pressure value of $13.7 \times 10^{-12} \text{ cm}^3 \text{ molecule}^{-1} \text{ s}^{-1}$ at room temperature [29].

Two room temperature studies have been carried out, both using the relative rate technique, on the reaction of OH radicals with o-ethyltoluene with the reported rate constants being in excellent agreement [75,76]. The unit-weighted average of these rate data results in a recommended value of $12.3 \times 10^{-12} \text{ cm}^3 \text{ molecule}^{-1} \text{ s}^{-1}$ [29]. The reactivity of o-ethyltoluene towards OH is equal to that of o-xylene, within the quoted errors, consistent with the dominant reaction pathway being OH addition to the aromatic ring.

Kinetic data for the reaction of OH with o-diethylbenzene has not been reported previously. The room temperature OH radical rate constant obtained in this study ($12.4 \pm 0.4 \times 10^{-12} \text{ cm}^3 \text{ molecule}^{-1} \text{ s}^{-1}$) is equal, within the experimental uncertainties, to that for o-xylene and o-ethyltoluene supporting the predominance of OH addition to the aromatic ring under these experimental conditions.

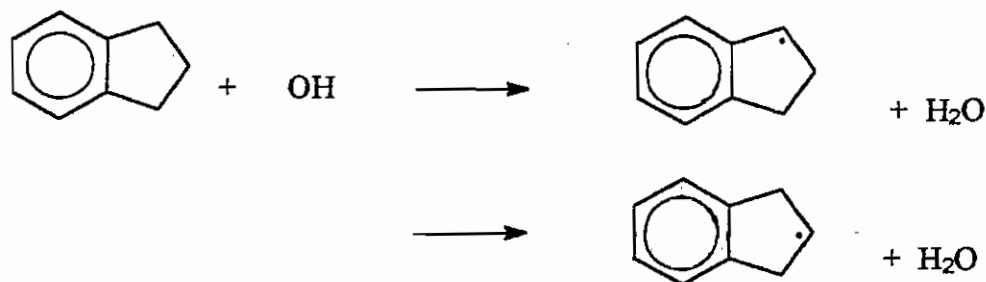
Table 5.4 Rate constants for the reaction of OH radicals with a series of Aromatic compounds at room temperature and at, or close to, the high pressure limit.

Aromatic	$10^{17} \times k_{OH}$ $\text{cm}^3 \text{ molecule}^{-1} \text{ s}^{-1}$	Technique	Reference
o-xylene 	12.6 ± 0.6	RR	Ohta and Ohyama [75]
	11.2 ± 3.4	RR	Doyle <i>et al</i> [59]
	15.3 ± 1.5	FP-RF	Hansen <i>et al</i> [90]
	14.3 ± 1.5	FP-RF	Perry <i>et al</i> [81]
	12.4 ± 1.2	FP-RF	Ravishankara <i>et al</i> [70]
	14.0	RR	Cox <i>et al</i> [94]
	14.2 ± 1.7	FP-RF	Nicovich <i>et al</i> [86]
	13.6	RR	Klöpffer <i>et al</i> [95]
	12.6	RR	Edney <i>et al</i> [91]
	12.2 ± 0.6	RR	Atkinson <i>et al</i> [88]
	13.7	E	Atkinson [29]
o-ethyltoluene 	12.0 ± 2.4	RR	Lloyd <i>et al</i> [76]
	12.5 ± 1.3	RR	Ohta and Ohyama [75]
	12.3	E	Atkinson [29]
o-diethylbenzene 	12.5 ± 0.4	RR	This work
Indane 	9.2 ± 2.0	DF-RF	Baulch <i>et al</i> [77]
	23.9 ± 1.9	RR	This work
Tetralin 	34.3 ± 0.6	RR	Atkinson and Aschmann [78]
	26.5 ± 1.3	RR	This work

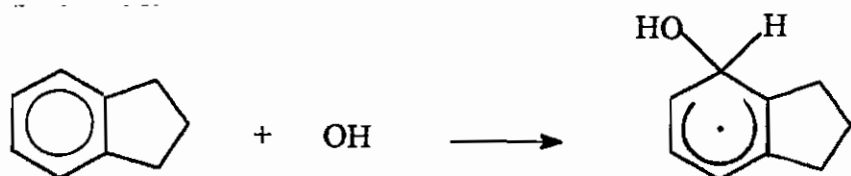
Previous kinetic studies on the reaction of OH radicals with aromatic compounds containing saturated cyclic substituents are limited to a single study on indane by Baulch *et al* [77] and on tetralin by Atkinson and Aschmann [78]. The almost factor of four difference between the reported rate constants for these compounds is surprising given the similarity in their structures. The value of $k(\text{OH} + \text{indane}) = 9.2 \pm 2.0 \times 10^{-12} \text{ cm}^3 \text{ molecule}^{-1} \text{ s}^{-1}$ reported by Baulch *et al* [77] is broadly in line with that obtained for ortho-dialkyl substituted benzenes suggesting that the dominant reaction pathway is OH addition to the aromatic ring. The corresponding rate constant for tetralin ($34.3 \pm 0.6 \times 10^{-12} \text{ cm}^3 \text{ molecule}^{-1} \text{ s}^{-1}$) reported by Atkinson and Aschmann [78] implies a much larger contribution from the abstraction channel if one assumes that the addition component is similar for all ortho-dialkyl substituted benzenes, both cyclic and acyclic. The difference in the reported rate data of these two aromatics does not seem plausible given that the only differences between these two compounds is the presence of an additional $-\text{CH}_2-$ group in tetralin and some degree of ring strain in the saturated five membered ring. While $k(\text{OH} + \text{tetralin}) = 26.5 \pm 1.3 \times 10^{-12} \text{ cm}^3 \text{ molecule}^{-1} \text{ s}^{-1}$ from this work is ~25% less than the value obtained by Atkinson and Aschmann [78], (using a similar experimental technique) the OH rate constant measured in this study for indane ($23.9 \pm 1.9 \times 10^{-12} \text{ cm}^3 \text{ molecule}^{-1} \text{ s}^{-1}$) at 298K and 1 atm of air is more than a factor of two greater than that previously reported by Baulch *et al* [77].

Baulch *et al* [77] used the absolute technique of discharge flow with OH detection by resonance fluorescence to measure the rate constant for indane at room temperature and at 40Pa (0.32 Torr) and 170Pa (1.3 Torr) total pressure. The results obtained at the two

different pressures were the same, within the error limits, and the absence of a pressure dependence was considered by the investigators to be consistent with the dominant reaction pathway being a labile hydrogen atom abstraction from the saturated ring:



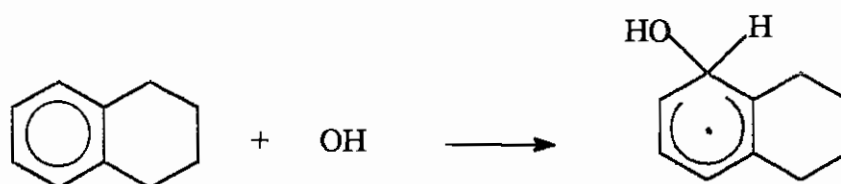
This is in sharp contrast to all previous work [29 and references therein] on the alkylated aromatics where it has been clearly demonstrated that the room temperature rate constant shows a pressure dependence below about ~25 – 50 Torr total pressure as a result of OH addition to the aromatic ring being the dominant reaction channel. Based on previous kinetic and mechanistic studies on *o*-dialkyl substituted benzenes the addition reaction would be expected to make a significant contribution:



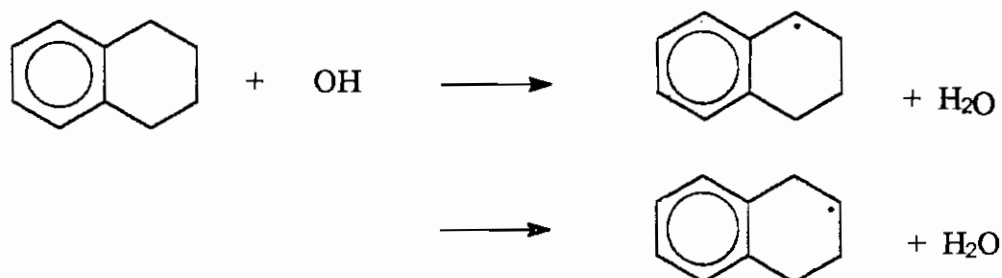
If the addition component to the overall room temperature rate constant for OH + indane is assumed to be similar to that for acyclic ortho-dialkyl substituted benzenes at, or close to, the high pressure limit ($\sim 12 \times 10^{-12} \text{ cm}^3 \text{ molecule}^{-1} \text{ s}^{-1}$), then this value, combined with that obtained in the low pressure study of Baulch *et al* [77], results in an overall rate

constant of $21.2 \times 10^{-12} \text{ cm}^3 \text{ molecule}^{-1} \text{ s}^{-1}$, close to the value of $23.9 \pm 1.9 \times 10^{-12} \text{ cm}^3 \text{ molecule}^{-1} \text{ s}^{-1}$ obtained in this study. Hence it is suggested that the rate constant reported by Baulch *et al* [77] reflects only the contribution of the abstraction channel and the pressure dependence of this reaction warrants further investigation.

The reason for the discrepancy in $k(\text{OH} + \text{tetralin})$ reported by Atkinson and Aschmann [78] and obtained from this study is not obvious but might be due to the use of different reference compounds in the relative rate studies. The enhanced reactivity of tetralin over other ortho-dialkyl substituted benzenes towards OH radicals suggests that the addition channel contributes only $\sim 50\%$ to the overall rate constant under atmospheric conditions:



with H-atom abstraction from the saturated ring making up the remainder:



Supporting evidence that the enhanced reactivity of indane and tetralin towards OH radicals, over that observed for acyclic dialkyl substituted benzenes, is due to an increase in the contribution of the abstraction channel comes from a comparison of the Arrhenius parameters obtained in this study for reaction of OH with toluene, indane and tetralin, and shown in Table 4.3. The negative temperature dependence obtained for toluene in this study ($k_{\text{OH}} = 2.41 \times 10^{-12} e^{269 \pm 24/T} \text{ cm}^3 \text{ molecule}^{-1} \text{ s}^{-1}$) and in previous investigations ($k_{\text{OH}} = 1.81 \times 10^{-12} e^{355 \pm 143/T} \text{ cm}^3 \text{ molecule}^{-1} \text{ s}^{-1}$) [29 and references therein] is indicative of addition being the dominant pathway. The essentially zero activation energy obtained in this work for indane ($k_{\text{OH}} = 21.6 \times 10^{-12} e^{30 \pm 7/T} \text{ cm}^3 \text{ molecule}^{-1} \text{ s}^{-1}$) implies a significant contribution from the abstraction channel, while the positive temperature dependence observed for tetralin ($k_{\text{OH}} = 42.5 \times 10^{-12} e^{-141 \pm 24/T} \text{ cm}^3 \text{ molecule}^{-1} \text{ s}^{-1}$) suggests an even greater importance of H-atom abstraction from the saturated ring.

As stated previously, a substantial fraction (~50%) of the overall OH + indane and OH + tetralin reaction appears to proceed via H-atom abstraction from the saturated ring at room temperature and atmospheric pressure. The average reactivity per $-\text{CH}_2-$ group in the saturated ring of $\sim 3 \times 10^{-12} \text{ cm}^3 \text{ molecule}^{-1} \text{ s}^{-1}$ is thus much greater than that observed for the corresponding cycloalkanes, cyclopentane and cyclohexane, where $k_{\text{OH}} \sim 1.2 \times 10^{-12} \text{ cm}^3 \text{ molecule}^{-1} \text{ s}^{-1}$ per $-\text{CH}_2-$ group [87].

Further support for facile H-atom abstraction from the saturated ring in indane and tetralin comes from a consideration of the kinetic data in Table 5.5 for the reaction of Cl atoms

with indane and tetralin and the reaction of NO_3 radicals with tetralin, both of which are postulated to proceed solely via H-atom abstraction from the saturated ring:

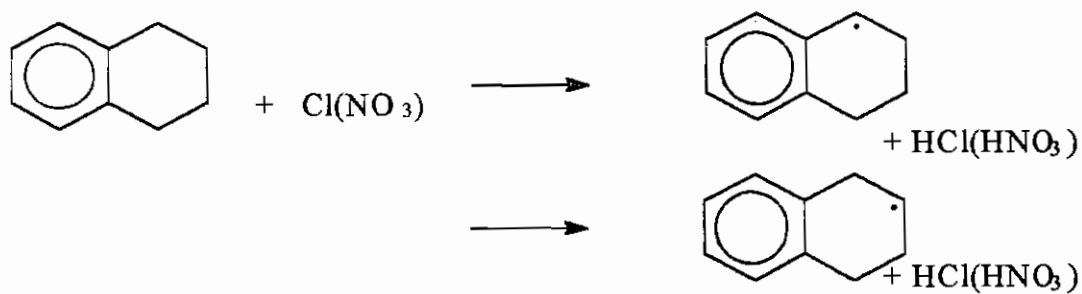
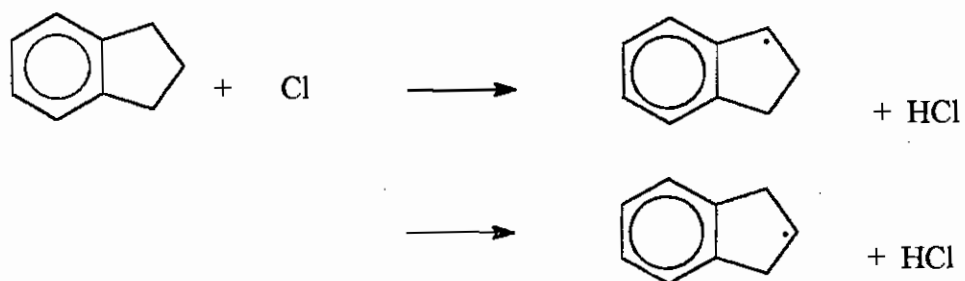
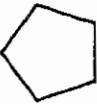
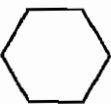
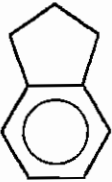
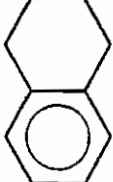


Table 5.5 Rate constants for the reaction of Cyclopentane, Cyclohexane, Indane and Tetralin with OH and NO₃ radicals and Cl atoms at 298K.

Organic	$10^{12} \times k_{OH}^a$	$10^{16} \times k_{NO_3}^a$	$10^{10} \times k_{Cl}^a$ (gas phase)	$10^{10} \times k_{Cl}^a$ (solution)	Reference
Cyclopentane 	5.08	-	-	1.2	Atkinson [87] Russel <i>et al</i> [96]
Cyclohexane 	7.49	1.35 ± 0.25	3.08 ± 0.14		Atkinson [87] Atkinson [97] Atkinson <i>et al</i> [88] Russel <i>et al</i> [96]
Indane 	23.9 ± 1.9	-	2.28 ± 0.18	2.4	Russel <i>et al</i> [96] This work
Tetralin 	26.5 ± 1.3	88 ± 2.6	3.30 ± 0.12	2.6	Atkinson <i>et al</i> [98] Russel <i>et al</i> [96] This work

a: in units of $\text{cm}^3 \text{ molecule}^{-1} \text{ s}^{-1}$

The reported room temperature rate constant for reaction of NO_3 radicals with tetralin [98] is almost two orders of magnitude greater than that for reaction with cyclohexane [97] ($0.23 \times 10^{-16} \text{ cm}^3 \text{ molecule}^{-1} \text{ s}^{-1}$ versus $22 \times 10^{-16} \text{ cm}^3 \text{ molecule}^{-1} \text{ s}^{-1}$ per $-\text{CH}_2-$ group). There appears to be no significant difference between the k_{C1} values for cyclopentane, cyclohexane, indane and tetralin which is not surprising given that these reactions are all close to the collision limit. However, on a per $-\text{CH}_2-$ basis, the $-\text{CH}_2-$ groups in indane and tetralin are $\sim 50\%$ more reactive than those in cyclopentane and cyclohexane.

Hydrogen atom abstraction in solution phase by ROO^\cdot , [99], CCl_3^\cdot , [100], $t\text{-BuO}^\cdot$ [101], and CH_3^\cdot [102] radicals has also been observed to proceed at a faster rate for indane and tetralin than for alkylsubstituted benzenes. The relative rate constants (per active H-atom) obtained by Meyer *et al* [102] for H-atom abstraction by methyl radicals from a series of aromatic compounds are listed in Table 5.6 together with the corresponding values for other radical species. While the difference in reactivity between toluene (or o-xylene) and indane (or tetralin) can be explained in terms of the ease of abstraction of secondary hydrogen atoms compared to primary hydrogen atoms, the tabulated data clearly shows that, regardless of the abstracting species, indane and tetralin are significantly more reactive than ethylbenzene. Meyer *et al* [102] proposed that in the case of ethylbenzene there is a significant loss of resonance energy in the transition state due to the skewed conformation of the alkyl side chain as a result of repulsion between the closest β -hydrogen on the alkyl side chain and the ortho-hydrogen of the ring. This is in contrast to indane and tetralin where there is no such repulsion due to more rigid

conformation of the bi-planar structure and hence no loss of stabilisation in the transition state resulting in greater reactivity.

Table 5.6 Relative rate constants (per active H Atom) for H-atom abstraction from a series of Aromatic compounds by various radicals in solution phase.

Substrate	ROO ^a	CCl ₃ ^b	t-BuO ^c	CH ₃ ^d
toluene	1.00	1.00	1.00	1.00
o-xylene	-	-	1.20	0.99
ethylbenzene	7.75	4.6	3.2	4.12
indane	37	7.1	-	8.3
Tetralin	134	25.6	15.2	23

a [99]; b [100]; c [101]; d [102].

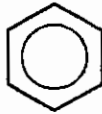
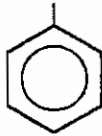
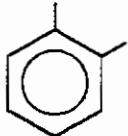
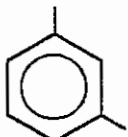
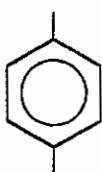
In summary, it would appear that the contribution of the abstraction pathway to the overall rate constant for reaction of indane and tetralin with OH radicals is considerably greater than for the corresponding ortho-dialkyl substituted benzenes. If this was simply due to the weaker C-H bonds in the -CH₂- group adjacent to the aromatic ring, as has been postulated by Atkinson [98] to account for the enhanced reactivity of tetralin with NO₃ radicals, one would expect ortho-diethyl benzene to be considerably more reactive towards OH radicals than o-xylene and closer to that observed for indane. Quite obviously this is not the case, suggesting that the rigid conformation in indane (and tetralin) due to the presence of the saturated ring leads to a more favourable transition state for H-atom abstraction by OH radicals, as suggested by Meyer et al [102].

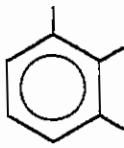
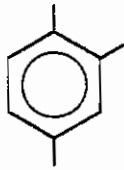
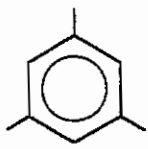
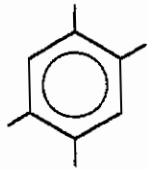
5.5 TRI- AND TETRAMETHYL SUBSTITUTED BENZENES

Table 5.7 shows the recommended room temperature rate constants for reaction of OH radicals with benzene, mono-, di- and tri-methyl substituted benzenes, together with the value obtained in this study for 1,2,4,5-tetramethylbenzene. A comparison of the reactivity of hydroxyl radicals with benzene and toluene reveals that addition of a methyl group to the aromatic ring increases the room temperature rate constant of the OH-aromatic reaction by a factor of ~5. Moreover, there is about another three-fold increase in reactivity with the addition of a second methyl group. The presence of a third methyl substituent on the aromatic ring leads to a further two-fold increase in k_{OH} . As discussed previously in *Section 2.0* the dominant reaction pathway for hydroxyl radicals with benzene and alkyl substituted aromatics is electrophilic addition to the aromatic ring. Hence, this observed trend can be rationalised in terms of an enhanced inductive effect with increased methyl group substitution making OH addition to the ring more facile.

It is well known that the electron donating ability of a substituent to an aromatic ring is also very sensitive to the position of substitution. A striking feature of di- and tri-methylbenzenes is the differences in reactivity of the different isomers towards OH radicals. For example, the room temperature rate constant for meta-xylene is almost twice that for ortho- or para-xylene. Similarly, 1,3,5-trimethylbenzene is considerably more reactive than 1,2,3- or 1,2,4-trimethylbenzene. These differences have not been rationalised in depth in any of the kinetic studies carried out to date.

Table 5.7 Rate constants for the reaction of OH radicals with a series of methyl substituted benzenes at room temperature and at, or close to, the high pressure limit.

Aromatic	$10^{12} \times k_{OH}$ $\text{cm}^3 \text{ molecule}^{-1} \text{ s}^{-1}$	Technique	Reference
benzene 	1.23	E	Atkinson[29]
Toluene 	5.96	E	Atkinson[29]
o-xylene 	13.7	E	Atkinson[29]
m-xylene 	23.6	E	Atkinson[29]
p-xylene 	14.3	E	Atkinson[29]

Aromatic	$10^{12} \times k_{OH}$ $\text{cm}^3 \text{ molecule}^{-1} \text{ s}^{-1}$	Technique	Reference
1,2,3-trimethylbenzene 	32.7	E	Atkinson[29]
1,2,4-trimethylbenzene 	32.5	E	Atkinson[29]
1,3,5-trimethylbenzene 	57.5	E	Atkinson[29]
1,2,4,5-tetramethylbenzene 	51.57 ± 3.4	RR	This work

The stability of the OH-aromatic adduct formed in the addition pathway is central to this discussion. As with carbocations, the stability order of alkyl radicals is tertiary > secondary > primary. This is due to the delocalisation of electrons through overlap between the p orbital occupied by the odd electron of the carbon radical centre and a σ orbital of the methyl group as shown below. Overlap of a filled orbital and a half-filled orbital has a net stabilising effect. This kind of stabilisation due to delocalisation of σ bond orbitals is known as hyperconjugation.

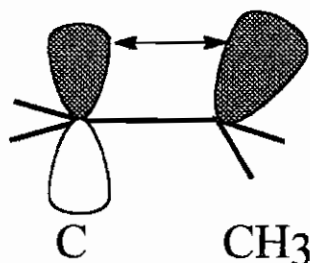
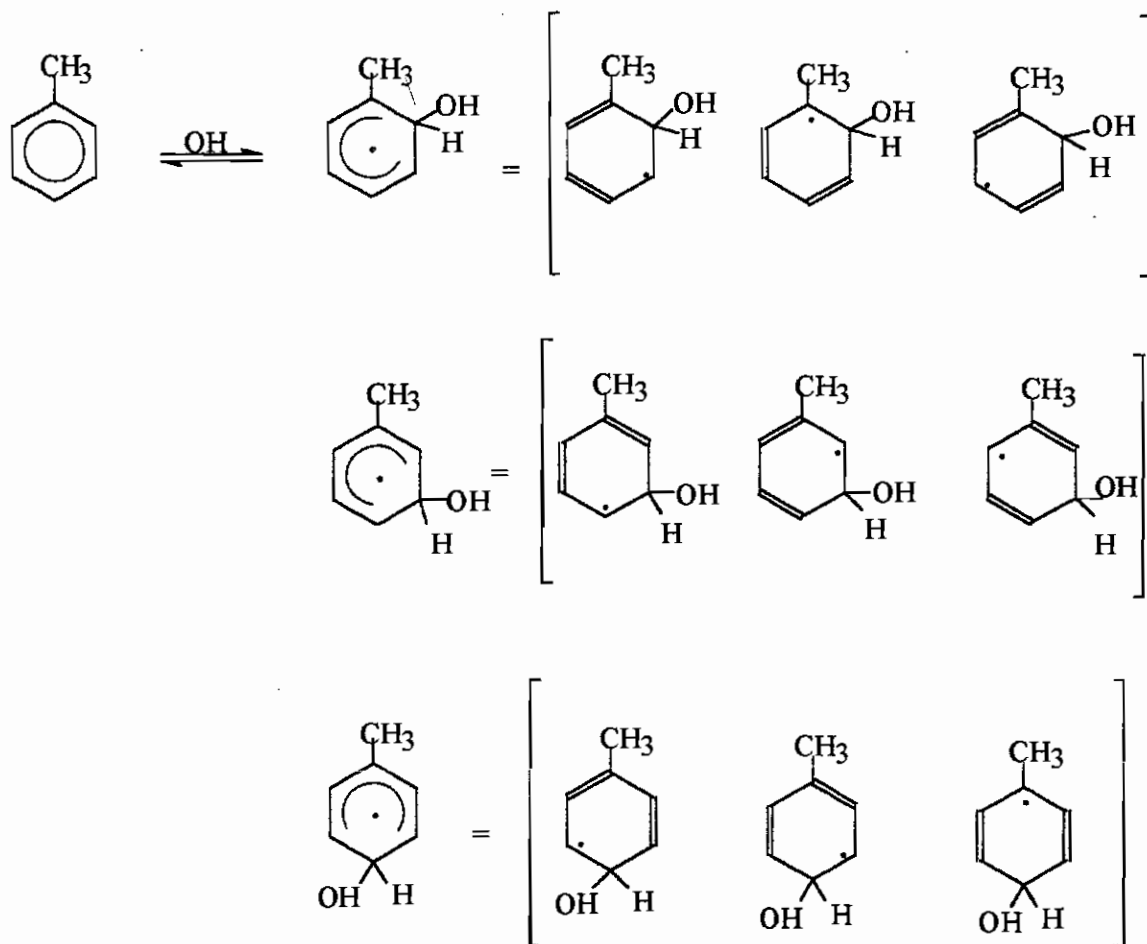
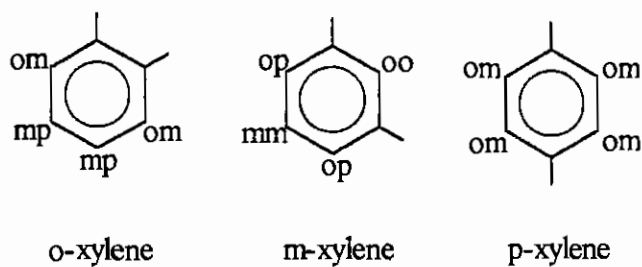


Figure 5.2 shows all possible resonance structures for addition of OH to the ortho, meta and para positions of toluene. The ortho and para addition adducts both have resonance structures that contain a tertiary carbon radical which can be stabilised by hyperconjugation. The meta addition pathway has no such resonance structures. As a result addition of OH to the ortho and para positions has a lower energy barrier than addition to the meta position. In a product study on the reaction of OH with toluene Gery *et al* [103] found that 81% of the total cresol yield was o-cresol, 17% was p-cresol and 2% was m-cresol. In aromatic substitution terminology this is expressed as the methyl group having an activating effect and ortho and para directing characteristics.

Figure 5.2 Resonance structures following addition of OH radicals to the ortho, meta and para positions of Toluene.

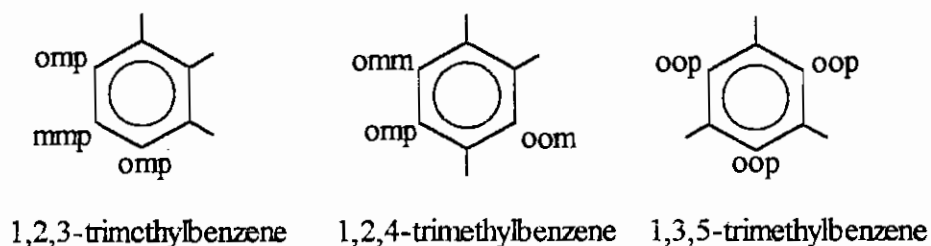


Applying this rationale to the xylenes isomers, the two methyl groups on each xylene will activate (i.e. the vacant sites will be ortho or para to a methyl group) and deactivate (meta) the following positions:



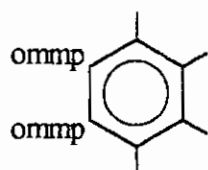
The vacant sites on ortho- and para-xylene are each activated by one methyl group so they are expected to have similar reactivities. Three of the four vacant sites on meta-xylene are activated by both methyl groups so it is expected that m-xylene will have a much greater reactivity. This is supported by the data in Table 5.7 with meta-xylene some 60-70% more reactive towards OH radicals than ortho- or para-xylene.

The trimethylbenzene isomers are shown below with the vacant sites labelled as being ortho, meta or para influenced:

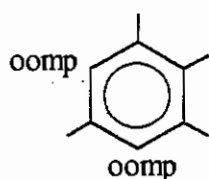


1,2,3- and 1,2,4-trimethylbenzene both have two vacant sites activated by two of the methyl groups with the third site activated by one methyl group so these compounds are expected to have similar reactivities with respect to reaction with the OH radical. 1,3,5-trimethylbenzene has all three vacant sites activated by all three methyl groups suggesting that this isomer should be significantly more reactive with OH. The recommended rate data in Table 5.7 supports this conclusion.

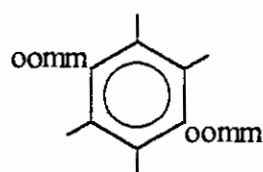
Applying this argument to the tetramethyl benzene isomers, (shown below with ortho,meta and para labelling) it is clear that the isomers will not exhibit similar reactivities towards the OH radical:



1,2,3,4-tetramethylbenzene



1,2,3,5-tetramethylbenzene



1,3,5-tetramethylbenzene

It is predicted that the room temperature rate constant for reaction of OH radicals with 1,2,3,4-tetramethylbenzene will be similar to that obtained in this study for OH + 1,2,4,5-tetramethylbenzene ($62.45 \pm 4.4 \times 10^{-12} \text{ cm}^3 \text{ molecule}^{-1} \text{ s}^{-1}$) as both isomers have two vacant sites activated by two of the methyl groups. It is also predicted that 1,2,3,5-tetramethylbenzene will be considerably more reactive with OH since the vacant sites are activated by three of the methyl substituents.

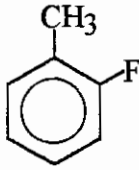
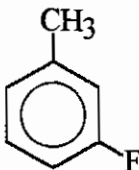
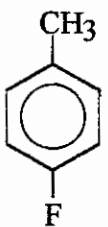
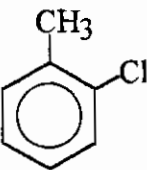
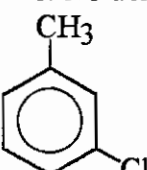
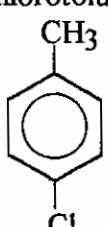
5.6 HALOTOLUENES

Rate data obtained in this work for the reaction of OH radicals with monofluorotoluenes and monochlorotoluenes at 298K and atmospheric pressure are listed in Table 5.8. This study represents the first reported kinetic data on the gas phase reactions of OH radicals with these aromatic substrates, previous studies being confined to halogenated benzenes.

The reactivity differences observed in this study between halobenzenes and their non-halogenated analogue, toluene, are consistent with the deactivating influence of halogen substituents. The presence of a F- or Cl- substituent on the aromatic ring leads to an approximately two-fold decrease in reactivity compared to toluene. The rate data also shows that fluorine is slightly more deactivating than chlorine, consistent with their Pauling electronegativity values.

The data in Table 5.8 also illustrate significant differences in reactivity between the different isomers with the same trend being observed for both fluoro- and chlorotoluenes, i.e. 3-halotoluene > 4-halotoluene > 2-halotoluene. This trend is similar to that observed for alkyl-substituted benzenes where meta- > ortho- ≥ para-. Despite the deactivating affect of F- and Cl- substituents towards the addition of an electrophilic species such as the OH radical, halogens have ortho- and para- directing characteristics which make them unique as substituents in electrophilic aromatic substitution reactions.

Table 5.8 Rate constants for the reaction of OH radicals with a series of Halotoluenes at 298±2K and 1 atm total pressure.

Aromatic	$10^{12} \times k_{OH}$ $\text{cm}^3 \text{ molecule}^{-1} \text{ s}^{-1}$	Technique	Reference
2-fluorotoluene 	2.09 ± 0.07	RR	This work
3-fluorotoluene 	4.40 ± 0.07	RR	This work
4-fluorotoluene 	3.03 ± 0.14	RR	This work
2-chlorotoluene 	2.45 ± 0.22	RR	This work
3-chlorotoluene 	4.72 ± 0.50	RR	This work
4-chlorotoluene 	3.46 ± 0.43	RR	This work

Support for the reactivity trends observed in this study comes from the previously reported kinetic data of Ohta and Ohyama [77], Atkinson *et al* [80], Rinke and Zetzsch [82], Wallington *et al* [83] and Edney *et al* [91] for the reaction of OH with halogenated benzenes. The room temperature rate constants for OH + chlorobenzene obtained by Rinke and Zetzsch [82], Atkinson *et al* [80], Wallington *et al* [80], and Edney *et al* [91] result in recommended value of $0.77 \times 10^{-12} \text{ cm}^3 \text{ molecule}^{-1} \text{ s}^{-1}$ [29], which is about 60% less than that recommended for OH + benzene ($1.23 \times 10^{-12} \text{ cm}^3 \text{ molecule}^{-1} \text{ s}^{-1}$) [29], confirming the deactivating effect of the chlorine substituent. The rate data of Wahner and Zetzsch [73] at 298K for reaction of OH with ortho-, meta- and para-dichlorobenzene of 0.42, 0.72 and 0.32 respectively (all in units of $10^{-12} \text{ cm}^3 \text{ molecule}^{-1} \text{ s}^{-1}$), shows that the presence of a second chlorine substituent leads to a further reduction in reactivity towards OH.

Systematic studies have also been carried out by Rinke and Zetzsch [82] and Wallington *et al* [83] on the reaction of fluoro-, chloro-, bromo- and iodobenzene with OH radicals. In both studies the reactivity was observed to decrease uniformly with increasing electronegativity of the halogen substituent.

5.6.1 Chlorine atom production in the reaction of OH radicals with halogenated aromatics

Studies have been carried out to investigate Cl atom production in the reaction of OH radicals with chloroalkenes and chlorinated aromatics [91,104,105,106]. A kinetic study

by Edney *et al* [91] on the OH + allyl chloride reaction showed that k_{OH} varied in the presence or absence of a scavenger species (methane) suggesting that Cl atom production was significant in this reaction. In a subsequent study on benzyl chloride and chlorobenzene. Edney *et al* [104] in a later study modified the rate expression used to calculate the OH radical rate constant in an attempt to take Cl atom production into account. In addition Tuazon *et al* [105] identified chlorinated products from the reaction of OH with chloroethenes that strongly suggested Cl atom production. Kleindienst *et al* [106] and Tuazon *et al* [105] have measured the Cl atom yield to be as low as 0.077 and 0.084 respectively from the OH + benzyl chloride reaction and no significant difference was observed in the value of k_{OH} in the presence and absence of a Cl atom scavenger.

Experiments were carried out in this work to investigate the potential for Cl atom production in the reaction of OH radicals with chlorotoluenes. The rate constant for reaction of 2-chlorotoluene with OH radicals was measured in the presence and absence of a Cl atom scavenger (methane). The rate coefficients obtained differed slightly but were within the overall experimental uncertainties:

$$\begin{aligned}
 k(\text{OH} + 2\text{-chlorotoluene}) &= 2.45 \pm 0.22 \text{ cm}^3 \text{ molecule}^{-1} \text{ s}^{-1} \\
 k(\text{OH} + 2\text{-chlorotoluene} + \text{methane}) &= 2.72 \pm 0.29 \text{ cm}^3 \text{ molecule}^{-1} \text{ s}^{-1}
 \end{aligned}$$

Hence the degree of Cl atom production in the reaction of OH radicals with chlorotoluenes appears to be negligible. The production of fluorine atoms from the reaction of OH with fluorotoluenes is not expected on thermochemical grounds.

In conclusion, reactivity trends observed in the present study for the halotoluenes are dictated by the nature and position of the halogen substituent and are totally consistent with the trends found in previous studies on other halogenated aromatics.

5.7 CORRELATIONS

Kinetic data are now available for the gas phase reactions of the OH radical with a wide variety of organic compounds [29]. These data allow possible trends and correlations to be examined for certain classes of organics such as aromatic compounds. Correlations are useful (i) as a method of highlighting the general trend in chemical behaviour of different compounds, (ii) in allowing an estimate of unknown rate coefficients to be made, and (iii) in pointing out experimental inconsistencies in a data set.

Zetzsch [107] has established two predictive tools for the estimation of rate constants for the reaction of OH radicals with aromatic compounds. The basis of these two techniques are a correlation between (a) rate data and the electrophilic substituent constants developed by Brown and Okamoto [108], and (b) rate data and ionisation potential of the aromatic.

(a) Electrophilic Substituent Constants

Zetzsch [107] has shown that for benzene, biphenyl and a series of substituted monocyclic aromatics, the room temperature rate constants for the addition of OH radicals to the aromatic ring correlate well with the sum of the electrophilic substituent constants $\sum\sigma^+$.

The following assumptions were made when calculating $\Sigma\sigma^+$:

- Steric hindrance is not taken into account, i.e. attack at ortho- and para- positions are equal.
- The total substituent constant $\Sigma\sigma^+$ is the sum of each of the individual substituent constants.
- OH attacks at the site which yields the most negative summation of $\Sigma\sigma^+$.
- If all positions are occupied, the ipso position is treated like a meta position.

A unit-weighted least squares analysis of k^{add} versus $\Sigma\sigma^+$ by Zetzsch [107] yielded the expression:

$$\log k^{\text{add}} (\text{cm}^3 \text{ molecule}^{-1} \text{ s}^{-1}) = -11.4 - 1.39\Sigma\sigma^+ \quad \text{XIII}$$

Using a more extensive kinetic database Atkinson [109] has modified XIII to yield:

$$\log k^{\text{add}} (\text{cm}^3 \text{ molecule}^{-1} \text{ s}^{-1}) = -11.64 - 1.31\Sigma\sigma^+ \quad \text{XIV}$$

Table 5.9 lists the sum of the electrophilic substituent constants, $\Sigma\sigma^+$, the rate constants calculated using expression XIV and the experimental rate constants from this work.

Table 5.9 Calculated rate constants based on Electrophilic Substituent Constants versus experimental rate constants for reaction of OH with selected Aromatic compounds.

Aromatic	Substituent Constant $\Sigma\sigma^+$	$10^{12} \times k_{calc}$ $\text{cm}^3 \text{ molecule}^{-1} \text{ s}^{-1}$	$10^{12} \times k_{exp}$ $\text{cm}^3 \text{ molecule}^{-1} \text{ s}^{-1}$
Toluene	-0.311	5.85	5.23
Ethylbenzene	-0.295	5.58	6.34
n-propylbenzene	-0.295	5.58	7.21
1,2,4,5-tetramethylbenzene	-0.754	22.27	51.57
1,2,3,4-tetramethylbenzene	-0.754	22.27	-
1,2,3,5-tetramethylbenzene	-0.999	46.63	-
2-fluorotoluene	-0.139	3.48	2.09
3-fluorotoluene	-0.384	7.29	4.40
4-fluorotoluene	-0.139	3.48	3.03
2-chlorotoluene	0.048	1.98	2.45
3-chlorotoluene	-0.197	4.15	4.72
4-chlorotoluene	0.048	1.98	3.46

It is clear from a comparison of the calculated and experimental rate constants listed in Table 5.9 that this correlation may be used to predict OH rate constants to within \pm a factor of typically ≤ 2 (with the exception of 1,2,4,5-tetramethylbenzene). The agreement between the calculated and experimental rate constants for toluene, ethylbenzene and n-propylbenzene is very good. The calculated value for 1,2,4,5-tetramethylbenzene is underestimated but supports the order of reactivity postulated in *Section 5.5* where by the 1,2,4,5- and 1,2,3,4- isomers have similar reactivities and that of the 1,2,3,5- isomer is greatly enhanced due to the positioning of the methyl groups on the ring.

The rate constants predicted for the halotoluenes are within a factor of ≤ 2 of the experimental values, while the 3-halo isomer is predicted to be the most reactive consistent with the experimental data. Since one of the basic assumptions in deriving expression XIV is that attack at the ortho and para positions are equal, the 2-halo and 4-halo toluenes are predicted to have the same reactivity. The chlorotoluenes are predicted to be less reactive than the corresponding fluorotoluene isomers, in contrast to the results obtained in this study and in the work of Wallington *et al*[83] on halobenzenes, where it was shown that the reactivity was observed to decrease with increasing electronegativity of the halogen substituent. The electrophilic substituent constants derived by Brown and Okamoto [108] for F- (-0.073) and Cl- (0.114) suggest that Cl- is more deactivating than F-.

(b) Ionisation Potentials (IP)

For addition reactions several examples exist which show a dependence of the rate constants on ionisation potential of the reactants. Gaffney and Levine [110] observed a linear correlation for $\log k_{\text{OH}}$ versus ionisation potential for the olefins and chlorinated olefins. Zetzsch [107] found that the reactivities of a series of substituted aromatics with OH radicals increase rapidly with decreasing ionisation potential of the reactant aromatic and derived the following expression using benzene, aniline, para-chloroaniline, phenol, 1,2,4-trichlorobenzene, benzonitrile, nitrobenzene and twelve alkyl substituted benzenes:

$$\log k (\text{cm}^3 \text{ molecule}^{-1} \text{ s}^{-1}) = 0.74 - 1.36 \text{ IP (eV)} \quad \text{XV}$$

Table 5.9 lists the ionisation potentials, the rate constants calculated from expression XV and the experimentally determined rate constants for the reaction of OH radicals with aromatics from this work. The calculated rate constants for the toluene, ethylbenzene and n-propylbenzene are in excellent agreement with the experimentally determined values.

It is interesting to note that the calculated rate constants for reaction of OH with indane and tetralin are an order of magnitude lower than the experimental values from this work, supporting the proposition that H-atom abstraction from the saturated ring contributes significantly to the overall reactivity for these two compounds. The calculated and experimental rate constants for the halotoluenes agree within a factor of ± 2 .

Table 5.10 Calculated rate constants based on Ionisation Potentials versus experimental rate constants for reaction of OH with Aromatic compounds.

Aromatic	Ionisation Potential ^a eV	$10^{12} \times k_{\text{calc}}$ $\text{cm}^3 \text{ molecule}^{-1} \text{ s}^{-1}$	$10^{12} \times k_{\text{exp}}^b$ $\text{cm}^3 \text{ molecule}^{-1} \text{ s}^{-1}$
Toluene	8.821 ± 0.01	5.54	5.94
Ethylbenzene	8.76 ± 0.01	6.70	6.34
n-propylbenzene	8.72 ± 0.01	7.60	7.21
n-butylbenzene	8.69 ± 0.01	8.40	9.52
Indane	9.05 ± 0.05	2.70	23.86
Tetralin	9.14 ± 0.05	2.04	26.46
2-fluorotoluene	8.915 ± 0.01	4.13	2.09
3-fluorotoluene	8.915 ± 0.01	4.13	4.40
4-fluorotoluene	8.785 ± 0.01	6.20	3.03
2-chlorotoluene	8.83 ± 0.02	5.38	2.45
3-chlorotoluene	8.83 ± 0.02	5.38	4.72
4-chlorotoluene	8.70 ± 0.02	8.09	3.46

a: Rosenstock *et al* [93].

b: This work.

5.8 ATMOSPHERIC IMPLICATIONS

It is well recognised that the reaction of the OH radical with aromatics is thinitial step in the oxidation leading to the formation of ozone. The effective time before these aromatics generate ozone is determined by their lifetimes with respect to reaction with the OH radical. The atmospheric lifetime, τ , can be determined from a knowledge of the OH radical reaction rate constant, k , and the atmospheric concentration of the hydroxyl radical, $[\text{OH}]$, using the expression:

$$\tau = 1/(k[\text{OH}]) \quad \text{XVI}$$

where $[\text{OH}]$ is taken as 5×10^6 per cm^{-3} which is typical of polluted urban air [111]. Table 5.11 shows the room temperature rate constants and atmospheric lifetimes calculated using expression XVI for the series of aromatics studied in this work. As expected the compounds which are more reactive with the OH radical reactive compounds such as indane, tetralin and 1,2,3,4-tetramethylbenzene have relatively short atmospheric lifetimes, of the order of one day and hence their initial oxidation processes will lead mainly to local photooxidant formation. The photochemical oxidation of halotoluenes, which have atmospheric lifetimes typically greater than five days, will contribute to regional oxidant formation.

Table 5.11 Room temperature rate constants and atmospheric lifetimes with respect to reaction with the OH radical for the Aromatic compounds studied in this work.

Aromatic	$10^{12} \times k_{OH}$ $\text{cm}^3 \text{ molecule}^{-1} \text{ s}^{-1}$	τ_{OH} days
toluene	5.94 ± 0.22	3.9
toluene-d8	5.77 ± 0.07	4.0
ethylbenzene	6.34 ± 0.29	3.7
n-propylbenzene	7.21 ± 0.29	3.2
n-butylbenzene	9.52 ± 0.50	2.4
o-diethylbenzene	12.47 ± 0.43	1.9
indane	23.86 ± 1.88	1.0
tetralin	26.46 ± 1.30	0.9
1,2,4,5-tetramethylbenzene	51.57 ± 3.4	0.4
2-fluorotoluene	2.09 ± 0.07	11.1
3-fluorotoluene	4.40 ± 0.07	5.3
4-fluorotoluene	3.03 ± 0.14	7.6
2-chlorotoluene	2.45 ± 0.22	9.4
3-chlorotoluene	4.72 ± 0.50	4.9
4-chlorotoluene	3.46 ± 0.43	6.4

6.0 LITERATURE REFERENCES

1. S. Chapman, *Mem. Roy. Meteorol. Soc.*, **3**, 103 (1930).
2. "Stratospheric Ozone 1988", UK Stratospheric Ozone Research Group, 2nd Report, HMSO, London (1988).
3. R.P. Wayne, "Chemistry of Atmospheres", 2nd Edition, Oxford (1991)
4. United Nations Environment Programme, "Montreal Protocol on the Protection of the Ozone Layer", Nairobi, Kenya (1992).
5. R.E. Hester and R.M. Harrison, "Volatile Organic Compounds in the Atmosphere" Royal Society of Chemistry (1995).
6. "Europe's Environment – The Dobvis Assessment", 1991.
7. "Air Pollution in Europe 1997", EEA Environmental Monograph No. 4.
8. H.J.T. Bloeman and J. Burns "Chemistry and Analysis of Volatile Organic Compounds in the Environment", Chapman and Hall (1993).
9. A.B. Pittock, *Q. J. R. Meteorol. Soc.*, **103**, 575 (1977).
10. J.A. Logan, *J. Geophys. Res.*, **90**, 10463 (1985).
11. J. Fishman, V. Ramanathan, P.J. Crutzen and S.C. Liu, *Nature*, **282**, 818 (1979).
12. B.E. Tilton, *Environ. Sci. Technol.*, **23**, 257 (1989).
13. W.W. Heck, O.C. Taylor, R. Adams, G. Bingham, J. Miller, E. Preston and L. Weinstein, *J. Air Pollut. Control. Assoc.*, **32**, 353 (1982).
14. J.N. Woodman and E.B. Cowling, *Environ. Sci. Technol.*, **21**, 120 (1987).
15. A.M. Hough and R.G. Derwent, *Atmos. Environ.*, **21**, 2015 (1987).
16. W.P.L. Carter and R. Atkinson, *Environ. Sci. Technol.*, **21**, 670 (1987).
17. W.P.L. Carter and R. Atkinson, *Environ. Sci. Technol.*, **23**, 864 (1989).
18. W.P.L. Carter, *J. Air and Waste Manage. Assoc.*, **44**, 881 (1994).
19. W.P.L. Carter, EPA 600/3-91-050, US EPA Research Triangle park, NC (1991).

20. F.M. Bowman and J.H. Seinfeld, *Atmos. Environ.*, **28**, 3359 (1994).
21. F.M. Bowman and J.H. Seinfeld, *J. Geophys. Res.*, **99**, 5309 (1994).
22. R.G. Derwent and M.E. Jenkin, *Atmos. Environ.*, **25A**, 1661 (1991).
23. Y. Andersson-Skold, P. Grennfelt and K. Pleijel, *J. Air and Waste Manage. Assoc.*, **42**, 1152 (1992).
24. R.G. Derwent, M.E. Jenkin and S.M. Saunders, *Atmos. Environ.*, **30**, 181 (1996).
25. B. Hamilton, <http://www.mustangworks.com>
26. E.L. Marshall and K. Owen, "Motor Gasoline", Royal Society of Chemistry (1995)
27. "Gasolines", Concawe 1992 Product Dossier No. 92/103.
28. U.K. Transport Committee, 6th Report "Transport Related Air Pollution in London", Volume II (1994).
29. R. Atkinson, *J. Phys. Chem. Ref. Data*, Monograph 1 (1989).
30. R. Snyder and C.C. Hedli, *Environmental Health Perspectives*, **104**, Supplement 6 (1996).
31. Integrated Criteria Document: Benzene, Report No. 75846001, National Institute of Public Health and Environmental Protection, Bilthoven, The Netherlands.
32. S. Shigeta, J. Misawa and H. Aikawa, *Neurobehav. Toxicol.*, **2**, 85 (1980).
33. A.K. Agrawal, S.P. Srivastava and P.K. Seth, *Bull. Environ. Contam. Toxicol.*, **29**, 400 (1982).
34. A. Mikiska, *Arch. Gewerbe Pathol. Gewerbe Hyg.*, **19**, 286 (1960).
35. J.T.F. Liao and F.W. Oehme, *Vet. Hum. Toxicol.*, **22**, 160 (1980).
36. J.M. Hesse, G.J.A. Speijers and R.D.F.M. Taalman, Integrated Criteria Document: Chlorobenzene effects, Appendix to Report No. 71041015. National Institute of Public Health and Environmental Protection, Bilthoven, The Netherlands.

37. U.G. Ahlborg and T.M. Thunberg, *Arch. Toxicol.*, **40**, 55 (1978).
38. S. DeFlora, P. Zannachi, A. Camoira, C. Bennicalli and G.S. Bandolati, *Mutat. Res.*, **133**, 161 (1984).
39. W.F. Van Oettigan, *Nat. Inst. Health Bull.* No. 190 (1949).
40. R.P. Wayne, I. Barnes, P. Biggs, J.P. Borrows, C.E. Canosa-Mas, J. Hjorth, G.Le Bras, G.K. Moortgat, D. Perner, G. Poulet, G. Restelli and H.W. Sidebottom, *Atmos. Environ.*, **25A**, No.1 (1991).
41. B. O'Leary, M.Phil. Thesis, Dublin Institute of Technology, 1992.
42. R. Atkinson, *J. Phys. Chem. Ref. Data*, Monograph 2 (1992).
43. S. Madronich and W. Felder, *J. Phys. Chem.*, **89**, 3556 (1985).
44. Y.Z. He, W.G. Mallard, and W. Tsang, *J. Phys. Chem.*, **92**, 2196 (1988).
45. D.F. Smith, C.D. McIver and T.E. Kleindeinst, *J. Atmos. Chem.*, **30**, 209 (1998).
46. F.P. Tully, A.R. Ravishankara, R.L. Thompson, J.M. Nicovich, R.C. Shah, N.M. Kreutter and P.H. Wine, *J. Phys. Chem.*, **85**, 2262 (1981).
47. B.J. Finlayson-Pitts and J.N. Pitts Jr., "Atmospheric Chemistry: Fundamentals and Experimental Techniques" J. Wiley, New York (1986).
48. H.J.L. Forstner, R.C. Flagan and J.H. Seinfeld, *Environ. Sci. Tech.*, **31**, 1345 (1997).
49. J. Yu, H.E. Jeffries and K.G. Sexton, *Atmos. Environ.*, **31**, 2261 (1997).
50. J. Yu and H.E. Jeffries, *Atmos. Environ.*, **31**, 2281 (1997).
51. L.J. Bartoltti and E.O. Edney, *Chem. Phys. Lett.*, **245**, 119 (1995).
52. R. Atkinson and S.M. Aschmann, *Int. J. Chem. Kinet*, **26**, 929 (1994).
53. N. Moschonas, D. Danalatos and S. Glavas, *Monatshefte fur Chemie*, **127**, 875 (1996).
54. D.F. Smith, C.D. McIver and T.E. Kleindeinst, *J. Atmos. Chem.*, **30**, 209 (1998).

55. H. Lay, J.W. Bozzelli and J.H. Seinfeld, *J. Phys. Chem.*, **100**, 6543 (1996).
56. R.G.W. Norrish and G. Porter, *Nature*, **164**, 658 (1949).
57. T. Ohta, *J. Phys. Chem*, **87**, 1209 (1983).
58. R.A. Cox, *J. Photochem.*, **3**, 291, (1974/1975).
59. G.J. Doyle, A.C. Lloyd, K.R. Darnall, A.M. Winer and J.N. Pitts Jr, *Environ, Sci. Technol.*, **9**, 237 (1975).
60. R. Atkinson, W.P.L. Carter, A.M. Winer and J.N. Pitts Jr., *J. Air Pollut. Contr. Assoc.*, **31**, 1090 (1981).
61. W.B. De More, *Int. J. Chem. Kinet*, **15**, 619 (1983).
62. E.C. Tuazon, W.P.L. Carter, R. Atkinson and J.N. Pitts Jr., *Int. J. Chem. Kinet.*, **15**, 619 (1983).
63. I. Barnes, V. Bastian, K.H. Becker, E.H. Fick and F. Zabel, *Atmos Environ.*, **16**, 545 (1982).
64. D.L. Baulch, I.M. Campbell and S.M. Saunders, *J. Chem. Soc., Faraday Trans.2*, **84**, 377 (1988).
65. K. Lorenz and R. Zellner, *Ber. Bunsenges. Phys. Chem.*, **87**, 629 (1983)
66. F. Witte, E. Urbanik and C. Zetzsch, *J. Phys. Chem.*, **90**, 3251 (1986).
67. A. Gourmi, J.F. Pauwels and P. Devolder, *Can. J. Chem.*, **69**, 1057 (1991).
68. D.D. Davis, W. Bollinger and S. Fischer, *J. Phys. Chem.*, **79**, 293 (1975).
69. N. Bourmada, P.Devolder and L.R. Sochet, *Chem. Phys. Lett.*, **149**, 339 (1988).
70. A.R. Ravishankara, S. Wagner, S. Fischer, R. Schiff, R.T. Watson, G. Tesi and D. D.Davis, *Int. J. Chem. Kinet.*, **10**, 783 (1978).
71. K. Kramp and S.E. Paulson, *J.Phys. Chem A*, **102**, 2685 (1998).
72. P.N.Anderson and R.A. Hites, *En viron. Sci. Technol.*, **30**, 301 (1996)..
73. A. Wahner and C. Zetzsch, *J. Phys. Chem.*, **87**, 4945 (1983).

74. R.R. Arnts, R.L. Seila and J.J. Bufalini, *J. Atmos. Pollut. Control Assoc.*, **39**, 453 (1989)
75. T. Ohta and T. Ohyama, *Bull. Chem. Soc. Jpn.*, **58**, 3029 (1985).
76. A.C. Lloyd, K.R. Darnall, A.M. Winer and J.N. Pitts Jr., *J. Phys. Chem.*, **80**, 789 (1976).
77. D.L. Baulch, I.M. Campbell, S.M. Saunders and P.K.K. Louie, *J. Chem. Soc., Faraday Trans. 2*, **85**, 1819 (1989).
78. R. Atkinson and S.M. Aschmann, *Int. J. Chem. Kinet.*, **20**, 513 (1988).
79. S.B. Corchnoy and R. Atkinson, *Environ. Sci. Technol.*, **24**, 1497 (1990).
80. R. Atkinson, S.M. Aschmann, A.M. Winer and J.N. Pitts Jr., *Arch. Environ. Contam. Toxicol.*, **14**, 417 (1985).
81. R.A. Perry, R. Atkinson and J.N. Pitts Jr., *J. Phys. Chem.*, **81**, 296 (1977).
82. M. Rinke and C. Zetzsch, *Ber. Bunsenges. Phys. Chem.*, **88**, 55 (1984).
83. T.J. Wallington, D.M. Neuman and M.J. Kurylo, *Int. J. Chem. Kinet.*, **19**, 725, (1987).
84. M. Semandi, D.W. Stocker and J.A. Kerr, *Int. J. Chem. Kinet.*, **27**, 287 (1995).
85. R. Knispel, R. Koch, M. Siese and C. Zetzsch, *Ber. Bunsenges. Phys. Chem.*, **94**, 1375 (1990).
86. J.M. Nicovich, R.L. Thompson and A.R. Ravishankara, *J. Phys. Chem.*, **85**, 2913 (1981).
87. R. Atkinson, *J. Phys. Chem. Ref. Data*, **26**, No.2 (1997).
88. R. Atkinson and S.M. Aschmann, *Int. J. Chem. Kinet.*, **21**, 355 (1989).
89. R. Atkinson, D.L. Baulch, R.A. Cox, F.M. Hampson, Jr., J.A. Kerr, M.J. Rossi and J. Troe, *J. Phys. Chem. Ref. Data*, **26**, 521 (1997).

90. D.A. Hansen, R. Atkinson and J.N. Pitts Jr., *J. Phys. Chem.*, **79**, 1763 (1975).
91. E.O. Edney, T.E. Kliendienst and E.W. Gorse, *Int. J. Chem. Kinet.*, **18**, 1355 (1986).
92. D.F. McMillian and D.M. Golden, *Ann. Rev. Phys. Chem.*, **33**, 493 (1982).
93. M. Rosenstock, K. Draxl, B.W. Steiner and J.T. Herron, *J Phys. Chem. Ref. Data*, **6**, Supplement No.1 (1977).
94. R.A.Cox, R.G. Derwent, M. R. Williams, *Environ. Sci. Technol.*, **14**, 57 (1980).
95. W. Klopffer, R. Frank, E.G. Kohl and F. Haag, *Chemiker-Zeitung*, **110**, 57 (1986).
96. G.A. Russel, A. Ito and D.G. Hendry, *J. Am. Chem. Soc.*, **85**, 2976 (1963).
97. R. Atkinson, *J. Phys. Chem. Ref. Data*, **26**, No. 2 (1997).
98. R. Atkinson, S.M. Aschmann and A.M. Winer, *Environ. Sci. Technol.*, **21**, 1123 (1987).
99. G.A. Russell, *J. Am. Chem. Soc.*, **78**, 1047 (1956).
100. C. Kooyman, *Discussions Faraday Soc.*, **10**, 163 (1951).
101. A.I. Williams, E.A. Oberright and J.W. Brooks., *J. Am. Chem. Soc.*, **78**, 1190 (1956).
102. J.A. Meyer, V. Stannett and M. Szwarc, *J. Am. Chem. Soc.*, **83**, 25 (1960).
103. M.W. Gery, D.L. Fox, H.E. Jeffries, L. Stockburger and W.S. Weathers, *Int. J. Chem. Kinet.*, **17**, 931 (1985).
104. E.O. Edney, P.B. Shepson, T.E. Kleindienst and E.W. Corse, *Int. J. Chem. Kinet.*, **18**, 597 (1986)
105. J E.C. Tuazon, R. Atkinson and S.M. Aschmann, *Int. J. Chem. Kinet.*, **22**, 981 (1990)
106. T.E. Kleindienst, P.B. Shepson and C.M. Nero, *Int. J. Chem. Kinet.*, **21**, 863 (1989)

107. C. Zetzsch, *15th Informal Conference on Photochemistry, Stanford CA, June 27-
July 1 (1982)*
108. H.C. Brown and Y. Okamoto, *J. Am. Chem. Soc.*, **80**, 4979 (1958).
109. R. Atkinson, *Chem. Rev.*, **85**, 69 (1985).
110. J.S. Gaffney and S.Z. Levine, *Int. J. Chem. Kinet.*, **11**, 1197 (1979)